

University of Vermont

ScholarWorks @ UVM

---

Transportation Research Center Research Reports

---

6-30-2014

## Tailpipe Emissions and Engine Performance of a Light-Duty Diesel Engine Operating on Petro- and Bio-diesel Fuel Blends

Britt Holmén

*University of Vermont*, [Britt.Holmen@uvm.edu](mailto:Britt.Holmen@uvm.edu)

Tyler Feralio

*University of Vermont*

James Dunshee

*University of Vermont*

Karen Sentoff

*University of Vermont*

Follow this and additional works at: <https://scholarworks.uvm.edu/trc>

---

### Recommended Citation

Holmén, Britt; Feralio, Tyler; Dunshee, James; and Sentoff, Karen, "Tailpipe Emissions and Engine Performance of a Light-Duty Diesel Engine Operating on Petro- and Bio-diesel Fuel Blends" (2014). *Transportation Research Center Research Reports*. 186.  
<https://scholarworks.uvm.edu/trc/186>

This Report is brought to you for free and open access by ScholarWorks @ UVM. It has been accepted for inclusion in Transportation Research Center Research Reports by an authorized administrator of ScholarWorks @ UVM. For more information, please contact [donna.omalley@uvm.edu](mailto:donna.omalley@uvm.edu).



A Report from the University of Vermont Transportation Research Center

# Tailpipe Emissions and Engine Performance of a Light-Duty Diesel Engine Operating on Petro- and Bio-diesel Fuel Blends

TRC Report 14-008 | Holmen, Feralio, Dunshee, Sentoff | June 2014

## DISCLAIMER

The contents of this report reflect the views of the authors, who are responsible for the facts and the accuracy of the information presented herein. This document is disseminated under the sponsorship of the Department of Transportation University Transportation Centers Program, in the interest of information exchange. The U.S. Government assumes no liability for the contents or use thereof.

# **Tailpipe Emissions and Engine Performance of a Light-Duty Diesel Engine Operating on Petro- and Bio-diesel Fuel Blends**

**University of Vermont Transportation Research Center**

**June 30, 2014**

*Prepared by:*

Britt A. Holmén, Professor, Civil & Environmental Engineering

Tyler Feralio, Graduate Research Assistant

James Dunshee, Graduate Research Assistant

Karen Sentoff, Research Specialist

Transportation Research Center  
Farrell Hall  
210 Colchester Avenue  
Burlington, VT 05405

Phone: (802) 656-1312

Website: [www.uvm.edu/trc](http://www.uvm.edu/trc)



## **Acknowledgements**

The Project Team would like to acknowledge the efforts of the following members of the UVM Transportation Air Quality (TAQ) Laboratory who assisted in collection of emissions data upon which the results of this report are based: Vaishali Sharma, Brad Haire, as well as undergraduate research assistants Scott Quinn, Michael Kreigh, Joseph Marri, David Wheeler, Daryl Deprey, Justin Jannone, John Nummy, Kristin Darby and Rose Long. U.S. DOT support under Project #025668 via the UVM TRC is gratefully acknowledged.

## **Disclaimer**

The contents of this report reflect the views of the authors, who are responsible for the facts and the accuracy of the data presented herein. The contents do not necessarily reflect the official view or policies of the UVM Transportation Research Center. This report does not constitute a standard, specification, or regulation.

# Table of Contents

<b>Tailpipe Emissions and Engine Performance of a Light-Duty Diesel Engine Operating on Petro- and Bio-diesel Fuels</b>	<b>i</b>
Acknowledgements	i
Disclaimer	i
 <b>TABLE OF CONTENTS .....</b>	 <b>ii</b>
 <b>List of Tables</b>	 <b>iv</b>
 <b>List of Figures</b>	 <b>i</b>
 <b>1. INTRODUCTION .....</b>	 <b>1</b>
<b>1.0 Overview and Introduction</b>	<b>1</b>
1.1 Study Motivation	1
1.2 Effect of Biodiesel Properties on Engine Operation	3
1.2.1 Fuel Consumption	3
1.2.2 Start of Combustion	4
1.2.3 Low Temperature Properties	5
1.3 Effect of Biodiesel use on Tailpipe Emissions	6
1.3.1 Particulate Emissions measured by Mass (PM)	7
1.3.2 Particulate Emissions Measured by Number (PN)	8
1.3.3 Regulated Gas-Phase Emissions from Diesel and Biodiesel Fueled Engines	10
1.3.4 Mobile Source Air Toxic (MSAT) Emissions	11
1.3.5 Summary	12
 <b>2. RESEARCH METHODOLOGY .....</b>	 <b>13</b>
2.1 Experimental Setup Overview	13
2.2 CM-12 Light-duty Diesel Engine Dynamometer	13
2.2.1 Armfield Software Control of CM-12 Engine and Dynamometer	14
2.2.2 Exhaust Sampling and Dilution	14
Ejector Diluter Mechanics.	15
Dilution Air Supply.	16
Raw Exhaust Sample Probe.	17
Dilution System Tuning.	17
Flow Measurement and Temperature Control.	19
2.2.3 Data Acquisition System	19
Armfield Engine and Dynamometer Parameters.	20
Scantool Engine Parameters	20
Labview Data Acquisition for Temperature, Flow and Pressure Sensors	21
2.2.4 Tailpipe Emissions Test Sequence	24
Fuel Purging	25
Drive Cycles.	26
Oil and Fuel Filter Changes.	27
2.3 (Bio)diesel Fuel Supply and Monitoring	28
2.3.1 Fuel Composition And Biodiesel Fuel Blending	28
2.4 Gas and Particle Emissions Measurement	28

2.4.1 Particle Mass & Number Measurement	29
Filters	29
EEPS	29
UCPC	29
EAD	30
2.4.2 Exhaust Gas Measurement	30
FTIR	30
5-Gas Analyzer	30
2.5 Data Processing	30
2.5.1 Data Pre-Processing: Temporal Alignment.	30
2.5.2 Engine Load Calculation.	31
2.5.3 Fuel Consumption.	32
2.5.4 Blank Corrections	33
2.6 System Validation Procedures	34
2.6.1 Logsheets and Checklists	34
2.6.2 Data Quality Control and Instrument Verification	35
<b>3. RESULTS .....</b>	<b>36</b>
3.1 Summary Of Data Collected	36
Ambient Air Conditions	37
3.2 Fuel Composition by IROX-D	37
3.3. Engine Operation: Run-to-Run Reproducibility	38
Engine Parameters	38
Fuel Consumption	40
3.4 Gravimetric Total Particulate Matter (PM) Emissions	42
3.5 Mean Particle Number Distributions by Biodiesel Blend	42
3.6 Particle Diameter Measurement	45
3.7 Gas-Phase Emissions	45
<b>4. CONCLUSIONS .....</b>	<b>49</b>
<b>REFERENCES CITED .....</b>	<b>50</b>
<b>Appendices</b>	<b>53</b>
Appendix A. Experimental Sampling Setup Instrumentation Detail	54
Appendix B. Biodiesel Fuel Blending & Analysis Procedures	56
Appendix C. Sampling Checklists and Logsheets	65
Appendix D. Raw Data Tables	71

## List of Tables

Table 1-1. Properties of No. 2 Diesel and Biodiesel Fuels (4).....	3
Table 1-2. Low temperature properties for No. 2 diesel fuel and B100 from various feedstocks (4) .....	5
Table 1-3. Mobile source contribution to 1999 National-Scale Air Toxics Assessment (NATA).....	12
Table 2-1. Armfield CM-12 Component Specifications.....	14
Table 2-2 Computers used for each sampling instrument.....	20
Table 2-3 Armfield Sensors on CM-12 Test Cell .....	20
Table 2-4. Rosstech Scantool Sensors and Calibration Equations* .....	21
Table 2-5. Data Acquisition Components.....	21
Table 2-6. Labview Parameters and Calibration Equations for Sensors.....	22
Table 2-7. Diluted Samples and Flows by Port Identifier. Minimum dilution system flow is 80 LPM resulting in a minimum of 5 LPM excess flow.....	28
Table 2-8. PM Filter Specifications used for PM mass and chemical composition .....	29
Table 2-9. Test runs completed at 40% and 80% load and the instruments that successfully logged.....	34
Table 3-1. Individual Run Test Conditions.....	36
Table 3-2. Mean IROX results for fuel biodiesel content.....	38
Table 3-3. Mean ( $\pm$ 1 sd) Gas-phase Concentrations for SS40 Tests: Total Run and SS portion of run only. .....	47
Table A.1. CM-12 Light-Duty Diesel Engine Dynamometer Test Equipment.....	54
Table A.2. Scantool 8-bit Interpretation Table .....	54
Table A.3. Labview Channel Setup.....	55
Table B.1 Fuel Purchase and Delivery Log .....	64
Table D.1. DILUTION RATIO AND TEST CONDITIONS TABLE.....	71
Table D.2. Steady-State Test Run Mean Engine Parameters .....	72
Table D.3. Particulate Matter Filter Mass Concentrations.....	73
Table D.4. Ambient conditions recorded from ExTech Temperature and Humidity Logger at beginning of Engine Runs.....	74
Table D.5. IROX RESULTS FOR 2012 CM-12 TEST FUELS .....	75
Table D.6. Steady-State 40% Load Engine Tests from Winter-Spring 2012 .....	77
Table D.7. Steady-State 80% Load Engine Tests from Winter-Spring 2012 .....	78
Table D.8. EEPS Channel Means for SS40 and SS80 Tests.....	79
Table D.9. Particle Number Distribution Diameter Modes and Corresponding DR-Corrected Concentrations by Blend .....	82
Table D.10. FTIR Gas-Phase Concentrations for SS40 Biodiesel Runs .....	83

## List of Figures

Figure 1-1. Biodiesel Production, Exports and Consumption in the United States, 2001 to 2011. (Source: EIA Annual Energy Review, 2011 Table 10.4 from the U.S. Energy Information Administration (1)).....	2
Figure 1-2. Depiction of crank angle (CA) for different piston positions in engine cylinder. ....	4
Figure 1-3. Cloud point, pour point, and cold filter plug point (CFPP) measurements for different blends of soy biodiesel in low sulfur No. 2 diesel (4) .....	6
Figure 1-4. EPA’s criteria pollutant emissions data for biodiesel blends. ....	7
Figure 1-5. Typical engine exhaust mass (dotted line) and number (solid black line) weighted size distributions (left axis) with alveolar deposition fraction (green line, right axis)(14).....	9
Figure 1-6. Particle number distributions from Aakko et al. (35) highlighting the effect of reformulating petrodiesel.....	10
Figure 2-1. Block diagram of emissions test systems configuration. ....	13
Figure 2-2. Schematic of Dekati ejector diluter flows to dilute raw exhaust for particle sampling. ....	15
Figure 2-3. Engine Exhaust Dilution System Configuration .....	16
Figure 2-4. Locations of orifices (A, B) and orifice meters (C, D) on dilution system. ....	18
Figure 2-5. Calibration curves for exhaust sample transfer line and dilution air magnehelics.. ....	23
Figure 2-6. Calibration setup for push-through flow of exhaust Pitot tube (a) and pull-through flow for MAF sensor (b). ....	23
Figure 2-7. MAF Sensor Calibration: (left) Raw voltage; (right) calibration curve based on Sierra flow meter flowrate data.....	24
Figure 2-8. Pitot MAG Calibration: (left) Raw voltage; (right) calibration curve based on Sierra flow meter flowrate data .....	24
Figure 2-9. Fuel Switching System with the valves in the ‘Biodiesel’ Position .....	26
Figure 2-10. Second-by-second drive cycles. ....	27
Figure 2-11. Volkswagen 1.9L SDi Torque Curve with Polynomial Trendlines.....	32
Figure 2-12. Fuel consumption data comparison .....	33
Figure 2-13. EEPS PN distribution verification against SMPS with standard aerosol.....	35
Figure 3-1. Ambient air temperature and relative humidity at start of SS test runs. ....	37
Figure 3-2. IROX Mid-FTIR Absorbance Spectra for raw B0 and B20 fuel samples (left) and B50 and B100 samples diluted to 25% with n-hexanes (right).....	38
Figure 3-3. IROX results for fuel biodiesel content .....	38
Figure 3-4. Mean CM-12 engine operating parameters for SS40 tests.....	39
Figure 3-5. Mean CM-12 engine operating parameters for SS80 tests.....	40
Figure 3-6. Mean CM-12 exhaust manifold temperature for SS40 (left) and SS80 (right) tests.....	40
Figure 3-7. Fuel consumption for SS80 tests determined by weight of fuel tank during test cycle. ....	41
Figure 3-8. Gravimetric PM mass concentration ( $\mu\text{g}/\text{m}^3$ ) results and laboratory test conditions.....	42
Figure 3-9. EEPS Particle Number Distributions for SS40 and SS80 tests. Data were corrected for measured dilution ratio. Log-Log plot.....	43
Figure 3-10. Relationship between ambient temperature and mean total particle number over SS40 and SS80 test cycle. ....	44
Figure 3-11. Electrical Aerosol Detector (EAD) Full Run Time Series Data for B0, B20, B50 and B100 blends. ....	45
Figure 3-12. MultiGas FTIR Instrument Check Parameter Mean Values for SS40 Runs .....	46
Figure 3-13. Pre- vs. Post Tunnel Blank Gas Concentration Comparison for B0 and B20 SS40 Runs .....	46
Figure 3-14. Selected Gas Concentrations for SS40 Runs (linear y-axis scale) .....	48
Figure 3-15. Selected Gas Concentrations for SS40 Runs (log y-axis scale).. ....	48

**List of Figures (continued)**

Figure C.1. Run Logsheet ..... 65

Figure C.2. Labels sheet for PM Filter Petri dishes..... 65

Figure C.3. EEPS and FTIR Instrument Logsheet ..... 66

Figure C.4. 5-Gas, EAD and SMPS Instrument Logsheet ..... 67

Figure C.5. Aggressive Drive Cycle Worksheet ..... 68

Figure C.6. Run Checklist..... 69

Figure D.1. IROX-Diesel Fuel Properties for fuel samples collected from the fuel tanks, before and after  
CM-12 tests..... 76

Figure D.2. SS40 and SS80 Average Tailpipe PM Mass Concentrations. n = number of replicate samples.  
Error bars are one standard deviation. .... 78

Figure D.3. Uncorrected EEPS mean number distributions by run..... 80

Figure D.4. EEPS Particle Number Distributions for SS40 and SS80 tests. Data were corrected for  
measured dilution ratio. .... 80

Figure D.5. Average Particle Number Distributions for replicate steady –state emissions tests at each  
biodiesel blend ratio. EEPS data are not corrected for tunnel blank and dilution ratio here. .... 81

Figure D.6. Mean Exhaust Gas Species Concentrations for (a) B0, (b) B20, (c) B50 and (d) B100 fuel  
blends. Error bars are one standard deviation. .... 84

# 1. Introduction

## 1.0 Overview and Introduction

This report summarizes the experimental apparatus developed in the Transportation Air Quality Laboratory (TAQ Lab) at the University of Vermont to compare light-duty diesel engine performance and exhaust emissions when operating on petroleum diesel (henceforth referred to as petrodiesel) and biodiesel fuel blends. This work was conducted between July 2008, when the Armfield, Ltd. Light-Duty Diesel (LDD) Engine Dynamometer Test System (Model CM-12) was received, and June 2013. The engine housed in the CM-12 unit is a Volkswagen (VW) SDi 1.9 liter industrial engine, similar to those used in on-road vehicles similar to the VW Jetta or Golf, but without a turbocharger or exhaust aftertreatment. The objective of the research was to evaluate how the alternative fuel, biodiesel, would affect emissions and engine performance (fuel economy and torque) relative to the baseline petrodiesel. In this preliminary report, the experimental apparatus is described in detail and emissions results are presented for a series of steady-state tests with petrodiesel and soybean biodiesel blends.

## 1.1 Study Motivation

The diesel engine is a well-established and widely used technology that is a vital component of modern day transportation networks. Emissions produced by diesel engines, however, have been linked to climate change, air pollution and adverse human health effects. The composition of diesel exhaust depends on several factors, including engine operating conditions and fuel composition. Hazardous products of diesel fuel combustion include particulate matter (measured by both particle mass (PM) and particle number (PN)) and gas phase substances such as carbon monoxide (CO), carbon dioxide (CO<sub>2</sub>, a greenhouse gas), oxides of nitrogen (NO + NO<sub>2</sub> = NO<sub>x</sub>), and various hydrocarbons (HCs). Of particular concern to public health are air toxics, including polycyclic aromatic hydrocarbons (PAHs), and particles with diameters less than 0.1 μm, ultrafine particles (UFP), which can deeply penetrate the human respiratory system due to their small size. Advancements in diesel engine technology and the emergence of alternative biofuels are promising means of reducing several harmful combustion products formed during diesel engine operation. Federal legislation mandating the use of renewable fuels that can be produced domestically such as the 2007 Energy Independence and Security Act (EISA) led to a surge in the production and use of biodiesel (**Figure 1-1**), despite the fact that relatively little was known about how the transition from conventional petroleum-based fuels to renewable biofuels would affect vehicle emissions profiles and, therefore, ambient air quality and human health.

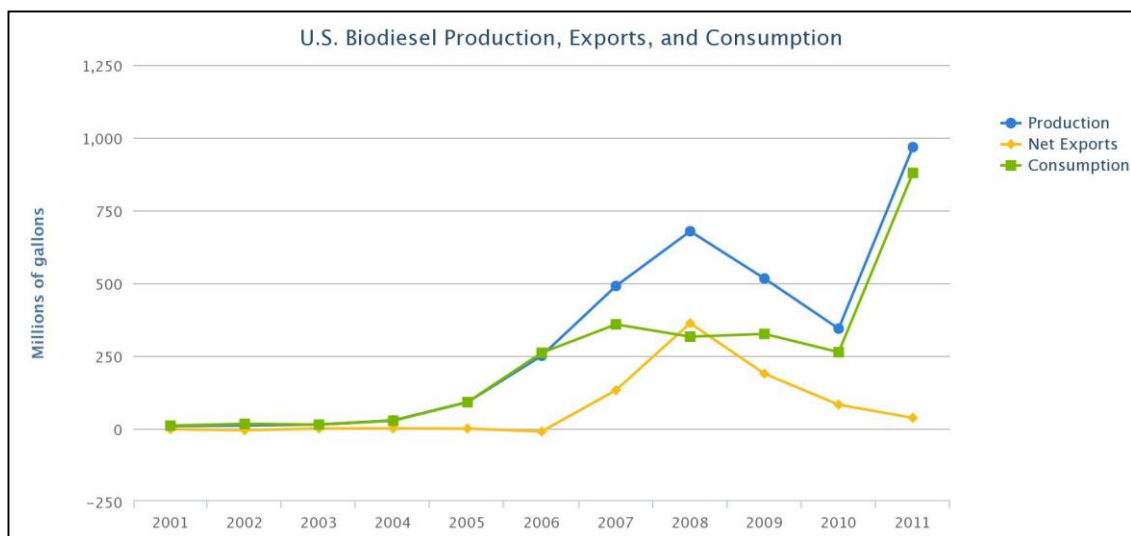


**Figure 1-1. Biodiesel Production, Exports and Consumption in the United States, 2001 to 2011. (Source: EIA Annual Energy Review, 2011 Table 10.4 from the U.S. Energy Information Administration (1))**

Vehicle emissions regulations have become more stringent over time in order to address air quality concerns. Currently, emissions of light-duty vehicles (LDV; i.e., passenger cars and trucks) in the U.S. are regulated by the Tier 2 emissions regulation. This regulation limits the emissions (on a g/mile basis) of non-methane hydrocarbons (NMHC), CO, NO<sub>x</sub>, PM, and formaldehyde (HCHO) measured while the vehicle follows the Federal Test Procedure (FTP) 75 drive cycle on a chassis dynamometer. The Tier 2 vehicle emission regulation went into full effect in 2009 (2). In March of 2013, the U.S. Environmental Protection Agency (EPA) signed a proposed rule that introduced Tier 3 emissions standards for LDVs. Tier 3 reduces the acceptable emissions levels from the Tier 2 and is slated to be phased in between 2017 and 2025 (3).

Because vegetable oils and animal fats are lipids that can be used as feedstocks for biodiesel fuel production through the transesterification process, biodiesel is a potential renewable energy source with a net benefit life-cycle greenhouse gas emissions profile (4). During the transesterification process, lipids react with alcohol in the presence of a catalyst to form mono-alkyl esters and glycerin. Current mass production of biodiesel commonly reacts methanol with the feedstock oil (typically soybean oil in the U.S. and rapeseed oil in Europe) resulting in a mixture of fatty acid methyl esters (FAMES). The regulations controlling the quality of biodiesel (EN14214 in Europe and ASTM D6751-12 in the U.S.), therefore, focus on the use of methanol as the alcohol reactant although ethanol could also be used which would result in a mixture of fatty acid ethyl esters (FAEE) (4). **Table 1-1** compares the properties of typical number 2 petrodiesel and 100% soybean biodiesel (B100) fuel. Biodiesel has a lower energy density, higher viscosity, higher cloud and pour point temperatures, higher cetane number, and higher oxygen content than petrodiesel. These properties affect fuel consumption, start of combustion, fuel handling under cold weather conditions as well as tailpipe emissions. The effect of each of these factors on tailpipe emissions is described in more detail below. Increasingly, biodiesel has been produced and used in on-road vehicles as blends with petrodiesel; typical in-use blends contain 5 to 20 percent biodiesel (B5 to B20), computed on a volumetric basis. The low blend percentage reflects the disadvantages of biodiesel use in cold weather relative to petrodiesel.



**Table 1-1. Properties of No. 2 Diesel and Biodiesel Fuels (4)**

Fuel Property	Diesel	Biodiesel
Fuel Standard	ASTM D975	ASTM D6751
Higher Heating Value, Btu/gal	~137,640	~127,042
Lower Heating Value, Btu/gal	~129,050	~118,170
Kinematic Viscosity, @ 40°C (104°F)	1.3–4.1	4.0–6.0
Specific Gravity kg/l @ 15.5°C (60°F)	0.85	0.88
Density, lb/gal @ 15.5°C (60°F)	7.1	7.3
Carbon, wt %	87	77
Hydrogen, wt %	13	12
Oxygen, by dif. wt %	0	11
Sulfur, wt %	0.0015 max	0.0–0.0024
Boiling Point, °C (°F)	180–340 (356–644)	315–350 (599–662)
Flash Point, °C (°F)	60–80 (140–176)	100–170 (212–338)
Cloud Point, °C (°F)	-35 to 5 (-31 to 41)	-3 to 15 (26 to 59)
Pour Point, °C (°F)	-35 to -15 (-31 to 5)	-5 to 10 (23 to 50)
Cetane Number	40–55	48–65

## 1.2 Effect of Biodiesel Properties on Engine Operation

### 1.2.1 Fuel Consumption

Biodiesel has a lower energy density than petrodiesel that suggests a larger volume of biodiesel is required to generate the same load as petrodiesel. The increase in fuel delivery needed is described by three separate mechanisms (5, 6): (1) operator compensation, (2) fuel viscosity, and (3) fuel density.

Operator compensation refers to the unconscious act of a driver increasing throttle when the vehicle is fueled with biodiesel to evoke the same power response from the engine compared to when it is fueled with petrodiesel (5). Although increasing the quantity of fuel injected in this way may seem innocuous, it may have associated engine control implications. Depending on engine control strategy, the engine control unit (ECU) may modify other engine parameters such as start of injection (SOI) and exhaust gas recirculation (EGR) duty cycles in response to a different throttle position sensor (TPS) signal. In such a case, these parameters may also have an effect on tailpipe emissions.

It has also been shown that pump-line-nozzle fuel injection systems actually inject more biodiesel than petrodiesel given the same throttle position (5, 6). This phenomenon occurs due to the higher viscosity of biodiesel relative to petrodiesel; the result is less leakage between internal components of the fuel injector pump, allowing a higher percentage of allocated fuel to reach the combustion chamber.

Biodiesel also has a higher density than petrodiesel and therefore mechanical fuel injectors, which operate on a *volumetric* basis, will inject a higher *mass* of biodiesel fuel even when injecting the same fuel *volume* as petrodiesel (6). Unlike operator compensation, the ECU, in many cases,

would not be ‘aware’ of the increased fuel injection, resulting in a reduced air-to-fuel ratio (fuel enrichment) assuming no other adjustments are made by the ECU. Fuel enrichment is of concern because it is typically associated with elevated tailpipe emission events.

### 1.2.2 Start of Combustion

In its simplest form, engine “tuning” refers to the adjustment of two factors: (a) the time combustion of the fuel starts in the cylinder relative to engine speed (revolutions per minute; RPM) and (b) the mass of fuel injected into the cylinder relative to the mass of air in the cylinder. Recent advances in diesel engine control have resulted in superior process control with respect to (a). A generational shift in fuel injection technology occurred around 2008: changing from pump-line-nozzle to common rail fuel injection systems. Common rail systems utilize electronically-controlled injectors rather than mechanically-controlled injectors, enable increased control of start of injection (SOI), and provide the ability to divide what used to be one large injection event into smaller, precisely-controlled multiple injection events. Manufacturers have also started using in-cylinder pressure sensors to accurately measure start of combustion (SOC) (7). Given how recent this generational technology shift occurred, however, the majority of the diesel vehicles on the road still utilize the older pump-line-nozzle fuel injection technology. On these vehicles, SOC is not measured, but SOI is, providing feedback to the ECU. Both SOI and SOC are measured in terms of crank angle (CA) relative to the top dead center (TDC) piston position (**Figure 1-2**). Biodiesel fuel can affect both of these events due to differences in fuel properties compared to the petrodiesel fuel for which the diesel engines were designed (8).

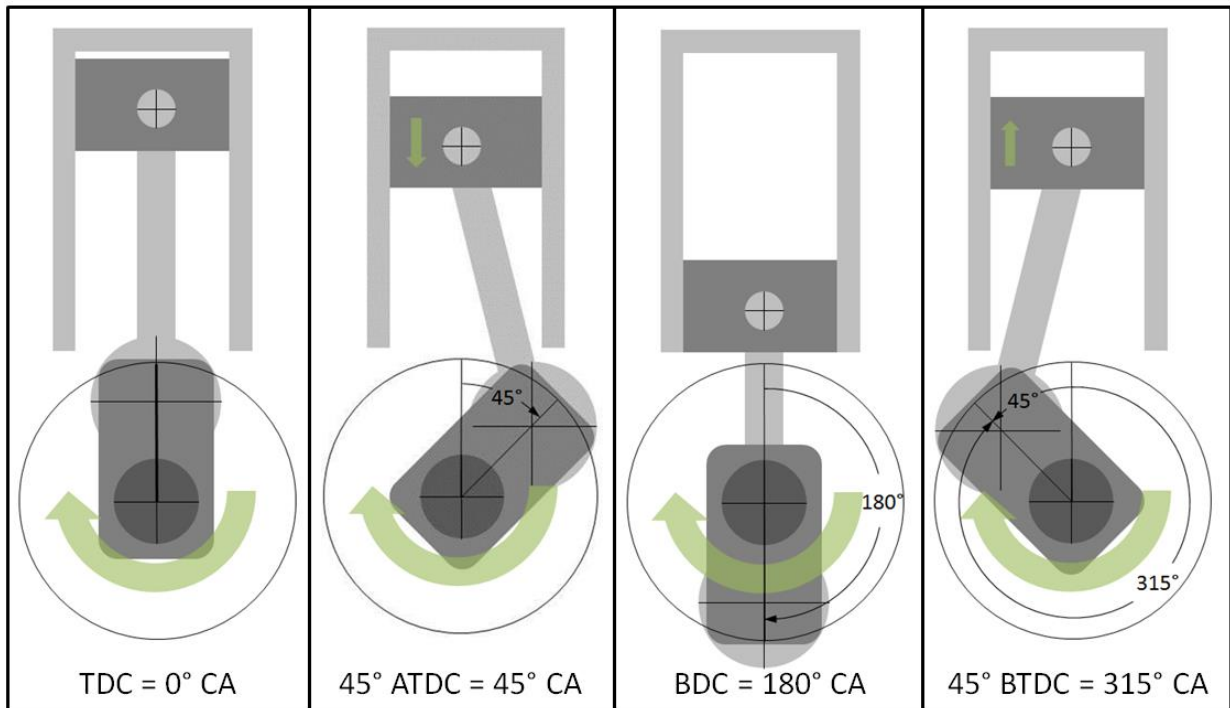


**Figure 1-2. Depiction of crank angle (CA) for different piston positions in engine cylinder.**  
Other acronyms: TDC = Top Dead Center; ATDC = After TDC; BDC = Bottom Dead Center; BTDC = Before TDC.

Vehicles equipped with engines that have pump-line-nozzle fuel injection systems are susceptible to an advance in SOI when using biodiesel due to its higher viscosity and higher bulk modulus relative to petrodiesel (5, 6, 8). The differences in these fluid properties result in quicker pressurization of the fuel line between the fuel pump and the injector and faster transmission of the

pressure pulse (8). These, in turn, advance the opening the mechanical fuel injector in relation to crank angle (CA) when using biodiesel. Thus, SOI occurs early when operating on biodiesel fuel.

Biodiesel also has a higher cetane number than petrodiesel (see **Table 1-1**). Cetane number is a measure of a diesel fuel's combustion quality and affects ignition delay: the higher the cetane number, the shorter the ignition delay of the fuel. Thus, for biodiesel the time delay between SOI and SOC is shorter than for petrodiesel. This means that, even if the ECU is capable of adjusting the injection timing to maintain the same SOI with different fuels, biodiesel combustion can still be advanced relative to petrodiesel combustion, resulting in fuel enrichment. This ignition advance is apparent on both pump-line-nozzle and common rail fuel injection systems without in-cylinder pressure sensors (5). This phenomenon, however, can be accounted for when the ECU utilizes in-cylinder pressure sensor feedback because SOC can then be directly measured.

### 1.2.3 Low Temperature Properties

One hurdle facing the widespread use of biodiesel is its low temperature behavior relative to petrodiesel. In cold weather, both petrodiesel and biodiesel can coagulate and freeze into a solid making it impossible for the fuel to be pumped and injected. The ambient temperatures at which the fuel “gels” for biodiesel is typically higher than for petrodiesel. The two metrics used to characterize a fuel's low temperature performance are cloud point and pour point. Cloud point is the temperature at which solids start to crystallize in the fuel as it is being cooled while pour point is the temperature at which the fuel has solidified to a point that it will no longer flow. Cloud point is typically considered the low temperature operability limit (4) of the fuel. **Table 1-2** summarizes typical cloud point and pour point values for petrodiesel and pure biodiesel (B100) produced from various lipid feedstocks.

**Table 1-2. Low temperature properties for No. 2 diesel fuel and B100 from various feedstocks (4)**

Fuel Type	Cloud Point		Pour Point	
	(°F)	(°C)	(°F)	(°C)
Typical No. 2 Diesel	-31 to 41	-35 to 5	-31 to 5	-35 to -15
Soy Methyl Ester (SME)	32	0	25	-4
Rapeseed (Canola) Methyl Ester (RME)	26	-3	25	-4
Lard Methyl Ester	56	13	55	13
Edible Tallow Methyl Ester	66	19	60	16
Inedible Tallow Methyl Ester	61	16	59	15
Yellow Grease 1 Methyl Ester	-	-	48	9
Yellow Grease 1 Methyl Ester	46	8	43	6

According to the data presented in **Table 1-2**, rapeseed methyl ester has the best low temperature properties relative to petrodiesel, however, its pour point is still 11°C higher than the highest petrodiesel pour point (i.e., the biodiesel will solidify in warmer weather conditions than petrodiesel). Pure biodiesel, however, is not typically used in on-road diesel engines. When biodiesel is blended with petrodiesel, the resulting low temperature properties lie between those of the neat fuels shown in **Table 1-2** as shown in **Figure 1-3**.

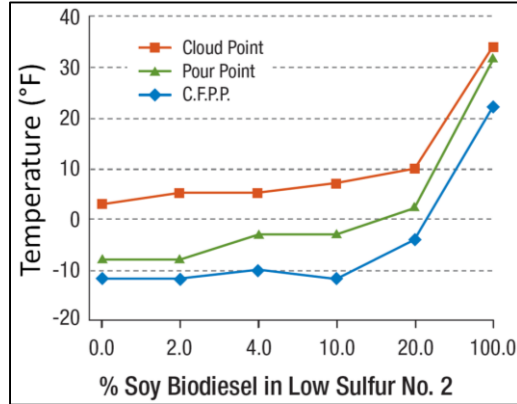


Figure 1-3. Cloud point, pour point, and cold filter plug point (CFPP) measurements for different blends of soy biodiesel in low sulfur No. 2 diesel (4)

### 1.3 Effect of Biodiesel use on Tailpipe Emissions

There have now been numerous studies on the effect biodiesel fuel has on the emissions from diesel engines compared to petrodiesel. Research is typically performed with direct injection, turbocharged, four cylinder, four stroke diesel engines or vehicles (5). Further, the majority of previous studies have examined emissions from heavy-duty diesel (HDD) engines, with fewer studies on light-duty diesel (LDD) emissions. The majority of these studies have shown that fueling with biodiesel typically reduces emissions of PM, HC, and CO while slightly increasing NO<sub>x</sub> emissions (4–6). Changes in these emission rates have been linked to different properties of biodiesel. One significant difference is that biodiesel, unlike petrodiesel, is an oxygenated fuel containing approximately 11% oxygen by weight [see **Table 1-1**]. Higher fuel oxygen content is thought to improve combustion quality, therefore, releasing fewer unburned and partially burned constituents (4, 5, 9). Additionally, advances of SOI and SOC relative to CA as discussed in **Section 1.2**, alter in-cylinder flame propagation and have a effect on combustion emissions.

The 2002 U.S. EPA report, *A Comprehensive Analysis of Biodiesel Impacts on Exhaust Emissions* (10), correlated the change in CO, HC, NO<sub>x</sub>, and PM mass emissions relative to biodiesel blend percentage using the results of numerous prior studies that utilized HDD engines with no EGR or aftertreatment systems. These relationships are depicted in **Figure 1-4** as solid red lines that overlay the individual data points used to generate the best-fit lines. It should be noted that the data are plotted in **Figure 1-4** as a percent change in pollutant emission rate for tests conducted with petroleum diesel, but the composition of this diesel fuel varied between studies as did the engine type and model year.

**Figure 1-4** not only depicts the general trends of the EPA findings but also the variability of the data found in the literature. This variability stems from the use of different engines with different control technologies, different loading scenarios used for testing, and different test fuels.

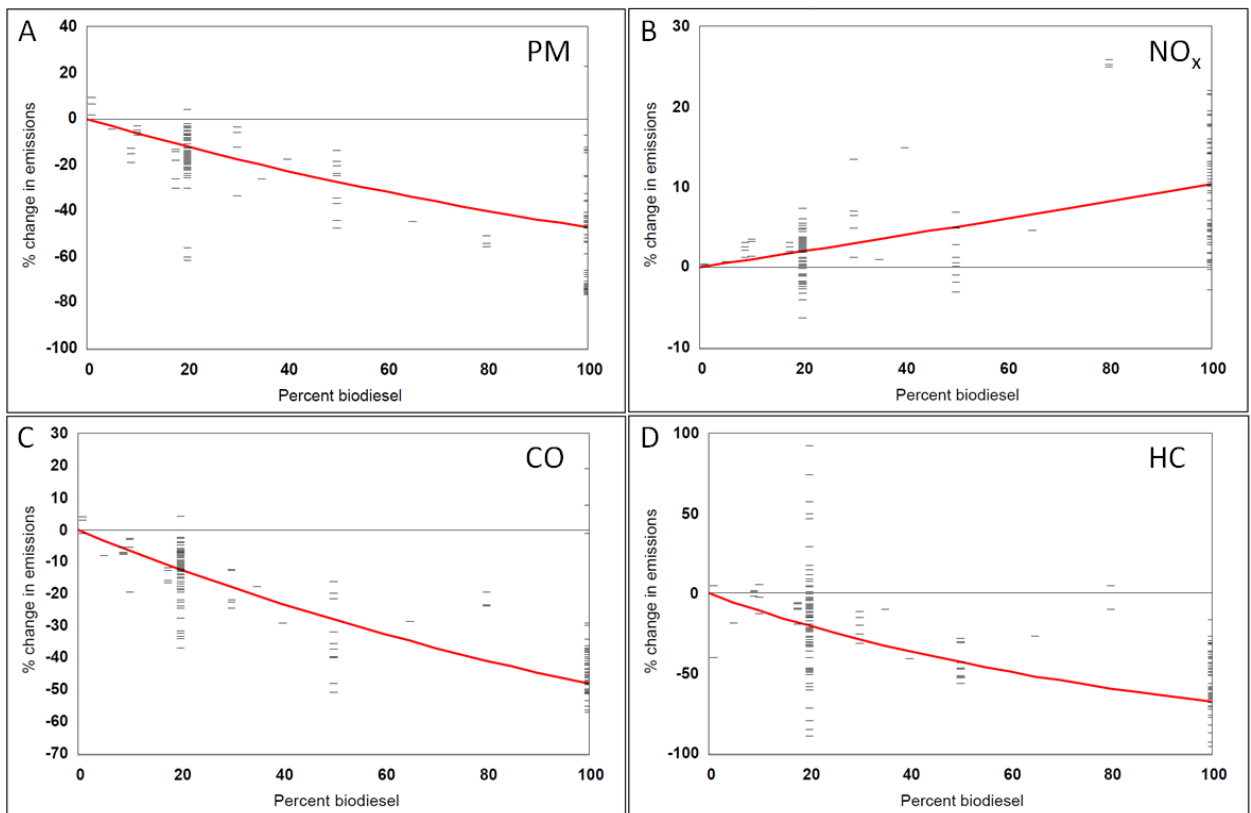


**Figure 1-4. EPA's criteria pollutant emissions data for biodiesel blends. A) PM; B) NO<sub>x</sub>; C) CO; D) HC (10)**

Beyond criteria pollutants PM, NO<sub>x</sub>, CO, and HC emissions, another area of concern is the emission of gas-phase mobile source air toxics (MSATs) as well as particle number emissions. MSATs include carbonyls and polycyclic aromatic hydrocarbons (PAHs). Many MSATs are known carcinogens for which a considerable amount of their emission inventory is attributed to mobile sources and are constituents of the broader hydrocarbons (HC) emissions category (10).

### 1.3.1 Particulate Emissions measured by Mass (PM)

In the U.S., exhaust particle emissions are currently regulated on the basis of gravimetric mass of particulate matter (PM). LDV PM emissions are measured while the vehicle is driven through the FTP-75 drive cycle on a chassis dynamometer. The tailpipe emissions are fed into a dilution system and samples of the diluted exhaust are pulled through pre-conditioned, pre-weighed filters during the entirety of the dynamometer test. Once the test is complete, the filters are post-conditioned and post-weighed. The difference between the post-weight and the pre-weight is the amount, by mass, of particulate collected. The emissions rate is then calculated by multiplying the measured particle mass by the dilution ratio (DR) and dividing it by the number of miles 'driven' during the dynamometer test cycle, resulting in an *emissions factor* in grams/mile. This value is then used to determine whether or not the LDV meets the emission standard criteria set forth by the current emission regulation.

The fuel and test engines used in PM emissions research for biodiesel fuel vary from study to study resulting in variation of the reported findings. In some cases, no significant change in PM was found, as in Durbin et al. (11), for which B20 and B100 were used. Yet,

Graboski et al. (12) reported a 66% reduction in PM while fueling with B100 derived from soybean oil. Although the literature reports considerable variability, the majority of previous studies reported reductions in PM emissions when fueling with biodiesel rather than petrodiesel (4, 6, 9–13), confirming the pattern shown in **Figure 1-4**.

Multiple reasons for decreased PM emissions from engines fueled with biodiesel have been put forth. Neat biodiesel has little to no sulfur, resulting in a reduction in sulfate formation when fueling with biodiesel blends (4–6, 8, 9). Biodiesel is also an oxygenated fuel (approximately 11% by weight) which promotes improved combustion in the fuel-rich zones of the combustion chamber (6, 9). Similarly, combustion is also improved during transient fuel-rich operating events associated with turbocharger lag due to the increased oxygen content of the fuel (6). It has also been suggested that the advance in SOC (due to both advanced SOI and higher cetane number) while using biodiesel provides more time for diffusion combustion which increases the oxidation of soot in the high temperature environment of the cylinder, effectively reducing the amount of soot emitted (6). Lastly, when operator compensation occurs to make up for the lower heating value of biodiesel (operator depresses throttle pedal further), the engine's ECU may also decrease the exhaust gas recirculation (EGR) duty cycle which increases cylinder temperature, promoting soot oxidation, and therefore reduces PM emissions (6).

### 1.3.2 Particulate Emissions Measured by Number (PN)

**Figure 1-5** depicts typical diesel engine exhaust mass- and number-weighted particle size distributions along with lung alveolar deposition fraction (14). The alveolar region is a sensitive area of the human lung that may have few natural defenses against large numbers of potentially harmful particles (15–19). As shown in **Figure 1-5**, ultrafine particles (UFP; diameter < 100 nm) account for the majority of the alveolar deposition in the human lung, but are not as well represented by the mass-weighted (PM) particle distribution as they are by the number weighting (PN) (14, 20–23). Because of they are readily deposited in the alveolar region of the lung, UFPs have a higher potential to cause adverse human health effects compared to the larger particles typically found in diesel exhaust (14, 15, 21, 24, 25). Recognizing that UFPs are better represented by the PN metric, the European Union's EURO 5b vehicle emissions standard, which came into effect in 2011, contained regulations for both PM and PN. The EURO 6 regulation, due to take effect in 2014, also addresses PN emissions (5, 26).

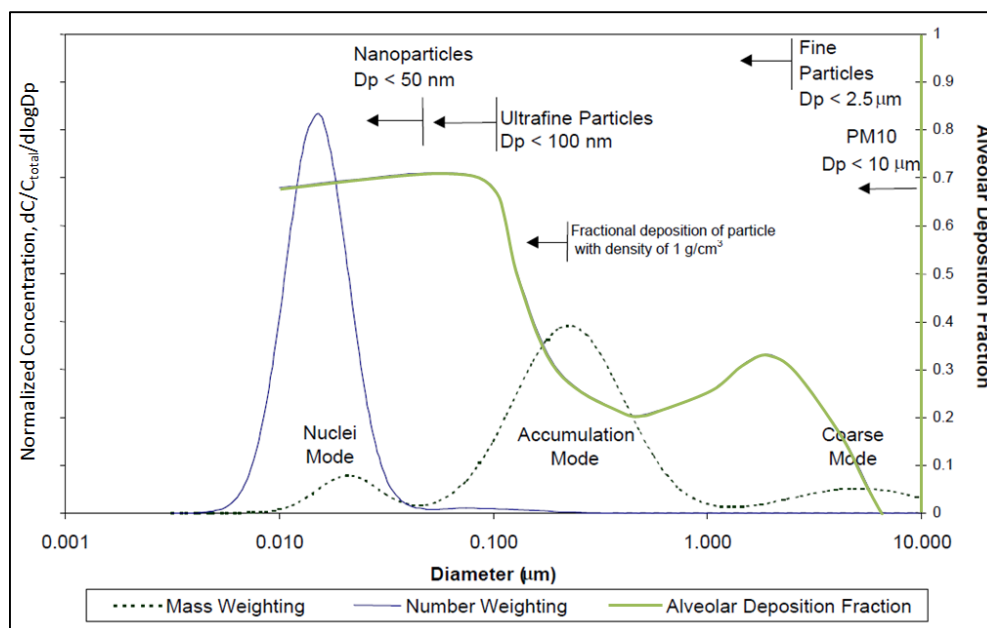


**Figure 1-5. Typical engine exhaust mass (dotted line) and number (solid black line) weighted size distributions (left axis) with alveolar deposition fraction (green line, right axis)(14)**

Many researchers have studied both the change in total PN emissions and in the PN size distributions during diesel engine operation on biodiesel fuel. The majority of these tests were performed with HHD engines running steady-state drive cycles. In general, the use of biodiesel relative to petrodiesel increases total particle number (TPN) and shifts the particle number distribution to smaller size bins (27–32), typically increasing the number of nuclei mode particles while decreasing the number of accumulation mode particles (28, 29, 33–35). These research results, however, are quite variable because of the many factors can affect particle formation and growth. These factors include: particle sizing and counting equipment (27, 36); the age and characteristics of the engine (5, 6, 8, 37); test cycle (high or low load) (28, 31, 38), and fuel composition (30, 34). Biodiesel’s low sulfur content relative to pre-2006 petrodiesel (after July 1, 2006, petrodiesel sulfur content was regulated to be < 15ppm in the U.S.) provided reductions in nuclei mode particles, however, as regulations regarding sulfur content in petrodiesel have become more stringent, this benefit has faded. This shift over time is highlighted by the particle number distribution data presented in Aakko et al. (35) for four fuels: (1) EN590 petrodiesel (similar to low sulfur diesel (LSD); sulfur <500ppm); (2) RFD - Reformulated petrodiesel (similar to ultra-low sulfur diesel (ULSD); sulfur <15ppm); (3) RME30 – 30% v/v Rapeseed methyl ester biodiesel, 70% EN590 petrodiesel; and (4) RME100 – 100% Rapeseed methyl ester biodiesel as shown in **Figure 1-6**.

These data shows that, relative to EN590 particulate emissions, neat RME and RME/EN590 blends result in an overall decrease in PN, presumably due to the reduction in sulfur content when introducing biodiesel into the fuel. The data for the RFD, however, suggests that reformulated petrodiesel fuel with sulfur content less than 15ppm (i.e., ULSD) may reduce nuclei mode particles to a higher degree than RME, resulting in less of a biodiesel emissions benefit.



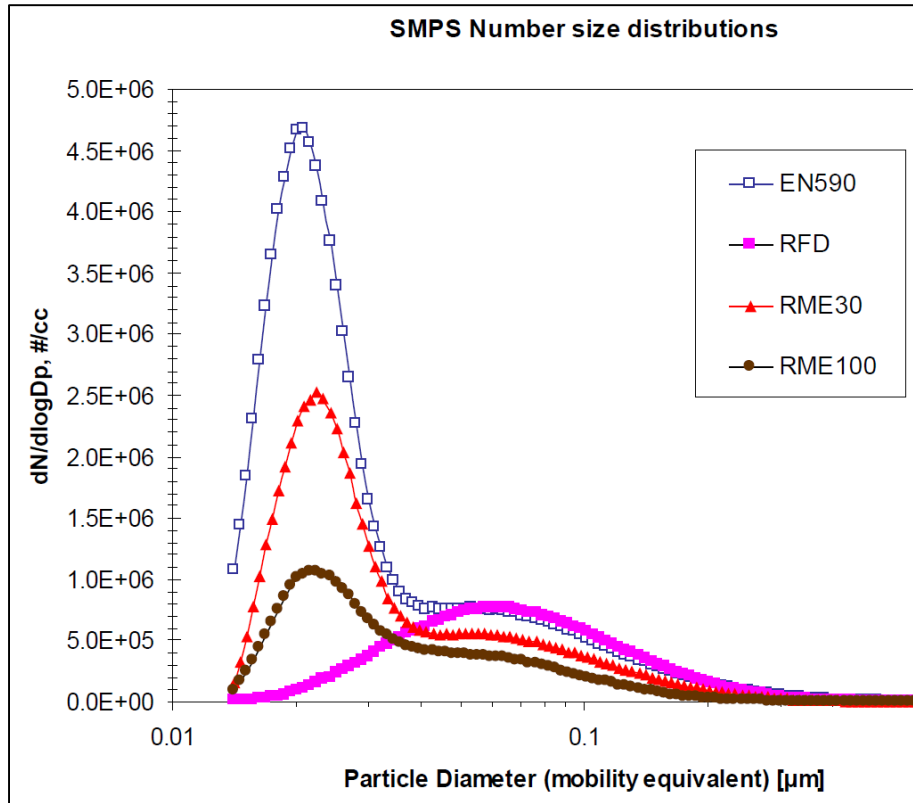


Figure 1-6. Particle number distributions from Aakko et al. (35) highlighting the effect of reformulating petrodiesel.

Explanations for why biodiesel generally increases total particle number (TPN) emissions relative to ULSD have been suggested:

- Biodiesel emissions increase the particle phase soluble organic fraction (SOF) and the effect of increased injection pressure and advanced injection timing as the percentage of biodiesel increases in the fuel have been proposed as possible causes of increased TPN (6, 39).
- The general reduction in accumulation mode particles reduces the availability of surface area for the nuclei mode particle precursor gases to adsorb to while traveling through the exhaust system, resulting in higher nuclei mode particles (28, 40).

Thus, while some studies have been found that diverge from the general trend (38, 40–42), most studies report an increase in the number of nuclei mode particles when fueling with biodiesel, resulting in higher TPN for biodiesel than for petrodiesel.

### 1.3.3 Regulated Gas-Phase Emissions from Diesel and Biodiesel Fueled Engines

#### Oxides of Nitrogen (NO<sub>x</sub>)

NO<sub>x</sub> emissions (NO and NO<sub>2</sub>) are associated with ground-level ozone (6, 43) and secondary organic aerosol (SOA) formation (44). Ground-level ozone presents significant human health risks, can be harmful to vegetation, and is one of the main components in urban smog (45). Diesel engines emit appreciable NO<sub>x</sub> and research has generally shown that NO<sub>x</sub> emissions from diesel engines running on biodiesel range from not significantly different from those for petrodiesel to slightly higher – up



to roughly a 23% increase for B100 in heavy-duty diesel engines (see **Figure 1-4**) (4–6, 28, 30, 31, 35, 41, 46). Although the general trend shows an increase in NO<sub>x</sub> emissions with biodiesel blend percentage, some researchers have reported reductions (47–49). A variety of mechanisms have been suggested to explain this phenomenon. Advanced SOI results in fuel entering the combustion chamber earlier and residing in elevated temperature and pressure conditions which are more favorable for NO<sub>x</sub> formation (6, 46). Also, in-cylinder temperatures increase due to the increased amount of biodiesel injected to produce an equivalent power output to that of petrodiesel (6). Furthermore, if the increase in biodiesel injected is due to operator compensation as described previously, differences in SOI and EGR control by the ECU could promote NO<sub>x</sub> production (6).

Recent data, however, has been presented suggesting that fuel injection and EGR control strategies that are designed specifically for the in-use fuel's properties can reduce biodiesel NO<sub>x</sub> emissions to levels at or below those of petrodiesel (46, 50).

### **Carbon Monoxide (CO)**

CO is emitted from all combustion processes and mobile sources contribute substantially to ambient CO in urban areas (51). Elevated CO levels can be harmful to human health because, when inhaled, oxygen that would normally go into the blood stream can be replaced by CO, blocking oxygen's pathway into the body and causing tissue damage and, possibly, death (52). When running on biodiesel, diesel engines generally produce less CO [Error! Reference source not found.C](4–6, 30, 33, 35, 47, 53), although some studies have reported increases in CO (28, 42). The range found in the literature is +95% (28) to -50% (10) CO emissions relative to petrodiesel. The reduction of CO emissions has primarily been explained by the increased oxygen content of biodiesel fuel leading to more complete combustion (4–6, 54).

### **Hydrocarbons (HC)**

Some HCs typically emitted by diesel engines are toxic or carcinogenic (4). When biodiesel is used to fuel diesel engines HC emissions generally decrease as shown in Error! Reference source not found.D (4–6, 30, 33, 35, 53, 54) although, again, some studies have shown the opposite trend with biodiesel blend percentage (28, 54). The range found in the literature is +58% (55) to -70% (10) HC emissions relative to petrodiesel. Again, the increased oxygen content of biodiesel has been credited with improved HC emissions (4–6, 54).

## **1.3.4 Mobile Source Air Toxic (MSAT) Emissions**

MSATs are air toxic compounds, defined by the U.S. EPA as known or suspected carcinogens (20), found in mobile source (vehicles) exhaust (10). Seven of the individual MSAT compounds focused on in the 2006 EPA report '*Control of Hazardous Air Pollutants From Mobile Sources*' are listed in **Table 1-3** with their percent contributions from mobile sources and on-road mobile sources (56).

The effect of biodiesel on MSAT emissions is under studied, but the majority of studies where MSATs have been measured show reductions in MSAT emissions with biodiesel compared to petrodiesel. The EPA (10) found a total MSAT reduction of approximately 15% when using B100.

Polycyclic aromatic hydrocarbons (PAHs), a subset of MSATs which are primarily from the soluble organic fraction (SOF) of diesel exhaust, are more widely studied because many of them are known or suspected carcinogens (20). Similar to the data found in the literature for regulated emissions, the reported effects of biodiesel on PAH emissions are variable, however, PAH emissions are generally reduced with biodiesel fuel (13, 41, 57, 58). Karavalakis et al. (57) reported both increases and decreases in PAH emissions which appeared to be dependent on drive cycle while Hensen and Jensen (41) reported total PAH reductions of more than 90% when using

rapeseed B100. An interesting note reported by Karavalakis et al. (57) is that the use of oxidized biodiesel increases PAH emissions relative to fresh biodiesel.

**Table 1-3. Mobile source contribution to 1999 National-Scale Air Toxics Assessment (NATA)**

1999 NATA risk drivers	Percent contribution from all mobile sources(percent)	Percent contribution from on-road mobile sources(percent)
Benzene	68	49
1,3-Butadiene	58	41
Formaldehyde	47	27
Acrolein	25	14
Polycyclic organic matter *	6	3
Naphthalene	27	21
Diesel PM and Diesel exhaust organic gases	100	38

\* This POM inventory includes the 15 POM compounds: benzo[b]fluoranthene, benz[a]anthracene, indeno(1,2,3-c,d)pyrene, benzo[k]fluoranthene, chrysene, benzo[a]pyrene, dibenz(a,h)anthracene, anthracene, pyrene, benzo(g,h,i)perylene, fluoranthene, acenaphthylene, phenanthrene, fluorene, and acenaphthene.

### 1.3.5 Summary

In summary, many studies report a decrease in emissions of harmful combustion products from use of biodiesel compared to diesel fuel. These include reductions in regulated pollutants (HCs and PM) as well as hazardous *unregulated* emissions (PAHs) in biodiesel exhaust (41). In general, the abundance of these compounds in exhaust decreases as biodiesel is used in greater blend proportions (**Figure 1-2**). However, these results are not widely conclusive as some studies have reported results which do not follow the general trend (13). Furthermore, other compounds of concern are reported to increase with higher biodiesel blend ratios, including NO<sub>x</sub> and polar oxygenated compounds (POCs), which are linked to cellular oxidative stress (42).

The majority of literature on biodiesel emissions pertains to experiments conducted with older model, heavy-duty diesel (HDD) engines. Marked differences in particle and gas emissions have been demonstrated between exhaust from pre-2007 diesel engines and New Technology Diesel Exhaust (NTDE) (37). Considering increased use of both biodiesel and light-duty diesel (LDD) engines in the United States and globally, it is important to understand how these factors interact to impact air quality, the environment, and public health under various conditions.

Bio-fuels have increased in popularity in the last ten years. For diesel vehicles, biodiesel is the bio-fuel of choice. As far as combustion is concerned, biodiesel is a ‘drop in’ fuel for compression ignition (diesel) engines (4), meaning that the compression ignition engine can run on both petrodiesel and biodiesel without any modification. This, however, does not mean that an engine designed to run efficiently with petrodiesel will run just as efficiently with biodiesel. The goal of this research is to better understand the factors that lead to UFP emissions from LDD vehicles, while taking into account the fuel used, in order to develop advanced emissions control technologies and improve ambient air quality.

## 2. Research Methodology

### 2.1 Experimental Setup Overview

The experimental setup consists of five subsystems and processes, each described in detail below. These systems are:

- (i) CM-12 light-duty diesel engine dynamometer & exhaust dilution (**Section 2.2**);
- (ii) Exhaust sampling and dilution (**Section 2.2**);
- (iii) (Bio)diesel fuel supply and monitoring (**Section 2.3**);
- (iv) Gas and particle emissions measurement (**Section 2.4**); and
- (v) Data Acquisition and Timing (**Section 2.2**).

In addition, the protocols used in the UVM Transportation Air Quality Laboratory (TAQ Lab) to ensure sample integrity and reproducibility in measurements are found in **Sections 2.5 and 2.6**.

Briefly, a Volkswagen light-duty diesel engine test stand with dynamometer is the central component for emissions testing. Engine exhaust is sampled for gases directly with two instrument (FTIR and 5-Gas), but must be diluted to obtain particle number measurements by a suite of time-resolved particle instruments (EEPS, EAD, UCPC). Custom-built systems monitor dilution ratio, temperatures, pressures and fuel consumption during the tests. Data acquisition at rates of 1Hz or faster are achieved with dedicated computers and a custom PC clock synchronization system. These systems are interconnected as shown in **Figure 2-1**. Detailed information on all instruments and sensors can be found in **Appendix A**.

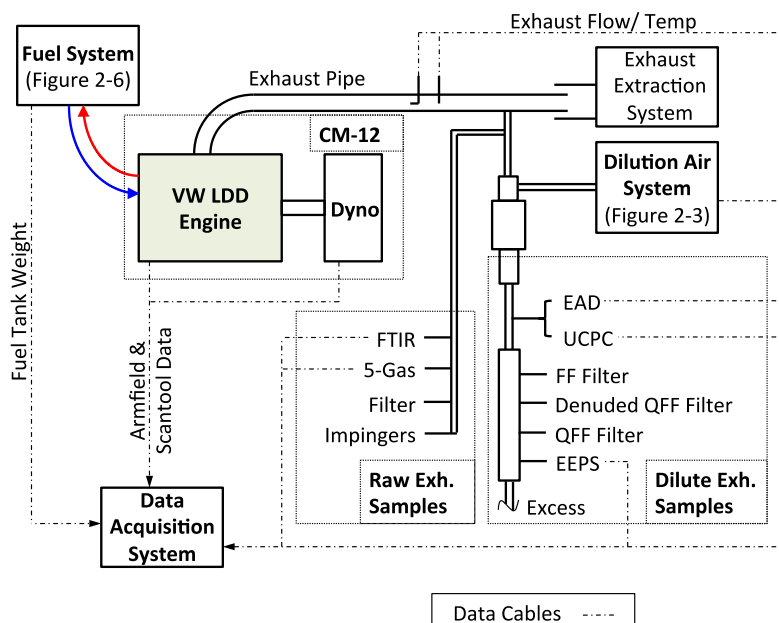


Figure 2-1. Block diagram of emissions test systems configuration.

### 2.2 CM-12 Light-duty Diesel Engine Dynamometer

An Armfield, Ltd. model CM-12 “Automotive Diesel Engine Test Cell” was used to generate light-duty diesel (LDD) engine exhaust in the University of Vermont’s Transportation Air Quality Laboratory (TAQLab). A 1.9 Liter Volkswagen SDi engine (similar to the engine found in the Volkswagen *Bora*, a European market sedan), a four cylinder, naturally aspirated engine with

pump-line-nozzle type fuel injection (Bosch VE injection pump) is coupled to a Zelu K-40 (air cooled; 145Nm max braking torque) eddy current dynamometer. Engine and dynamometer specifications can be found in **Table 2-1**. The CM-12 engine emissions certification falls under the European Union directive EC 97/68, Stage IIIA. These emission limits are 5.0 g/kWh for carbon monoxide (CO), 4.7 g/kWh for combined hydrocarbon and oxides of nitrogen emissions (HC + NO<sub>x</sub>) and 0.4 g/kWh for particulate matter (PM).

### 2.2.1 Armfield Software Control of CM-12 Engine and Dynamometer

Both engine and dynamometer are controlled with software supplied by Armfield that allows both ‘manual’ and ‘automatic’ control. In ‘manual’ mode, the operator can change % brake (power to the dynamometer which loads the engine) and % throttle (equivalent to pressing the accelerator pedal in a car). When in ‘automatic’ mode, a set point RPM can be specified and a proportional–integral–derivative (PID) controller adjusts the % brake setting to achieve the RPM set point while the operator continues to control the throttle. Experiments were conducted to evaluate the beta version of Armfield ‘scheduler’ control software that allows the user to pre-define a drive cycle that the software will then follow as the engine is running. Use of the scheduler ensures that the engine is cycled through the same ‘driving conditions’ for each replicate test. Armfield implemented the scheduler software in March of 2011 and it was first utilized in the TAQLab in June 2011. All data reported here were collected by operating with ‘automatic’ control (steady-state test cycles).

**Table 2-1. Armfield CM-12 Component Specifications**

Engine	
Manufacturer	Volkswagen
Identification Code	ARD
Charge Air	Naturally Aspirated
Capacity	1896cm <sup>3</sup>
Cylinders	4
Bore	79.5mm
Stroke	95.5mm
Compression Ratio	19.5:1
Nominal Output	44 kW @ 3600 RPM
Max Torque	130Nm @ 2000 - 2400 RPM
Fuel	Diesel DIN EN590
Control System	Bosch EDC
Exhaust Gas Recirculation	NO
Power Absorption Unit/ Eddy Current Dynamometer	
Manufacturer	Zelu/ Klam
Model Number	K-40 PAU
Max Power	60kW
Max Torque	145Nm

### 2.2.2 Exhaust Sampling and Dilution

The exhaust sampling and dilution system consists of: (A) a dilution air source and conditioning system, (B) exhaust and dilution air transfer lines, (C) ejector diluter, (D) flow measuring system, and (E) sample ports manifold. A custom-built mini-dilution system provided clean, dry dilution air for mixing with a subsample of raw engine exhaust from the CM-12 tailpipe. A Dekati Diluter

(Dekati, LTD, Finland) served to both sample the tailpipe exhaust and mix the raw exhaust with dilution air without the need for an additional sampling pump.

### Ejector Diluter Mechanics.

Raw exhaust temperature and particle concentrations are too high for current instruments to quantify particulate emissions in diesel engine exhaust without dilution. For this research, a single-stage mini-diluter setup based on a Dekati ejector diluter was employed to mix clean, dry dilution air with a raw exhaust subsample from the tailpipe, at a fixed temperature. Ejector diluters utilize the Bernoulli principal to draw sample flow into the diluter without the use of a mechanical pump. Clean, dry air is fed into the side port of the diluter under pressure (32 psi) and passes through an annular opening which surrounds the ejector nozzle through which the raw exhaust sample enters (**Figure 2-2**). As the dilution air passes the annular opening, ejector geometry widens substantially allowing the air to expand which creates a low pressure zone at the tip of the ejector nozzle. The pressure difference between the tip of the ejector nozzle and the sample inlet induces the raw exhaust sample to flow from the exhaust pipe and into the mixing chamber of the Dekati ejector diluter (**Figure 2-2, inset**). Subsequently, the well-mixed dilute exhaust exits the diluter and is sampled by a variety of particle instruments (EEPS, PM Filters, EAD, UCPC; See **Section 2.4** below). The total dilute exhaust volumetric flow is determined by the sum of dilution air flow and exhaust sample flow entering the diluter. The dilution air flow of this particular system is between 80 and 85 L/min. With a dilution air flow of 80 L/min, if a dilution ratio (DR) of 50 is required, an exhaust sample inlet flow of 1.63 L/min is necessary to give a final total dilute exhaust flow of 81.63 L/min. The total flow of all the instruments sampling this dilute exhaust should not exceed 90-95% of this total flow (or 73.5- 77.5 L/min) to ensure sufficient excess flow exists in the sample setup.

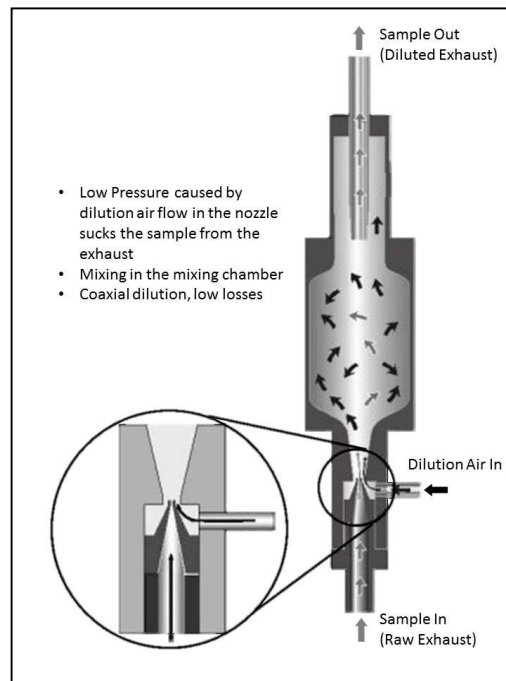


**Figure 2-2. Schematic of Dekati ejector diluter flows to dilute raw exhaust for particle sampling.**

### Dilution Air Supply.

A low-cost compressed air system was developed to provide clean, dry air to the Dekati diluter (**Figure 2-3**). To compress room air and supply sufficient total air flow to the diluter, two oil-less air compressors (**1 and 2 in Figure 2-3**), one with a pump flow rating of 6.4 SCFM (181.2 LPM) at 90 psi and a 22 gallon tank and the other with a pump flow rating of 6.2 SCFM (175.6 LPM) at 90 psi and a 33 gallon tank, both of which have a maximum duty cycle of 50%, were connected in parallel. In order for both compressors to consistently turn on at a specified ‘kick on’ pressure, they were both wired and plumbed to a Condor MDR3 (31GC3FXX) pressure switch (**3 in Figure 2-3**). This switch closes, turning the compressor on, when the pressure in the system drops below 100 psi and opens, turning the compressors off, when the pressure in the system reaches 125 psi. This pressure range is staggered from the 120/150 psi kick on/ kick off pressures of the pressure switches on the individual compressors resulting in full control by the Condor MDR3 pressure switch. The compressors are both run on 120V and have a max amperage rating of 15A. In order to run two compressors from a common pressure switch, the power for both compressors came from one 30-amp, 120V circuit breaker. Because the compressors both drew more than 15A for a split second at start up, if started simultaneously, they would trip the breaker. To get around this, a normally open Schneider Electric contactor (199AX-9) in series with an Artisan delay-on-make relay (438USA) was installed on the power feed between the pressure switch and one of the compressors. These components provide a delay in power delivery to the second compressor allowing the current spike that occurs during start of the first compressor to occur in advance of the current draw from the second compressor start.

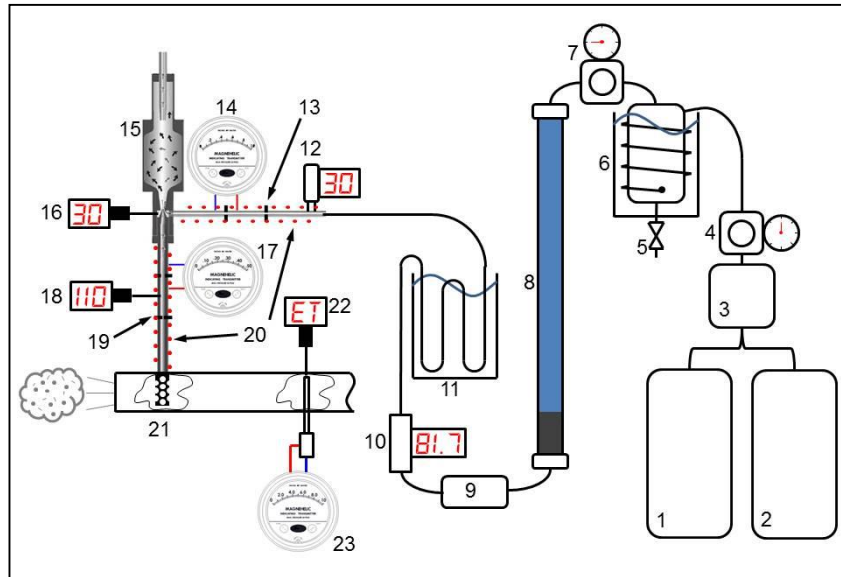


**Figure 2-3. Engine Exhaust Dilution System Configuration:** 1. Compressor One; 2. Compressor Two; 3. Pressure Switch; 4. Coarse Dilution Air Pressure Regulator; 5. Condensation Drain Valve; 6. Condenser/ Expansion Tank in Ice Bath; 7. Precision Air Pressure Regulator; 8. Desiccant Tube (Silica Gel and Activated Carbon); 9. HEPA Filter; 10. OMEGA Mass Air Flow Meter; 11. Ice Bath; 12. Pressure Sensor; 13. Orifice A/ Critical Orifice; 14. Dilution Air Orifice Flow Meter Utilizing Orifice C; 15. Dekati Diluter; 16. Dilution Air Thermocouple; 17. Raw Exhaust Sample Orifice Flow Meter Utilizing Orifice D; 18. Raw Exhaust Sample Thermocouple; 19. Orifice B/ Pinhole Orifice; 20. Heat Cord (represented by red dots); 21. Perforated Sampling Probe; 22. Exhaust Temperature Thermocouple; 23. Exhaust Pipe Pitot Tube Flow Meter

Beyond the electrical demands of the dilution air system, the air quality is maintained to ensure that the dilution air is not introducing contaminants into the diluted exhaust sample prior to measurement. In addition to purifying the air with silica gel (to remove moisture), activated carbon (hydrocarbons) and HEPA filtration (particle removal), the dilution air pressure and temperature at the side port of the Dekati diluter are precisely maintained to ensure a consistent mass flow rate of air into the diluter. Once the air passes through the pressure switch (**3**), the air pressure is regulated to 50 psi with a ‘coarse’ air pressure regulator (**4**). From here the air travels through 3/8” OD metal

tubing coiled around an expansion tank. Both the metal coil and the expansion tank are submerged in an ice bath (6), substantially dropping the air temperature resulting in condensation of the majority of the moisture in the air into the expansion tank which is equipped with a drain valve (5). After the expansion tank, the air passes through an Ingersoll Rand precision air pressure regulator (PR4031-100) (7) which regulated the pressure down to 30psi with an accuracy of 0.1%. Utilizing the 'coarse' air pressure regulator shields the precision air pressure regulator from the large pressure changes in the compressor tanks, which result in finer overall pressure control. After the air passes through the precision pressure regulator, it flows through a 4' long x 2" diameter tube containing silica gel desiccant beads and a small section of activated charcoal to remove any remaining moisture and organic compounds (8). After the desiccant tube, the air flows through a Whatman HEPA-CAP 150 (6702-9500) HEPA filter (9) to remove any particles from the air stream. The air then flows through an OMEGA FMA 1700/1800 mass flow meter (10) which monitors the flow through the dilution air system. The desired temperature of the dilution air at the diluter was 30°C, however, room temperature often exceeded 30°C when the engine was running. Even though the dilution air was cooled as it passed through the condenser/ expansion tank (6), there was sufficient residence time in the dilution system after this point for the dilution air to warm back up to room temperature. To ensure that the dilution air did not go above 30°C, the flow then passed through another coil of 3/8" OD metal tubing submerged in an ice bath (11). After this ice bath, the flow entered the side arm of the Dekati diluter. Because the mass flow rate of the dilution air entering the diluter was critical to the overall Dilution Ratio, multiple parameters were measured/ controlled in this location. First, an OMEGA pressure transducer (PX319-100GI) (12) logged and displayed dilution air pressure. This pressure display was used to set dilution air pressure with the precision air pressure regulator. Then, the volumetric flow rate was metered with a critical orifice (13). Another orifice, in conjunction with a magnehelic gage, (14) was used as an orifice flow meter to measure volumetric flow. Finally, a thermocouple (16) logged dilution air temperature and served as feedback to the temperature controller that maintain a set point dilution air temperature of 30°C by modulating the power going to a BriskHeat heat cord (20) wrapped around the entirety of the diluter side arm which was also insulated with fiberglass insulation tape.

### **Raw Exhaust Sample Probe.**

Because an exhaust sample collected close to the wall of an exhaust pipe has the potential to be different than that collected at the center, a perforated sample probe (21) was fabricated and installed that spans the diameter of the exhaust pipe. This ensured that the sample was representative of the exhaust leaving the tailpipe. The probe was connected to a 3/8" OD, 17-inch long stainless steel transfer line that transported the exhaust sample to the inlet port of the Dekati diluter. A pinhole orifice (19) installed in the transfer line 7.5 inches from the exhaust sample probe controlled the amount of raw exhaust sample entering the Dekati diluter and downstream orifice, in conjunction with a magnehelic gage (17), located 6 inches from the pinhole orifice was used as an orifice flow meter to measure raw exhaust sample flow. A thermocouple (18) measured temperature within the transfer line and provided temperature feedback to a heat cord controller that maintained a raw exhaust sample temperature set point of 110°C by modulating the power going to the Briskheat heat cord (20) wrapped around the entirety of the transfer line. The transfer line was also insulated with fiberglass insulation tape.

### **Dilution System Tuning.**

The Dekati diluter was originally designed to provide a dilution ratio (DR) of ~8. This research, however, demanded a minimum DR of 50. From the factory, the diluter came with a 1.3mm (0.0512") diameter critical orifice at the dilution air inlet and was calibrated while maintaining a dilution air pressure of 2 bar (29.0psi) on this orifice. In order to increase the DR, the original critical orifice was removed and replaced with a new critical orifice (**Orifice A**) drilled with a #50



(1.778mm / 0.0700" dia.) drill bit (**Figure 2-4**). A ‘pinhole’ orifice (**Orifice B**) which was drilled with a #76 (0.508mm / 0.020" dia.) drill bit, was then installed in the raw exhaust sample transfer line to reduce the flow of exhaust sample and increase the DR. The dilution air pressure was set at 2.068Bar (30.0PSI). The combination of these modifications resulted in a new DR of ~80, measured as the ratio of total diluted exhaust outflow ( $Q_{total,out}$ , L/min) to raw exhaust sample flow entering the Dekati diluter ( $Q_{in}$ , **Equation 2-1**).

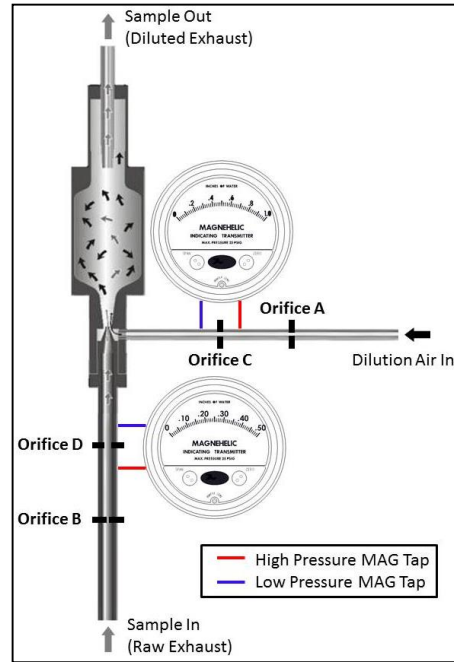


**Figure 2-4. Locations of orifices (A, B) and orifice meters (C, D) on dilution system.**

$$DR = \frac{Q_{total,out}}{Q_{in}} = \frac{Q_{DilutionAir} + Q_{Sample}}{Q_{Sample}} \quad (2-1)$$

Rather than assuming a constant DR, both ‘Exhaust Sample Inflow’ and ‘Dilution Air Inflow’ were logged at a rate of 1 Hz using calibrated transmitting magnehelics (MAGs) to measure the pressure difference across orifice meters in both the dilution air line and the raw exhaust transfer line. Specific magnehelic model numbers are found in **Appendix A**. The largest pressure difference that can be measured by a MAG sold by Dwyer is 50 inches of water (inH<sub>2</sub>O) (~1.81 psi). Considering that the pressure difference across **Orifice A** is essentially 30 psi, a MAG could not be used in conjunction with this orifice to measure dilution air flow; instead, an additional orifice was installed downstream of **Orifice A**, on the low pressure side, for dilution air flow measurement. This orifice, **Orifice C**, was drilled with a letter H (6.756mm / 0.2660" dia.) drill bit, and a 0-1.0 inH<sub>2</sub>O transmitting MAG (Dwyer Inc., Model 605-1) measured the differential pressure across it. In the raw exhaust sample transfer line, **Orifice B** could not be used to reliably measure flow due to the pressure pulses from the engine’s exhaust. To measure transfer line flow, **Orifice D**, drilled with a #43 (2.261mm / 0.0890" dia.) drill bit, was installed on the low pressure side/ downstream of **Orifice B** and a 0-0.5 inH<sub>2</sub>O transmitting MAG (Dwyer Inc., Model 605-0) measured differential pressure across this orifice. With the transfer line orifices in this orientation, **Orifice B** isolated **Orifice D** from the engine exhaust pressure pulses, resulting in a relatively stable measurement of differential pressure (flowrate is ~ 1.04 L/min) in this location.



### Flow Measurement and Temperature Control.

Orifice flow meters measure volumetric flow rate, not mass flow rate. Because the density of a gas is sensitive to temperature, mass flow will change as a function of temperature while volumetric flow remains constant. Temperature variation also affects particle evolution – as the exhaust gases cool, gas phase constituents can nucleate as new particles or condense onto existing larger particles. To ensure that flow rates and particle nucleation/condensation rates were consistent during each run and from run to run, both the raw exhaust transfer line and the dilution air line were temperature controlled. The set point temperatures for the gases in the raw exhaust transfer line and in the dilution air line were 110 °C and 30 °C, respectively. To tightly control and monitor these gas temperatures, two 1/16” ungrounded, dual element J-type thermocouples (**16 and 18 in Figure 2-3** above) fed back gas temperature data to custom-built heat cord controllers (Fuji Electronics Controller - PXR3-TEY1-4V0A1 and Carlo Gavazzi solid state relay - RM1E23AA25) which, in turn, modulated the temperature of the BriskHeat HWC1060 heat cords wrapped around each line. The average gas temperatures measured during the most recent transient run (1\_06AUG2013\_B000) were 107.25°C (StDev = 0.375) and 25.78°C (StDev = 0.340) for the transfer line and the dilution air line, respectively. These measurements are slightly offset from the set point temperatures due to thermocouple calibration differences between the heat cord controllers and the Labview system.

### 2.2.3 Data Acquisition System

The experimental apparatus was instrumented to acquire real-time system operation and emissions data. Up to eight instruments were used to measure different parameters simultaneously. Two of the instruments, Armfield and Scantool, shared a computer while all of the other instruments utilized a dedicated computer. The computers used for data acquisition from various instruments are listed in **Table 2-2**.

**Computer Clock Synchronization.** There are four possible sources of time misalignment between data collected from different instruments/computers. The first is clock synchronization error – a simple time shift from one data set to another – for example, the clock on one PC could be 30 seconds behind that of another PC. The second is a misalignment due to sensor response – the time necessary for a sensor to ‘see’ a change in the parameter it is measuring. The third is a real, physical lag – for example, the time it takes combustion gases to travel from the combustion chamber to the sampling location in the exhaust system. The fourth source of time misalignment is that of sampling residence time – the time it takes for a sample to flow from the sample port to the instrument where it is measured. To minimize the amount of time alignment necessary after data collection, procedures were developed to improve instrument clock synchronization.

Initially, in order to minimize temporal misalignment, a large clock was displayed on a computer screen that could be seen from all of the other computers used for data acquisition. The clocks on the other computers were then manually synchronized to that clock before each data collection event. In September 2012, all of the computers were linked through a local area network (LAN) and one of the computers was designated as a time server. This allowed automatic synchronization of all LAN-connected computers prior to each collection event using the ‘Date and Time’ application embedded in the Windows operating system. Even with this synchronization, the clocks on some of the computers would desynchronize in less than 10 minutes. To address this issue, Automachron simple network time protocol (SNTP) software was installed on the computers in May 2013. This software automatically synchronized the clock of the computer to the time server every 16 seconds, minimizing the chances of the computers becoming asynchronous over the 2 plus hour experiment duration.

**Table 2-2 Computers used for each sampling instrument**

	Instrument	Computer	Processor (GHz)	Core	RAM (GB)	OS
System Operation	Armfield/ Scantool	DELL Optiplex 755	2.66	Dual	2.00	Windows XP Pro
	Labview	DELL Latitude D630	2.20	Dual	2.00	Windows XP Pro
Particle Emissions	EEPS	DELL Optiplex GX620	3.60	Single	3.50	Windows XP Pro
	UCPC	DELL Latitude C400	1.20	Single	0.25	Windows XP Pro
	EAD	DELL Latitude D505	1.60	Single	0.50	Windows XP Pro
Gas Phase Emissions	FTIR	DELL Latitude D630	2.40	Dual	1.00	Windows XP Pro
	5-Gas	DELL Latitude E6400	2.40	Dual	3.50	Windows XP Pro

### Armfield Engine and Dynamometer Parameters.

The CM-12 came from Armfield with a rudimentary data acquisition system read through the Armfield software using sensors that Armfield had installed. The parameters that were acquired through the Armfield software are listed in **Table 2-3**. Initially, the Armfield software was set to log data at a frequency of 1Hz but the logging frequency was increased to 2Hz in April of 2013 while developing a transient drive cycle.

**Armfield Sensor Calibration.** The majority of the parameters logged through the Armfield software were assumed to be factory calibrated. The only adjustment made was in February of 2012 when the 'zero' and 'span' potentiometers associated with the Armfield throttle position were adjusted so that the throttle position reported Armfield and Scantool were the same.

**Table 2-3 Armfield Sensors on CM-12 Test Cell**

Sensor	Type	Signal Conditioning	Sensor Manufacturer
Throttle Position (%)	Measured from control portion of software	N/A	N/A
Brake Setting (%)	Measured from control portion of software	N/A	N/A
Heat Exchanger Water Flow (LPM)	Paddle wheel flowmeter	Buffer Amplifier/attenuator	GEMS RFA 3/4
Manifold Air Pressure (kPa)	Differential Pressure Sensor across orifice	Amplifier	Honeywell, 26PC
Manifold Air Temp (°C)	'K' type thermocouple	Compensated Amplifier	Armfield
Heat Exchanger Water Inlet Temp (°C)	'K' type thermocouple	Compensated Amplifier	Armfield
Heat Exchanger Water Outlet Temp (°C)	'K' type thermocouple	Compensated Amplifier	Armfield
Exhaust Manifold Temp (°C)	'K' type thermocouple	Compensated Amplifier	Armfield
Engine Speed (RPM)	Magnetic pick-up	Firmware counter	RS
Torque (Nm)	Load Cell	Differential Amplifier	Strain Measurement Devices, S200
Cylinder Pressure	piezo	Proprietary Charge amplifier	Kistler

### Scantool Engine Parameters

Engine operating parameters were also acquired from the On Board Diagnostics (OBD-II) system embedded in the Volkswagen engine control unit (ECU). The OBD-II system was accessed with Rosstech VCDS Scantool software through which specific engine operating parameters were selected for acquisition. The Scantool software does not allow the user to specify an acquisition frequency, therefore, these parameters were acquired at a variable 'as fast as possible' rate. Initially, multiple engine parameters from different measuring blocks were accessed through

‘Advanced Measuring Blocks’ in the VCDS software. Selecting the parameters logged in this manner resulted in a data collection frequency of ~0.5Hz. After further investigation, it was found that all desired parameters could be read through measuring block ‘000’. Switching from data collection through multiple measuring blocks to data collection through one measuring block increased the sampling rate to ~3Hz. Measuring block ‘000’, however, did not output measurement physical units. Instead, because the ECU is an 8-bit system, this measuring block reports raw byte values in the form of decimal numbers between 0 and 255 (**Table A-3 in Appendix A**).

**Scantool Sensor Calibration.** In order to assign physical units to each measuring block ‘000’ parameter, a series of engine tests were performed while logging measuring block ‘000’ and other measuring blocks that output the desired parameters with physical units. These data were then used to calibrate measuring block ‘000’ data to physical units. The parameters read by the Scantool and their calibration equations can be found in **TABLE 2.4**.

**Table 2-4. Rosstech Scantool Sensors and Calibration Equations\***

Position	Parameters	Calibration Equation
000-1	Engine Speed (RPM)	$=21 * (\text{byte})$
000-2	Start of Injection (° BTDC)	$=10.08 * (\text{byte}) - 3.12$
000-3	Throttle Position (%)	$= (\text{byte}) / 2.55$
000-4	Injection Quantity (mg/stroke)	$=10.2 * (\text{byte})$
000-5	Not Used (No Sensor Data)	N/A
000-6	Atmospheric Pressure (mbar)	$=24.914 * (\text{byte}) + 7.3506$
000-7	Engine Coolant Temp (°C)	$= (-0.68878) * (\text{byte}) + 135.983$
000-8	Intake Temp (°C)	$= (-0.68182) * (\text{byte}) + 135.191$
000-9	Fuel Temp (°C)	$=10.5625 * (\text{byte}) - 30.4875$
000-10	Not Used (No Sensor Data)	N/A

\* byte indicates the 0-255 value logged from the ECU measuring block ‘000’.

**Labview Data Acquisition for Temperature, Flow and Pressure Sensors**

A Labview (v. 8.6; National Instruments) data acquisition system specifically built for this research acquired data pertaining to both engine operation and exhaust dilution conditions at a rate of 1Hz. The data collection system was comprised of five components (**Table 2-5**). The Labview data acquisition system was configured to log sixteen single-ended signals through a single PCMCIA data acquisition card. In total, 14 of these channels were used (**Appendix A, Table A-##**). All of the sensors were connected to the connector enclosure with BNC cables which are intrinsically electrically shielded. The enclosure itself electrically shielded the connector block and the cable that connected the connector block to the PCMCIA card was electrically shielded as well. This shielding minimized the noise in the signals and helped ensure that the data collected was of the highest quality. In addition to the data logged through the PCMCIA card, the labview virtual instrument (vi) also logged fuel tank weight through the laptop’s RS-232 port which was connected to the fuel tank scale.

**Table 2-5. Data Acquisition Components**

Number	Component Description	Model Number
1	Dell Laptop (2.20GHz Processor, 2GB RAM)	Latitude D630
2	PCMCIA Data Acquisition Card	NI DAQCard 6024A
3	Shielded Cable (DAQ card to Connector Block)	NI SH68-C68-S
4	Connector Accessory Enclosure	CA-1000
5	Unshielded 68-pin I/O Connector Block	NI CB-68LPR

**Labview Sensor Calibration.** Factory calibration equations were used for all of the sensors logged through Labview except for the three differential pressure sensors that were connected to the Dwyer MAGs and the VW/BOSCH mass flow meter (MAF). **Table 2.6** lists the 15 parameters logged at 1 Hz by Labview and their calibration equations. Calibration procedures are described below.

**Table 2-6. Labview Parameters and Calibration Equations for Sensors**

Parameter	Sensor	Range	Model	Calibration Equation
1 Fuel Weight (lbs)	Adam Equipment Co. Scale	70lb/32kg x 0.002lb/0.001kg	GBK 70a	RS-232 Direct Read
2 Dilution Air Flow (SLPM)	Dwyer Magnehelic	0-1 inH <sub>2</sub> O	605-1	25.523*(V)-7.0439
3 Aerosol Inlet Flow (SLPM)	Dwyer Magnehelic	0-0.5 inH <sub>2</sub> O	605-0	0.3032*(V)+0.2982
4 Pitot Ex Flow (SLPM)	Dwyer Magnehelic	0-10 inH <sub>2</sub> O	605-10	sqrt(6888000*(V)-0.995))
5 Ambient Temp (°C)	OMEGA RH/ TEMP Transmitter	Temp: -15 to 60 °C	EWS-RH	18.863*(V)-34.457
6 Ambient RH (%)	OMEGA RH/ TEMP Transmitter	RH: 5 to 95%	EWS-RH	25*(V)-25
7 Dil Air P (PSIG)	OMEGA Pressure Transducer	0 - 100 PSIG	PX319-100GI	25.0193*(V)-25.167
8 Dil Air Temp (°C)	OMEGA Dual Element J-Type Thermocouple	0-750°C	SICSS-062U-3-DUAL	94.753*(V)+1.8464 (AD594CDZ Calibration)
9 Fuel Temp (°C)	Grounded J-Type Thermocouple (1/8" Dia)	0-750°C	N/A	94.753*(V)+1.8464 (AD594CDZ Calibration)
10 Downstream Ex Temp (°C)	Exposed J-Type Thermocouple (1/8" Dia)	0-750°C	N/A	94.753*(V)+1.8464 (AD594CDZ Calibration)
11 Diluted Sample Temp (°C)	Ungrounded J-Type Thermocouple (1/8" Dia)	0-750°C	N/A	94.753*(V)+1.8464 (AD594CDZ Calibration)
12 OMEGA Dil Air Flow (SLPM)	OMEGA Mass Flow Meter	2-100 LPM	FMA 1742	20*(V)
13 MAF (SLPM)	VW/ BOSCH Mass Flow Meter	Calibrated to 4000LPM	VW 037 906 461 C	53.135*(V)^3 + 104.38*(V)^2 + 56.724*(V) - 13.702
14 Transfer line Temp (°C)	OMEGA Dual Element J-Type Thermocouple	0-750°C	SICSS-062U-3-DUAL	94.753*(V)+1.8464 (AD594CDZ Calibration)
15 Flow Totalizer Pressure (PSIA)	Dwyer Pressure Transducer	0-30PSIA/ (-14.7)-15.3PSIG	626-01-GH-P1-E1-S1	7.5*(V)-22.2

\*\*\*Note: All J-Type thermocouples amplified with Analog Devices AD594CDZ Monolithic Thermocouple Amplifier\*\*\*

**Magnehelics.** Calibration of the dilution air and exhaust sample transfer line MAGs was performed with the heat cords at the 30 and 100°C set point temperatures. With the temperatures held constant, the magnehelic calibrations are effectively mass flow rate calibrations. To perform calibration, the dilution air pressure was adjusted with the precision regulator to affect both dilution air flow rate and transfer line flow rate. Calibration was performed with all components in the dilution system connected, with one exception - to calibrate the aerosol inlet transfer line flow, the dilution system was disconnected from the tailpipe probe so a bubble flow meter could be used to measure transfer line flow. The air source was the dilution air system as described above. Dilution air pressure was adjusted in steps around the 30 psi pressure set point used during engine tests to generate different flow rates for both the transfer line and dilution air magnehelics. The calibration dilution air pressures were (in psi) 15, 20, 25, 27, 28, 29, 30, 31, 32, 33 and calibration proceeded from high pressure to low pressure. Altering this pressure changed the amount of dilution air forced through Orifice A and into the Dekati diluter which, in turn, altered the inlet flow in the raw exhaust transfer line. The dilution air flow (~82 LPM) was measured with an OMEGA mass flow meter (FMA 1700/1800) with a range of 0-100 LPM. A 200 mL bubble flow meter was used to calibrate the raw exhaust transfer line flow (~1 LPM) because this type of flow meter introduces minimal pressure drop to the system, resulting in little to no effect on the flow measurement. During calibration, the dilution air pressure was adjusted to various settings around the standard 30psi set point while MAG data, OMEGA flow meter, dilution air pressure, and temperature data were logged continuously and 10 manual replicate measurements of the time necessary for the soap film in the bubble flow meter to travel through the 200mL volume were measured at each setting. At least 7.45 minutes were spent at each pressure setting to obtain the manual bubble flow meter measurements while the 1Hz data used to determine average MAG readings for each pressure setting was collected simultaneously. The calibration curve relationships between measured flow rate and the transmitting magnehelic voltage readings are shown in **Figure 2-5** and best-fit curves

are found in **Table 2-aaa**. The dilution ratios determined for each engine run are shown in **Table 2-bbb** and ranged from 50 to 92.

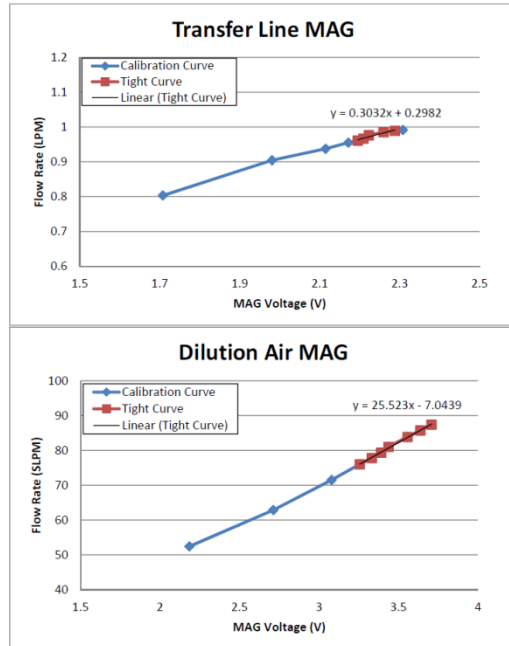


**Figure 2-5.** Calibration curves for exhaust sample transfer line and dilution air magnehelics. MAGs were calibrated while the dilution system was at the heat cord temperature setpoints (100°C and 30°C, respectively). The transfer line flow data (top plot) were collected with the bubble flow meter and dilution air flow rate (bottom plot) was measured by an Omega 0-100Lpm mass air flow meter.

**Pitot Tube and Mass Air Flow Sensor.** Calibration of both the pitot tube exhaust flow meter and the MAF sensor on the air intake of the engine were performed using an Ametek Nautilair 12.3” Variable Speed Blower and a Sierra Instrument mass flow meter (model number: 620S-L04-M1-EN2-V1-DD-0) with a calibrated 0 to 4000 sLPM range. To calibrate these sensors, they were attached to the blower with the Sierra flow meter inline (upstream for the pitot tube (**Figure 2-6a**), downstream for the MAF Sensor (**Figure 2-6b**)).

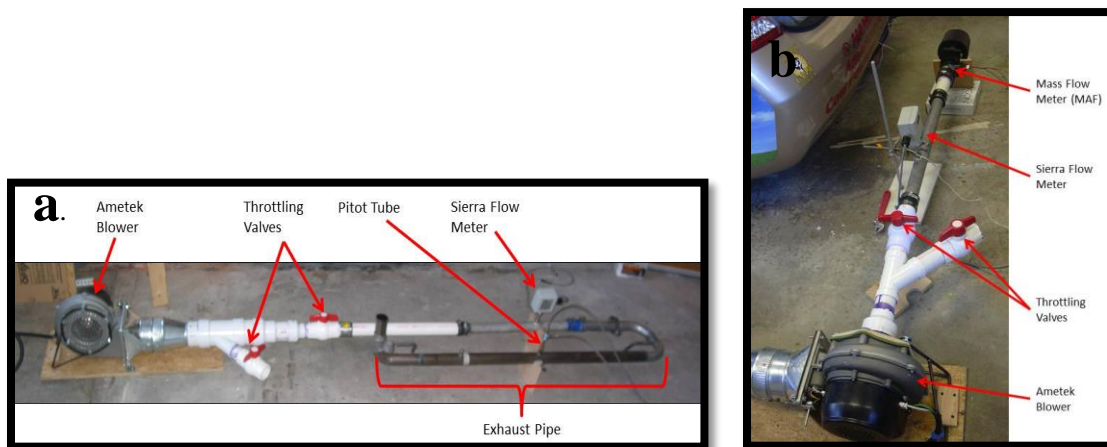


**Figure 2-6.** Calibration setup for push-through flow of exhaust Pitot tube (a) and pull-through flow for MAF sensor (b).

Flow was pushed past the pitot tube and pulled through the MAF sensor to simulate their actual use. Once connected, data for the Sierra flow meter, the MAF sensor and the pitot tube transmitting MAG (Dwyer, 605-10) were logged at 1Hz with Labview software. The blower was set to various flow rates between 0 and 4000 LPM (maximum calculated pumping rate of the 1.9L engine with a maximum RPM of 4000 is ~3800LPM). For each flow setting, flow was allowed to stabilize and then approximately one minute of data were collected for calibration. The factory calibration equation was applied to the logged Sierra flow meter voltage. The resulting Sierra flow rates and sensor voltages were then averaged for each flow position and used to compute the calibration equations for the sensor. The raw voltage data collected for the MAF sensor and its calibration curve can be seen in **Figure 2-7** and **Figure 2-8** shows the calibration data for the pitot tube exhaust flow sensor.

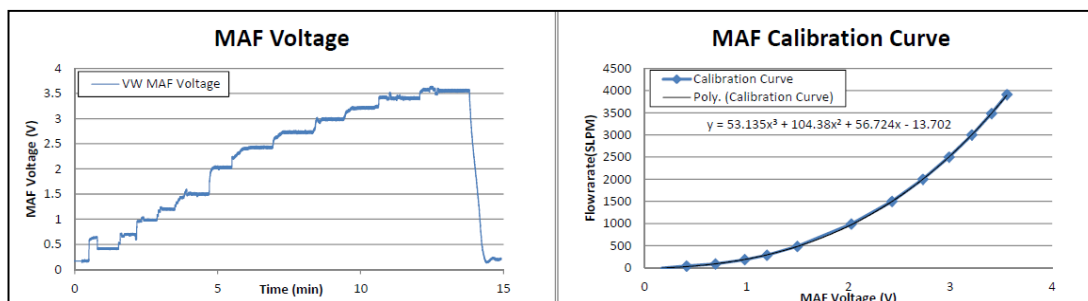


**Figure 2-7. MAF Sensor Calibration: (left) Raw voltage; (right) calibration curve based on Sierra flow meter flowrate data**

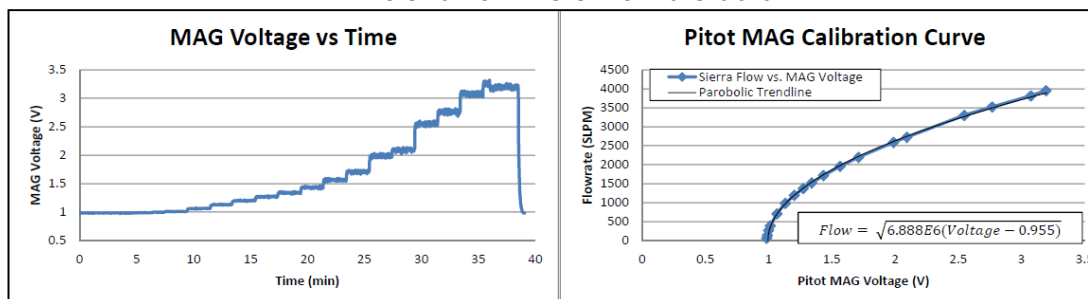


**Figure 2-8. Pitot MAG Calibration: (left) Raw voltage; (right) calibration curve based on Sierra flow meter flowrate data**

## 2.2.4 Tailpipe Emissions Test Sequence

Emissions tests for a certain biodiesel fuel blend involved the following sequence of steps: (a) if using a different fuel than what is currently in the fuel system, purge engine fuel system of previous fuel (1 day prior to test); (b) warm-up all instrumentation and data acquisition systems (minimum of 1 hr); (c) collect instrument blank (IB) data on all real-time instruments; (d) collect tunnel blank (TB) data on all real-time instruments; (e) Start CM-12 diesel engine; (f) run engine Warm-Up cycle until the engine coolant thermostat opens [ $92 \pm 1^\circ\text{C}$ ]; (g) conduct emissions test run with gas, particle number and PM filter sampling trains; (h) cool down engine (idle for 3-5 minutes); (i) CM-12 engine off; (j) collect post-run TB; (k) collect post-run IB with real-time instruments. Copies of run logsheets and SOPs for all test procedures are found in **Appendix C**.

Periodically, “Engine Blank” runs were performed where the entire test sequence was replicated except that the CM-12 engine was not started. During all tests, log sheets were filled out by TAQ Lab personnel to ensure test-to-test reproducibility and keep track of ambient sampling conditions, deviations from standard operating procedures (SOPs) and electronic data filenames.

Every CM-12 engine emissions test was given a unique TestID indicating the test replicate number for that date – sample date – fuel blend. For example, a B20 blend run as the first test on February 9, 2012 would have a TestID of **1 – 09FEB2012 – B020**. All electronic data were immediately copied to the HolmenGroup server after every engine test run and all data files collected during a specific TestID were stored in a separate folder.

### Fuel Purging

The CM-12 was equipped with a fuel purging system to minimize the chance of fuel crossover between tests with different fuel types. To further minimize the possibility of fuel contamination, each fuel blend had a designated 6-gallon plastic fuel tank. These fuel tanks were connected to the fuel system by self-sealing quick connect fittings. Because this engine has both a fuel feed line and a fuel return line, two valves were used to switch the fuel system from biodiesel to petrodiesel. As shown in **Figure 2-9**, the valve on the feed line switched between the biodiesel fuel tank and the petrodiesel fuel tank while the valve for the return line switched between the biodiesel fuel tank, a waste fuel storage tank, and the petrodiesel fuel tank. The procedure to purge the fuel system from petrodiesel to biodiesel is as follows:

1. Start engine and allow idle to stabilize (both valves initially on *petrodiesel*).
2. Simultaneously, switch the feed line valve to *biodiesel* and the return line valve to *waste*.
3. Allow the engine to idle for 5 minutes to completely clear the fuel system (fuel lines, fuel filter, and fuel pump) of petrodiesel.
4. Switch the return line valve to *biodiesel*.

One might think that when purging from one biodiesel blend to another, the fuel tank for the new biodiesel blend could just replace the petrodiesel fuel tank in **Figure 2-9**, however, because the engine is equipped with just one dedicated petrodiesel fuel filter, this is not the case. To avoid contaminating the petrodiesel fuel filter with any biodiesel, the procedure used to purge the fuel system from one biodiesel blend to another was as follows:

1. With the engine off, remove the feed and return fuel lines from the original biodiesel fuel tank.
2. Replace the original biodiesel fuel tank with the new biodiesel fuel tank without connecting the fuel lines.
3. Connect the return line that typically connects to the biodiesel tank to the waste tank.
4. Start the engine – as soon as the engine is running, connect the biodiesel feed line to the new biodiesel tank. This ensures that there is suction on the line and that any remnant of the original biodiesel in the line will not drip into the new tank.
5. Run the engine for 5 minutes to allow the system to purge to the new fuel.
6. Shut the engine off.
7. Disconnect the biodiesel return line from the waste tank and connect it to the new biodiesel tank.

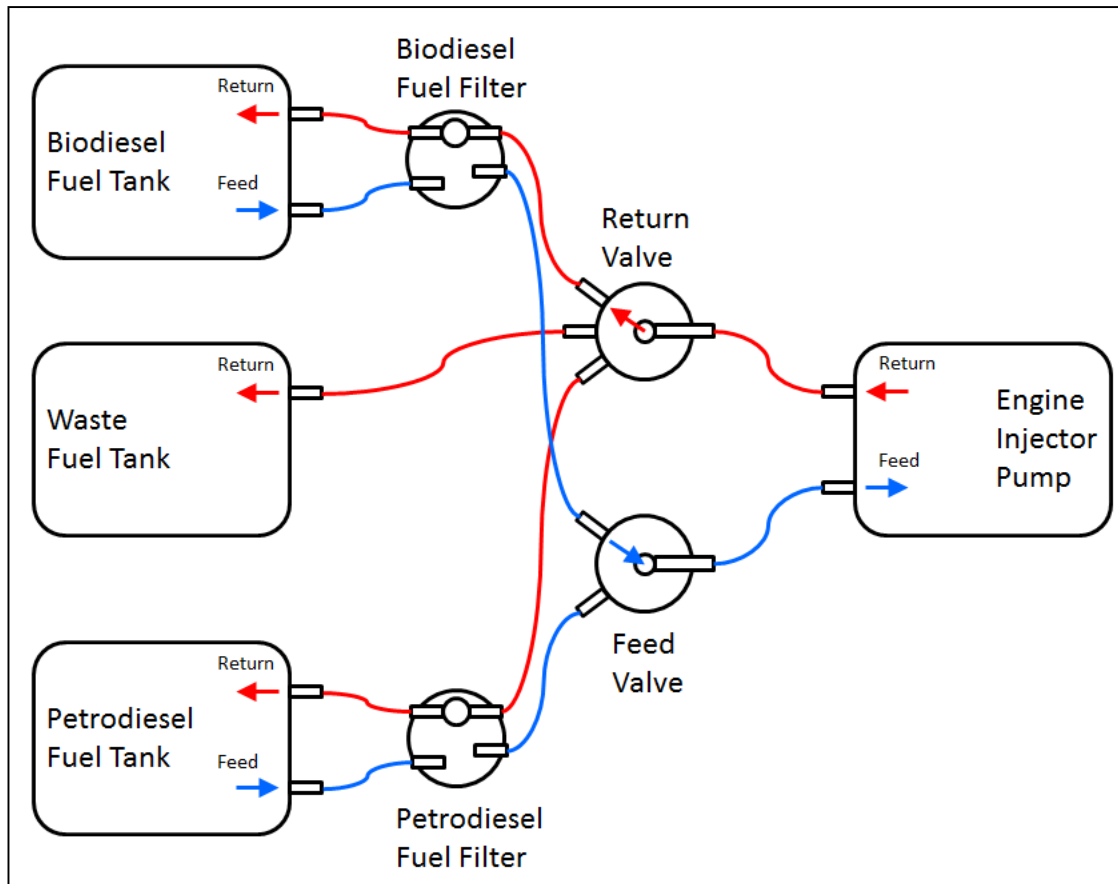


**Figure 2-9. Fuel Switching System with the valves in the 'Biodiesel' Position**

The 5-minute purge duration used in both procedures was determined by collecting fuel samples from the return line every minute after the feed line was switched to the new fuel. These samples were then analyzed for FAME content with the IROX-D; the fuel sample collected at 5 minutes was consistently found to have the same FAME content as the new fuel.

### Drive Cycles.

Multiple drive cycles were developed for collecting emissions data. The drive cycle primarily used from July 2010 to October 2011 was the “semi-transient” cycle depicted in **Figure 2-10**. From October 2011 to December 2012, a series of steady-state operating cycles were run at 40% load (2000RPM 40% Throttle) and 80% load (2200RPM, 67% Throttle). Development of a real-world transient drive cycle (**Figure 2-10**) began in December 2012 and was finalized in May 2013. A ‘burn out’ cycle was also developed to burn FAMEs residue out of the exhaust system after B100 runs. This cycle was a steady-state, extremely high load, hot exhaust run at 85% throttle and 3300 RPM. It is run for about 10 minutes; longer operation at these conditions result in excessive dynamometer temperatures indicated by incandescence of the dynamometer rotors.



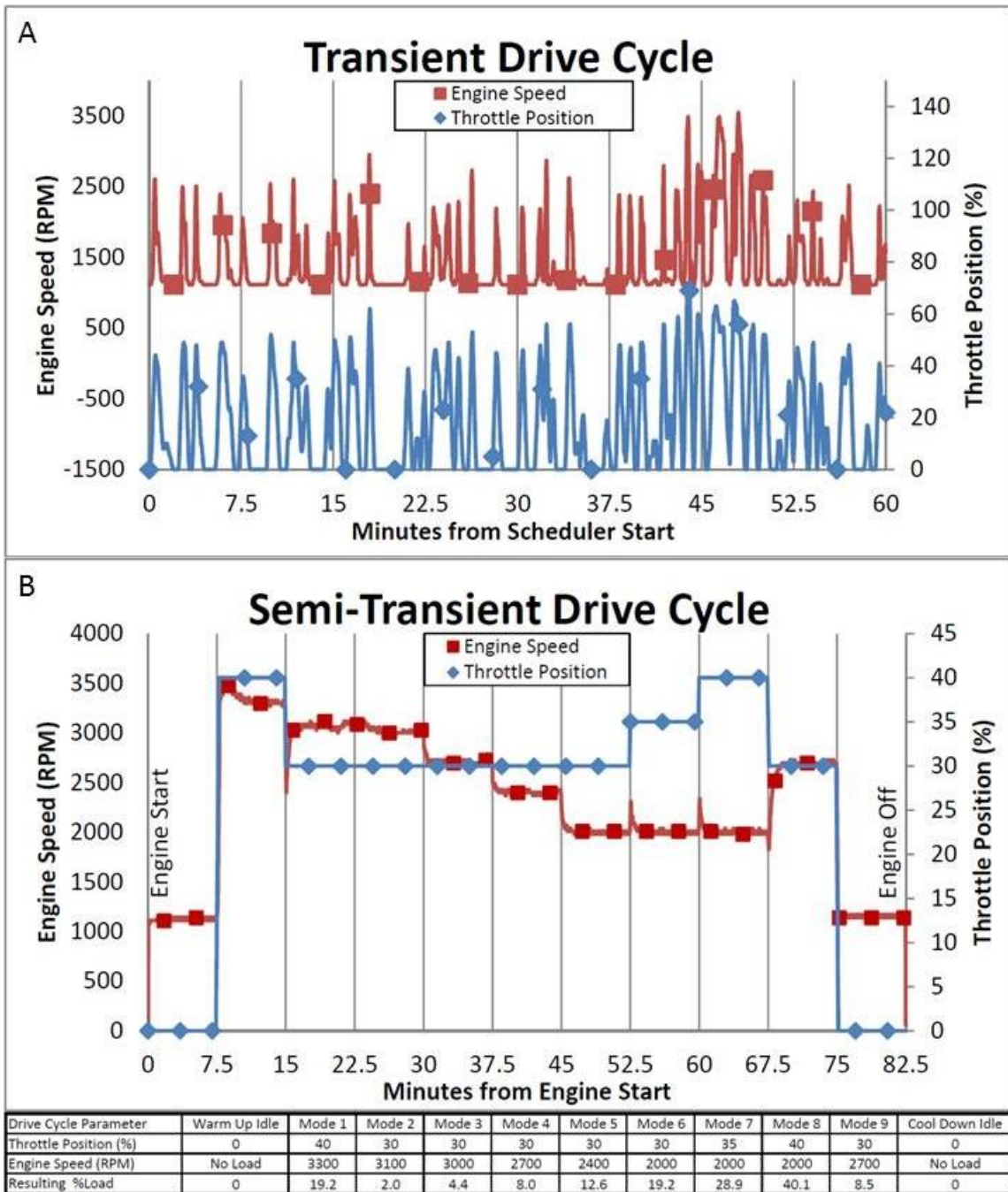


Figure 2-10. Second-by-second drive cycles. Measured RPM (squares) on left scale; throttle position (diamonds) on right scale A. Transient drive cycle. MAX Throttle position 72%; MAX measured RPM ~3500. B. Semi-transient drive cycle. MAX Throttle position 40%; MAX measured RPM ~3500.

### Oil and Fuel Filter Changes.

Engine oil was changed between different sets of tests to minimize lubrication oil contamination from fuel type to fuel type. Since receiving the CM-12, Castrol ‘EDGE with STP’ SAE 5W-40 engine oil has exclusively been used. This is a full synthetic motor oil that meets Volkswagen oil specifications 501 01, 502 00, and 505 00. Small quantities have been purchased from the local

auto parts store and, when controlling for production lot, large quantities have been purchased from a regional distributor, Windward Petroleum, Rutland, VT. Oil filters have also typically been purchased from the local auto parts store, however, when controlling for production lot, multiple filters were purchased from idparts.com (Pembroke, MA) along with fuel filters.

## 2.3 (Bio)diesel Fuel Supply and Monitoring

### 2.3.1 Fuel Composition And Biodiesel Fuel Blending

Neat ultra-low sulfur on-road petro-diesel, used as a baseline fuel, and neat soybean oil based biodiesel were obtained for this testing and blended when necessary (petro-diesel - Trono Fuels, Burlington, VT; biodiesel - Denis K. Burke, Inc., Chelsea, MA). The results for four different biodiesel/petrodiesel blends, denoted as BXXX, where XXX is the percentage (by volume) of biodiesel in the blend are reported here. These blends were B000 (petro-diesel), B020, B050, and B100 for the steady-state tests conducted at 40% load (SS40) and B0 and B100 for the steady-state 80% load (SS80) tests. All biodiesel blends were prepared as small volumes using a splash blending procedure (See SOP in **Appendix B**). Future emissions testing will utilize biodiesel fuels made from feedstocks of both waste vegetable oil (WVO) and soybean oil that was processed specifically for the UVM TAQlab at the University of Connecticut's Biofuel Consortium.

An IROX-Diesel mid-infrared instrument was used to characterize the fuel composition and physical properties. The IROX-Diesel instrument uses Fourier transform infrared (FTIR) spectroscopy to determine characteristics of fuel. The instrument determines the mid-range infrared absorption spectrum over the  $650\text{cm}^{-1}$  to  $3100\text{cm}^{-1}$  wavenumber analysis range. The IROX-D sample data are compared to the instrument's database on well-characterized petroleum diesel and biodiesel blends to interpolate the fuel sample blend volume (FAME content), density, and distillation temperatures (T90 and T95) based on the FTIR spectrum. The instrument is capable of measuring biodiesel content up 40% by volume. Above this content, samples must be diluted to within the measureable range (0-40%) by dilution with n-Hexane. Hexanes were used as the blanks for all IROX-D measurements. Fuel samples were collected from the fuel tank before and after emissions testing and stored in clean, amber glass vials at  $-4^{\circ}\text{C}$  until IROX-D analysis.

## 2.4 Gas and Particle Emissions Measurement

Multiple samples were collected from the diluted flow, one of which had to be forced to instrumentation in an adjacent laboratory. To force the flow necessary for this sample, the port on the Dekati diluter typically used to exhaust the excess sample flow was plugged and a 'T' fitting followed by a ball valve were connected to the outlet of the diluter. The ball valve was then used as a throttling valve to pressurize the diluted sample below it just enough to push flow through the 'T' fitting, denoted as port 'DL-A', and into the other room. In addition to pushing sample flow into the other room, the pressure induced by the valve also slightly decreased the transfer line flow, increasing the DR. The remainder of the flow went through the ball valve and into an 8-port stainless steel manifold (SMARTFLOW, 8SS-8-3-A) which enable additional sampling in the same room as the engine (ports labeled DL-B through DL-I). **Table 2-7** summarizes the final arrangement of emissions sampling instruments on each manifold port.

**Table 2-7. Diluted Samples and Flows by Port Identifier. Minimum dilution system flow is 80 LPM resulting in a minimum of 5 LPM excess flow.**

Port	Use	Max Flow (LPM)
DL-A	Pushed flow to alternate room - UCPC (1.5LPM), EAD (2.5LPM)	15
DL-B	Fiber Film 47mm Filter	20
DL-C	Denuded Quartz Fiber Film 47mm Filter	15
DL-D	Quartz Fiber Film 47mm Filter	15
DL-E	-	-
DL-F	Engine Exhaust Particle Sizer (EEPS)	10
DL-G	-	-
DL-H	-	-
DL-I	Diluted Sample Thermocouple	-
Total Sample Flow Required =		75

## 2.4.1 Particle Mass & Number Measurement

### Filters

Particle mass measurements were made using stainless steel filter holders containing pre-conditioned and pre-weighed 47mm diameter Teflo or Fiberfilm filters (Pall Gelman see **Table 2-8**). In various engine emissions tests, PM filters were located either on a separate raw exhaust sample line or at one of the dilution system manifold ports. PM was sampled at a flowrate of 20 L/min. In addition, quartz fiber filters (QFFs, Tissuquartz, Pall 2500QAO-UP) were collected from the manifold to enable chemical analysis as discussed in a separate report (**TRC 14-009**).

**Table 2-8. PM Filter Specifications used for PM mass and chemical composition**

TAQLab Name	Material	Pallflex Name	Manufacturer	Product Number	Model Number	Filter Diameter (mm)	Pore Size (µm)	Lot Numbers	Storage Condition	Pre-sampling Conditioning	Post-sampling Conditioning
<i>QFF</i>	Quartz Fiber Filters <i>Binder free pure quartz</i>	Tissuquartz	Pall	7194	2500QAO-UP	47		57249	Desiccant Chamber	1) Combusted in muffle furnace >8hrs at 450°C 2) 24hrs in Coy Chamber	24hrs in Coy Chamber
<i>FF</i>	Quartz Fiber with Teflon membrane <i>Pure borosilicate glass fibers with fluorocarbon (tetrafluoroethylene, TFE) coating</i>	Fiberfilm	Pall	7212	T60A20	47		18713C	Coy Chamber	24hrs in Coy Chamber	24hrs in Coy Chamber
<i>Teflo</i>	Teflon (PTFE) membrane with PMP <i>(polymethylpentene) support ring</i>	Teflo	Pall	R2PJ047		47	2	T02298	Coy Chamber	24hrs in Coy Chamber	24hrs in Coy Chamber

### EEPS

A TSI, Inc. Model 3090 Engine Exhaust Particle Sizer (EEPS) was used to measure the particle number (PN) concentration (#/cc) in the diluted exhaust simultaneously for 32 different particle diameter channels from 5.6nm to 560nm. The EEPS data was logged at 10Hz using proprietary EEPS software (*TSI Engine Exhaust Particle Sizer Software, Release Version 3.1.0.0*).

Diluted engine-out particle number emissions were measured with a TSI 3090 Engine Exhaust Particle Sizer (EEPS) (32 channels, 5.6 - 560nm) at a frequency of 1Hz. The bio-diesel blends used were soy-based B0, B20, B50, and B100. The engine was operated at 45% throttle and loaded to maintain 2000 RPM for all tests (approximately 40% load for this RPM). During the steady state operation the average calculated dilution ratio was 55 with a standard deviation of 2.4.

### UCPC

To verify the EEPS data, a TSI Model 3025A Ultrafine Condensation Particle Counter (UCPC) also counted total particle number concentration with a particle diameter detection range of 3–3000 nm. Because the total PN concentration from the entire particle distribution routinely surpassed

the maximum detection limit of the UCPC, a TSI Model 3080 Electrostatic Classifier was used to select a specific particle size range with a midpoint of 10.75nm for the UCPC to measure. The total concentration measured by the UCPC is then compared to the data collected for the corresponding EEPS bin.

### **EAD**

A TSI Model 3070A Electrical Aerosol Detector (EAD) was used to measure aerosol diameter concentration (mm/cc) in the diluted exhaust. The EAD measures a particle diameter range of 10-1000nm at 3.75Hz resolution with a one second averaging interval.

## **2.4.2 Exhaust Gas Measurement**

### **FTIR**

Raw exhaust sampled from the tailpipe probe was transported via heated line (191°C) into the sampling cell of the MKS MultiGas 2030 high-speed FTIR at a flowrate between 12 and 16LPM and sampled at a rate of 1 Hz. The FTIR simultaneously quantified the concentrations of 31 gas-phase pollutants based on manufacturer calibration curves using select absorbance regions. Before and after each sampling run, an instrument blank was acquired while the sample cell was purged with dry nitrogen gas to verify proper signal alignment and maximal signal-to-noise instrument response across the 500 to 5000 cm<sup>-1</sup> wavenumber region. In addition, a ten-minute tunnel blank (TB) was collected immediately before and after each run to obtain background gas concentrations in the exhaust system. These values were used to compute the daily quantitation limits of the FTIR instrument. For the 2012 steady-state emissions tests reported here, the FTIR gas-phase concentrations for the following compounds were averaged over the steady-state portion of the test cycle: Acetylene (ppm), CH<sub>4</sub> (ppm), CO (%), CO (ppm), CO<sub>2</sub> (%), Diesel (ppm), Ethane (ppm), Ethylene (ppm), Formaldehyde (ppm), H<sub>2</sub>O (%), HNCO (ppm), N<sub>2</sub>O (ppm), NH<sub>3</sub> (ppm), NO (ppm), NO<sub>2</sub> High (ppm), NO<sub>2</sub> Low (ppm), O<sub>3</sub> (ppm), Propane (ppm), Propylene (ppm), Urea ByProduct (ppm). These compounds were recommended by the instrument manufacturer for testing of diesel and biodiesel exhaust.

### **5-Gas Analyzer**

In addition to the FTIR an Applus+ AutoLogic Inc. 5-Gas analyzer was used to collect gas data for CO, CO<sub>2</sub>, NO<sub>x</sub>, HC and O<sub>2</sub>. In some instances, the 5-gas sampled raw exhaust along with the FTIR to determine the relationship between what the instruments were reporting. In other instances the 5-gas analyzer sampled diluted exhaust to allow DR calculation via gas data to corroborate the DR calculation based on measured volumetric flow data.

## **2.5 Data Processing**

### **2.5.1 Data Pre-Processing: Temporal Alignment.**

Although the clocks on the computers used for data collection were synchronized, the time stamps associated with each instrument were not aligned perfectly. The exhaust emissions (EEPS, CPC, FTIR) data were also subject to a time lag associated with the time necessary for the exhaust sample to travel from the sample port in the exhaust pipe to the instrument. The raw data from Scantool, Armfield, Labview, and EEPS were aligned as follows.

First, because Scantool data were logged at a variable ‘as fast as possible’ rate, they were interpolated to the same frequency as the Armfield data using the Matlab function ‘Interp1’ and the ‘linear’ method. Then, Armfield output file record numbers were translated to Armfield timestamps (hh:mm:ss:ddd) using the manually recorded start time and the known data collection sampling rate. Because of the error associated with generating the Armfield timestamps, the Armfield data were aligned to the Scantool data collected for the same parameter measurement. The Pearson’s correlation method was then used to determine the time lag to be assigned to each data set. The Armfield data set was shifted in intervals of one time step from  $-t$  seconds to  $+t$  seconds (where  $t$  is large enough to obtain a maximum correlation coefficient). The shifted Armfield parameters (throttle position, RPM, intake air pressure, and torque) were correlated to corresponding Scantool parameters (throttle position, RPM, RPM, and injection quantity respectively) and the lag with the highest correlation coefficient was recorded for each parameter being compared. The average of the four recorded lags was then applied as the Armfield instrument offset. Once the time offset was applied to the Armfield data, it and the Scantool data were interpolated to the frequency of the remaining instruments (1Hz). Next, the Labview data were aligned with the Armfield/ Scantool data by correlating multiple time shifts of the Labview mass air flow (MAF) parameter to the Armfield intake air pressure; both are measures of intake air flow. Again, the time offset associated with the highest correlation coefficient was selected and applied to time-align the Labview data set with Armfield/Scantool. To align particle and gas emissions instrument (EEPS, CPC, FTIR) to the engine operating data, the Scantool fuel injection quantity parameter was correlated to EEPS total particle number (TPN) to determine the lag based on the highest correlation coefficient.

### 2.5.2 Engine Load Calculation.

The CM-12 dynamometer is instrumented to measure engine torque in real time. In order to evaluate the data collected here in a broader context, it was necessary to calculate percent load, the amount of torque currently being generated **divided by** the maximum torque that could be generated at a given engine speed. To facilitate this calculation, the torque curve provided by Volkswagen for the 1.9L SDi engine (**Figure 2-11**) was interpolated into a piecewise function so that ‘maximum torque’ could be calculated across the RPM range. The maximum torque was calculated for every time step using the associated engine speed. Percent load was then calculated with the following equation:

$$\% \text{ Load} = ((\text{Measured Torque})/(\text{Maximum Calculated Torque})) * 100 \quad 2-2$$

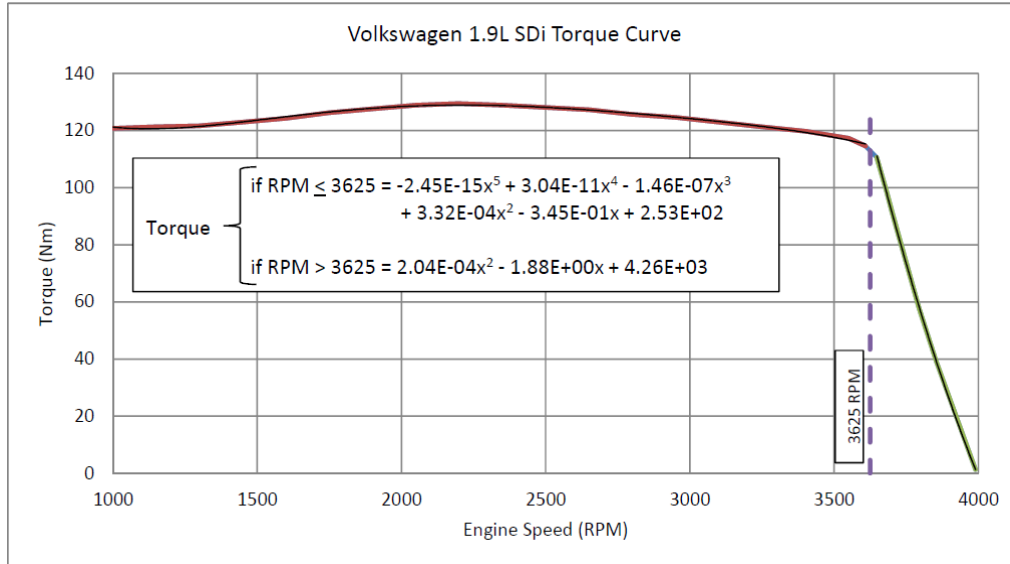


Figure 2-11. Volkswagen 1.9L SDi Torque Curve with Polynomial Trendlines

### 2.5.3 Fuel Consumption.

Fuel injection quantity (mass of fuel per engine stroke) is logged by the scantool. It is reported in units of mg/stroke. To calculate fuel consumption, the following equation was used:

$$Fuel\ Consumption\ (gal) = \frac{m_{fuel}}{Stroke} \times \frac{2}{rev} \times RPM \times \frac{lb}{453592\ mg} \times \frac{Dt(sec) \times \frac{min}{60sec}}{r_{fuel}(lb/gal)} \quad 2-3$$

Equation 2-3 was used to calculate the volume of fuel used for every time step in the data set and these instantaneous values were summed to give the overall fuel consumption during the test period. In April 2012, after the SS40 data was collected, an ADAM Equipment GBK 70a scale (0-70lb/0-32kg x 0.002lb/ 0.001kg) was added to the Labview system which logged the weight of the fuel tank at a frequency of 1 Hz. The fuel weight measured with this scale, in conjunction with the fuel density measured with the IROX-D, provide another measure of fuel consumption. To compare these two measures of fuel consumption the data collected during SS80 testing were analyzed. Because the duration of these tests were not all the same, steady state fuel consumption was normalized to gallons per hour. First, fuel consumption was calculated from the scantool data with the equation above and compared to the scale data (labeled ‘Uncorrected Injection Quantity’ and ‘Scale Data’ in **Figure 2-12**).

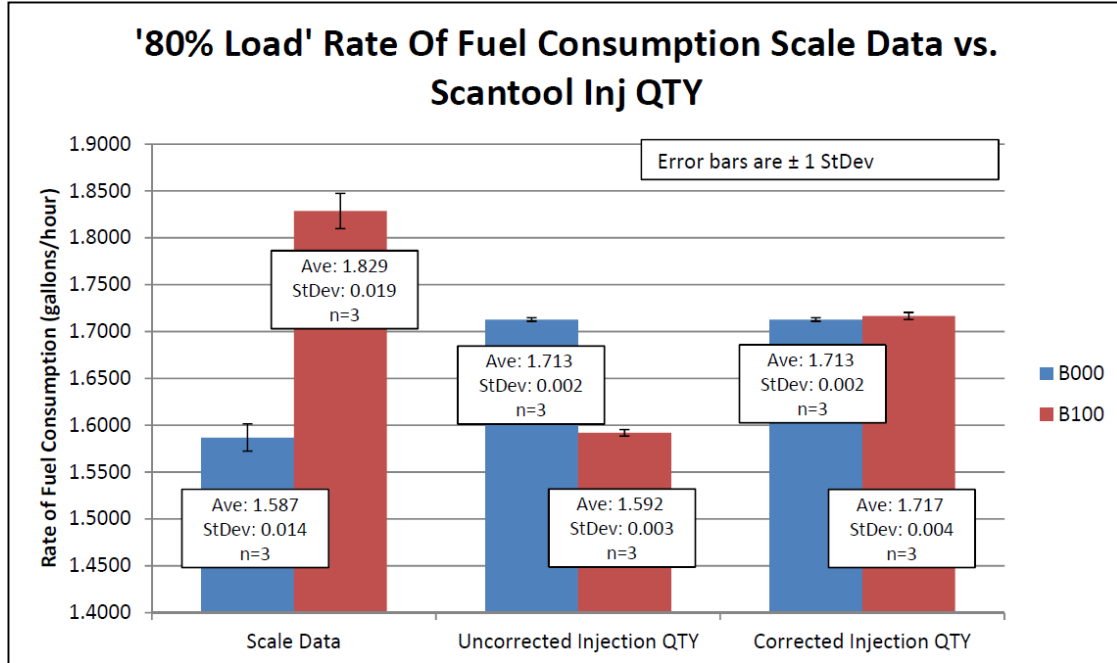


Figure 2-12. Fuel consumption data comparison

Fuel consumption calculated from the scantool data overestimated B000 fuel consumption and underestimated B100 fuel consumption as compared to scale data. Realizing that the scantool measure is based on average B000 fuel properties, and that fuel density was used in the fuel consumption calculation, a density ratio was applied to the scantool calculation which yielded the ‘Corrected Injection QTY’ data shown in **Figure 2-12**. The ‘Corrected Injection QTY’ scantool data shows a statistically insignificant difference between B000 fuel consumption and B100 fuel consumption according to the scantool data. This suggests that the scantool Injection QTY data is, in actuality, merely a crudely estimated volumetric flow measurement even though it is reported in units of mass flow. For this reason, fuel consumption calculated via fuel tank weight is considered to be more accurate.

### 2.5.4 Blank Corrections

To ensure that particle and gas phase data reported were not influenced by background levels, each instrument collected 5 data files - a pre-instrument blank, a pre-tunnel blank, run data, a post-tunnel blank, and a post instrument blank. The instrument blanks were used to verify that the instruments were operating similarly before and after the run as well as from run to run. The tunnel blank data were used to correct the gas and particle concentration data collected during the run for changes in ambient conditions. All data were blank corrected based on Equation 2-4

$$Corrected\ Data = RawData - \left( \bar{C}_{TB_{pre-run}} + 3S_{TB_{pre-Run}} \right) \quad 2-4$$



## 2.6 System Validation Procedures

A total of 10 test runs were completed at 40% steady-state load (SS40) and 6 runs were completed at 80% load (SS80). The engine and dilution system electronic data successfully logged for each test is summarized in **Table 2-9**. Lists of the complete test runs can be found in **Appendix D**.

**Table 2-9. Test runs completed at 40% and 80% load and the instruments that successfully logged**

40 % Load Tests	Fuel	Armfield Data	Scantool Data	Labview Data
1_07FEB2012_B000	B000	✓	✓	✓ (No Scale)
1_08FEB2012_B000	B000	✓	✓	✓ (No Scale)
1_09FEB2012_B020	B020	✓		✓ (No Scale)
1_10FEB2012_B020	B020	✓	✓	✓ (No Scale)
1_02MAR2012_B050	B050	✓		✓ (No Scale)
1_07MAR2012_B050	B050	✓		✓ (No Scale)
1_13MAR2012_B050	B050	✓	✓	✓ (No Scale)
1_20MAR2012_B100	B100	✓	✓	✓ (No Scale)
1_22MAR2012_B100	B100	✓	✓	✓ (No Scale)
1_26MAR2012_B100	B100	✓	✓	✓ (No Scale)
80 % Load Tests				
1_14MAY2012_B100	B100	✓	✓	✓
1_16MAY2012_B100	B100	✓	✓	✓
1_17MAY2012_B100	B100	✓	✓	✓
1_28AUG2012_B000	B000	✓	✓	✓
1_12SEP2012_B000	B000	✓	✓	✓
1_24OCT2012_B000	B000	✓	✓	✓

### 2.6.1 Logsheets and Checklists

Over the course of this project, multiple log sheets and check lists were developed to ensure adequate test run records are collected daily and that the experimental procedure was as repeatable as possible from run to run. Example log sheets used during this study can be found in **Appendix C**. There were a total of 5 logsheets (Run, EEPS, MultiGas, 5-Gas, Cycle) recorded for each emissions test. In addition, each emissions instrument and the CM-12 engine has its own hardbound logbook where information on instrument use, calibration and maintenance activities are recorded.

Beyond the real time monitoring of the equipment that is captured on the log sheets, Matlab code was written to quickly process the raw data collected during an experiment. The data from an experiment is typically processed with this code within 24 hours to generate plots of key parameters such as engine speed and torque, dilution system temperatures, ambient conditions, the calculated dilution ratio, exhaust temperature, and EEPS total particle number. These plots are then compared to those of previously collected data to make sure there are not any unexplained deviations. If deviations occurred or instruments malfunctioned, an additional replicate test was performed.



## 2.6.2 Data Quality Control and Instrument Verification

Procedures are also in place to ensure data quality. Particle number (PN) distributions measured by the EEPS were verified against an SMPS system, which is considered to be the “gold standard” for PN distribution measurement. For this purpose, a 100ppm emery oil in isopropanol solution was prepared in order to generate a standard aerosol of emery oil spheres. The aerosol was generated with a TSI Constant Output Atomizer (Model 3076), which produces an aerosol by pressurizing a given solution. The aerosol flowed through silica gel and activated carbon to remove moisture and organic contaminants from the sample before simultaneous measurement from the EEPS and SMPS on a “tee” fitting. Average results from the EEPS measuring a second-by-second distribution for seven minutes and the SMPS measuring the distribution three times (3 scans, 150 sec each) over the same time-frame are presented in **Figure 2-13**. The results indicate that the two instruments were able to measure the same distribution mode within this test, although the SMPS total particle number (TPN) measurement was almost twice that of the EEPS. This result has been reported by other studies, with the two instruments often displaying a difference in TPN between 25-38% due to their slightly different particle measurement methodologies (Zimmerman et al., 2013 REF 36). Because our experimental procedure are comparative in nature, utilizing baselines to determine percent differences between conditions (e.g., biodiesel percentage), accurate time-resolved PN distribution measurements are more important than absolute TPN values.

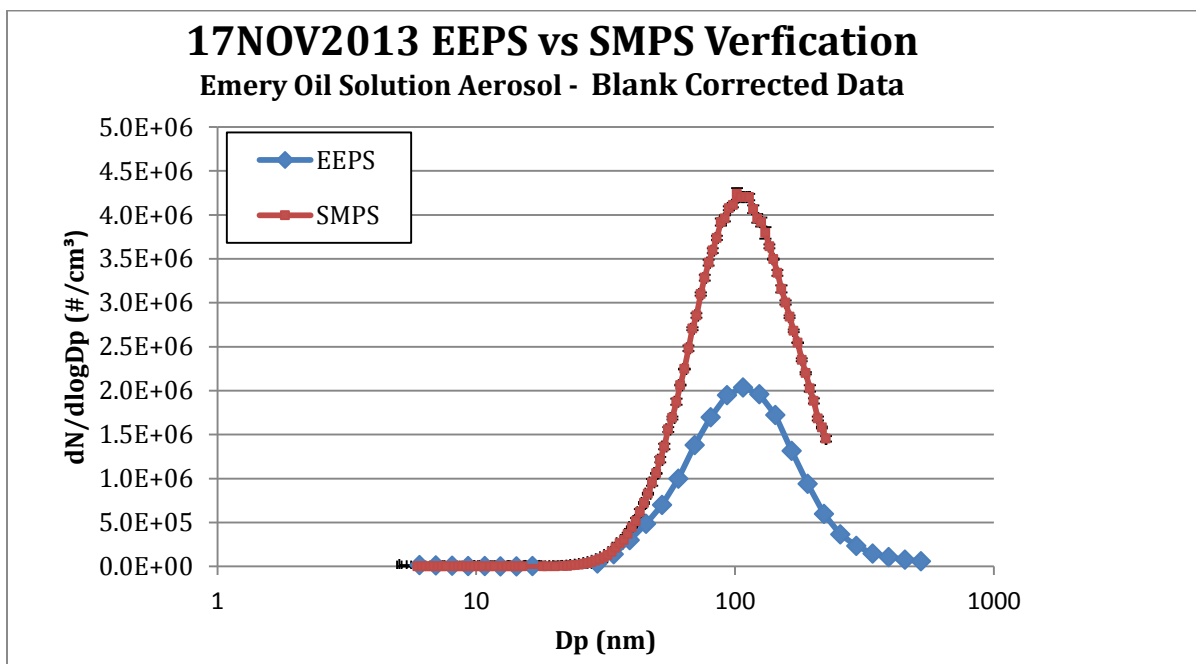


**Figure 2-13. EEPS PN distribution verification against SMPS with standard aerosol**

For the MKS MultiGas, measurement of gas-phase emissions, the quality assurance/quality control procedures described in detail by Sentoff (2013) were employed. These procedures include daily instrument zero checks using dry nitrogen gas, calibration using a certified emissions mix and a daily startup sequence based on manufacturer guidelines to ensure instrumentation was operating within specifications.

### 3. Results

#### 3.1 Summary Of Data Collected

Between January – December 2012, a total of 45 engine tests were performed to evaluate a number of research questions related to the Armfield CM-12 light-duty diesel engine and the sampling system design as well as the effect of fuel composition on CM-12 emissions and engine performance. **Table 3-1** summarizes the test information. These 2012 tests represent the first series of runs with the near-final CM-12 testing apparatus described previously in **Section 2**. Emissions from the tailpipe were sampled for gases and particles simultaneously and soybean biodiesel fuel from Burke Oil was mixed with petrodiesel from a single local commercial supplier (Trono Fuels). Thus, this dataset represents that for which the research team could evaluate the quality of the test procedures and collect preliminary emissions data for comparison to the literature.

**Table 3-1. Individual Run Test Conditions**

Date (dd Mon-YYYY)	Test #	Fuel Blend (Biodiesel el % by Vol)	Petrodiesel Feedstock (Distributor, Fuel Type, Purchase Year)	Biodiesel Feedstock (Distributor, Oil Type, Purchase Year)	Test Cycle (Test, Purge, Aggressive, Steady State, Transient, Hot Cleanout)	Number of False Start/ Cutout Events	Engine Start Time	Engine Off Time	Run Duration (min)	Engine Hours Start	Engine Hours End	Ignition Time On (min)	Clg In Dil Sys?	Calculated Dilution Ratio	Notes/Issues	
<b>Changed Dilution System Orifice setup</b>																
23-Jan-2012	N/A	B0	Trono Petro 2010	None	Purge	0	17:48:50	17:59:00	10.2	105.33	105.44	11	N		Purge to B0	
24-Jan-2012	N/A	B0	Trono Petro 2010	None	Test	0	15:55:20	16:02:30	7.2	105.44	105.52	8	N		Testing Mags	
26-Jan-2012	N/A	B0	Trono Petro 2010	None	Test	0				105.52	105.55	3	N		Testing Aerosol Inlet	
30-Jan-2012	1	B0	Trono Petro 2010	None	Steady State 40%	0	14:20:57	15:45:30	84.6	105.55	107.20	85	N		"Qnd" - Only collecting PM	
31-Jan-2012	1	B0	Trono Petro 2010	None	Steady State 40%	0	15:02:47	16:27:15	84.5	107.20	108.46	86	N		"Qnd" - Only collecting PM	
6-Feb-2012	N/A	B0	Trono Petro 2010	None	Test	0				108.46	108.58	12	N		Testing DilSys changes	
6-Feb-2012	N/A	B0	Trono Petro 2010	None	Test	0				108.58	109.04	6	N		Testing DilSys changes	
7-Feb-2012	1	B0	Trono Petro 2010	None	Steady State 40%	0	15:13:05	16:53:30	100.4	109.04	110.46	102	N	54		- 5-Gas did not detect CO2
8-Feb-2012	1	B0	Trono Petro 2010	None	Steady State 40%	0	15:47:00	17:25:00	98.0	110.46	112.32	106	N	50-51		- EEPS - "Concentration Overage" message - Scantool disconnected but was successfully reconnected
9-Feb-2012	1	B20	Trono Petro 2010	Burke Soy 2010	Steady State 40%	0	16:21:00	17:59:00	98.0	112.32	114.11	99	N	50		- Scantool disconnected
10-Feb-2012	1	B20	Trono Petro 2010	Burke Soy 2010	Steady State 40%	1	12:11:00	13:50:00	99.0	114.11	115.50	99	N	53		
1-Mar-2012	N/A	B50	Trono Petro 2010	Burke Soy 2010	Purge	0	11:55:00	12:00:00	5.0	116.17	116.24	7	N			Purged to B50
2-Mar-2012	1	B50	Trono Petro 2010	Burke Soy 2010	Steady State 40%	0	11:45:00	13:23:00	98.0	116.24	118.03	99	N	57-58		- Heat tape malfunction - EEPS - "Concentration Overage" message - Adjusted Armfield Throttle position to match OBD-II throttle position since last run. Maintained the same OBD-II throttle position throughout runs. - Scantool disconnected - Building water left on for the night prior - cylinder head cooler then usual
7-Mar-2012	1	B50	Trono Petro 2010	Burke Soy 2010	Steady State 40%	1	14:15:00	15:51:30	96.5	118.03	119.42	99	N	55-56		- Heat tape only on Aerosol Inlet - Scantool disconnected
13-Mar-2012	1	B50	Trono Petro #012	Burke Soy 2010	Steady State 40%	1	14:22:30	16:00:00	97.5	119.42	121.20	98	N			- Heat tape only on Aerosol Inlet
19-Mar-2012	N/A	B100	Burke Soy 2010	Burke Soy 2010	Purge	0	17:36:00	17:41:00	5.0	121.20	121.26	6	N			Purge to B100
20-Mar-2012	1	B100	Burke Soy 2010	Burke Soy 2010	Steady State 40%	0	13:58:00	15:35:30	97.5	121.26	123.04	98	N	56-57		- EEPS turned off between pre IB & TB - Both heat tapes operational again - Adjusted both heat tape controllers to try to maintain correct temperature
22-Mar-2012	1	B100	Burke Soy 2010	Burke Soy 2010	Steady State 40%	1	13:13:00	14:26:30	73.5	123.04	124.17	73	N	56		- Engine turned off early due to low fuel - EEPS - "Concentration Overage" message - Making sure engine starts back up
22-Mar-2012	N/A	B100	Burke Soy 2010	Burke Soy 2010	Test	1	18:15:00			124.17	124.33	16	N			
26-Mar-2012	1	B100	Burke Soy 2010	Burke Soy 2010	Steady State 40%	0	15:24:30	17:02:30	98.0	124.33	126.12	99	N	55		- Adjusted heat tape setpoint to achieve correct gas temp - Much colder Ambient temp then previous B100 runs (15.15°C) - Grounded thermocouple used to collect dilution air and transferline gas temperatures are reporting erroneously
5-Apr-2012	N/A	B0	Trono Petro #012	None	Purge	0				126.18	126.27	9	N			Purge to B0
20-Apr-2012	N/A	B0	Trono Petro #012	None	Test	0				145.33	145.36	3	N			Testing new fuel system
2-May-2012	1	B0	Trono Petro #012	None	Steady State 80%	0	15:21:30	17:21:31	120.0	145.48	147.49	121	N	58		- Scantool disconnected momentarily but reconnected successfully (went back to idle momentarily after warm-up to reconnect)
3-May-2012	N/A	B100	Burke Soy 2010	Burke Soy 2010	Purge	0							N	58		Purge to B100
3-May-2012	1	B100	Burke Soy 2010	Burke Soy 2010	Steady State 80%	0	15:29:00	17:24:30	115.5	147.49	149.50	121	N			- Tried Armfields '2 controller project work' control. It did not work with the setting changes I made. Had to shut down and restart with control typically used. - Forgot to reinstate Armfield data collection after restart - No Armfield data. Torque toggled between 103 and 104 Nm during SS. - Manually logged fuel tank weight
7-May-2012	1	B0	Trono Petro #012	None	Steady State 80%	0	13:12:00	15:10:00	118.0	149.50	151.48	118	N			Purged to B0 during warm-up Aerosol Inlet orifice clogged
11-May-2012	N/A	B100	Burke Soy 2012	Burke Soy 2012	Purge	0	16:15:00	16:22:30	7.5	151.48	151.56	8	N			Purge to B100
14-May-2012	1	B100	Burke Soy 2012	Burke Soy 2012	Steady State 80%	0	10:03:15	12:00:00	116.8	151.56	153.53	117	N	86.33		Day 1 of 3 day exposures - 10 mice SNAPS data - many scans, one sample
15-May-2012	1	B100	Burke Soy 2012	Burke Soy 2012	Steady State 80%	0	9:28:00	11:23:30	115.5	153.53	155.52	119	Y	128.59		Day 2 " - Aerosol Inlet orifice clogged
16-May-2012	1	B100	Burke Soy 2012	Burke Soy 2012	Steady State 80%	0	9:18:00	11:13:30	115.5	155.52	157.48	116	N	85.8		Redo day 2 of 3 day exposures - 10 mice 5-Gas missed engine start & warm-up
17-May-2012	1	B100	Burke Soy 2012	Burke Soy 2012	Steady State 80%	0	8:34:00	10:29:30	115.5	157.48	159.44	116	N	85.11		Day 3 of 3 day exposures - 10 mice
24-May-2012	N/A	B100	Burke Soy 2012	Burke Soy 2012	Steady State	0	14:26:30	14:49:00	22.5	159.44	160.06	22	N			Determining source of odor
4-Jun-2012	1	B0	Trono Petro #012	None	Steady State 40%	0	13:42:00	15:14:00	92.0	160.06	161.39	93	N	82		Dilution System Manifold Test
27-Jun-2012	1	B0	Trono Petro #012	None	Steady State 40%	0	11:18:00	14:00:32	162.5	161.39	164.21	162	N	82.95		Dilution System Manifold Test
28-Aug-2012	1	B0	Trono Petro #012	None	Steady State 80%	0	13:24:30	14:50:00	85.5	164.21	165.47	86	Y	85.24		Impinger Redesign Test - Tall Impinger
6-Sep-2012	1	B0	Trono Petro #012	None	Steady State 80%	0	11:03:43	12:28:30	84.8	165.56	167.22	86	Y	99.07		Impinger Redesign Test - Vortex Impinger Clog in Aerosol Inlet
10-Sep-2012	N/A	B0	Trono Petro #012	None	Test	0	10:57:20	10:59:40	2.3	167.32	167.32		N	83.32		Testing Scantool measuring block
10-Sep-2012	N/A	B0	Trono Petro #012	None	Test	1	17:28:00	17:33:49	5.8	167.32	167.49	17	N			Testing Scantool measuring block
12-Sep-2012	1	B0	Trono Petro #012	None	Steady State 80%	0	10:30:30	12:26:00	115.5	168.42	170.38	116	N			Impinger Redesign Test - Vortex Impinger
21-Sep-2012	1	B0	Trono Petro #012	None	Steady State 80%	0	11:18:30	12:47:30	89.0	171.04	172.34	90	Y	88.63		Impinger Redesign Test - Diffused Impinger Clog in Aerosol Inlet
5-Oct-2012	N/A	B0	Trono Petro #012	None	Test	0				172.34	172.44	10	N			Testing cold air intake
8-Oct-2012	N/A	B0	Trono Petro #012	None	Test	0				172.44	172.50	6	N			Demonstrating engine operation
16-Oct-2012	N/A	B0	Trono Petro #012	None	Transient	0				172.50	172.52	2	N			Testing Transient Cycle schedule
24-Oct-2012	1	B0	Trono Petro #012	None	Steady State 80%	0	15:04:30	16:58:00	113.5	172.52	174.46	114	Y	91.57		Impinger Redesign Test - Swirling Impinger
8-Nov-2012	1	B0	Trono Petro #012	None	Steady State 80%	1	10:13:00	12:20:00	127.0	174.46	176.53	127	Y	85.73		
12-Nov-2012	1	B0	Trono Petro #012	None	Steady State 80%	0	10:09:00	12:04:00	115.0	176.54	178.49	115	N	64.87		Impinger Test - Heat Exchanger, Swirling Imp
21-Nov-2012	N/A	B0	Trono Petro #012	None	Transient	0	13:16:30	13:22:30	6.0	178.54	179.01	7	N			Developing Transient Cycle
27-Nov-2012	N/A	B0	Trono Petro #012	None	Transient	0	14:50:30	14:57:00	6.5	179.01	179.09	8	N			Developing Transient Cycle
11-Dec-2012	1	B0	Trono Petro #012	None	Steady State 80%	0	14:15:00	16:10:00	115.0	179.23	181.18	115	N	83.81		Impinger Test - Heat Exchanger w/ catch-can
17-Dec-2012	N/A	B0	Trono Petro #012	None	Transient	0	15:50:00	16:05:00	15.0	181.18						Developing Transient Cycle
17-Dec-2012	N/A	B0	Trono Petro #012	None	Transient	0	16:15:30	16:30:00	14.5	181.34	181.49	15	N			Developing Transient Cycle

Steady-state 40% load (SS40) tests were conducted at four biodiesel blend ratios: B0, B20, B50 and B100. Steady-state 80% load (SS80) tests were conducted at just two blend ratios: B0 and B100. Replicate tests were collected for each fuel blend and results are reported below both by individual test and as averages of the combined replicate runs on a single fuel blend.

### Ambient Air Conditions

The mean ambient air temperature and relative humidity (RH) at the beginning of each test are plotted in **Figure 3-1**. For the SS40 tests conducted between January 30, 2012 – March 26, 2012 the average temperature was 18.4°C and average RH was 28.4%. The temperature and humidity were higher for the SS80 tests that were conducted between May 2-17, 2012: 20.6°C and 46.6% RH, respectively. These differences reflect the fact that the TAQ Lab air is unconditioned and seasonal changes in ambient air properties will be incorporated into the experimental conditions. This test condition mimics real-world seasonal vehicle operation, but demands careful assessment of how ambient conditions might influence experimental procedures and emission results.

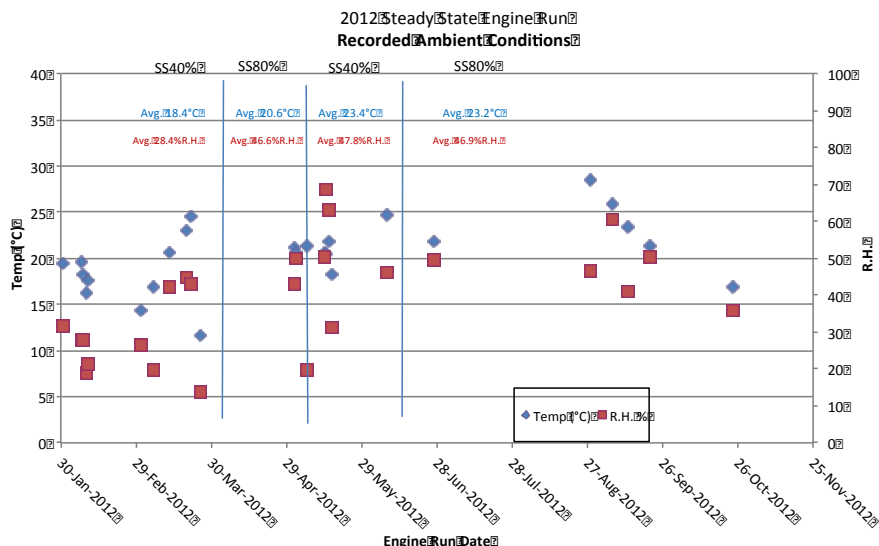


Figure 3-1. Ambient air temperature and relative humidity at start of SS test runs.

### 3.2 Fuel Composition by IROX-D

**Figure 3-2** below shows the mid-FTIR absorbance spectra for fuel samples measured by the IROX-D instrument. Fuel samples of the same biodiesel blend content are plotted as the same color, which may not be immediately visible due to the high similarity of the spectra measured within each blend. As the biodiesel content increased, the intensity of the signal response at the 1195cm<sup>-1</sup> wavenumber region also increased, as expected. This ester (C-O) peak is used by the IROX to measure biodiesel (FAME) concentrations between 7-30% by volume. The measured biodiesel content for fuel sample is presented in **Figure 3-3**, and average results are shown in **Table 3-2**. Although results were consistent, B50 and B100 biodiesel content was likely underestimated due to the need to dilute samples with n-Hexane. Despite this, the results indicate that biodiesel content for all samples of fuels used in testing were within an acceptable range of target biodiesel blend composition values.

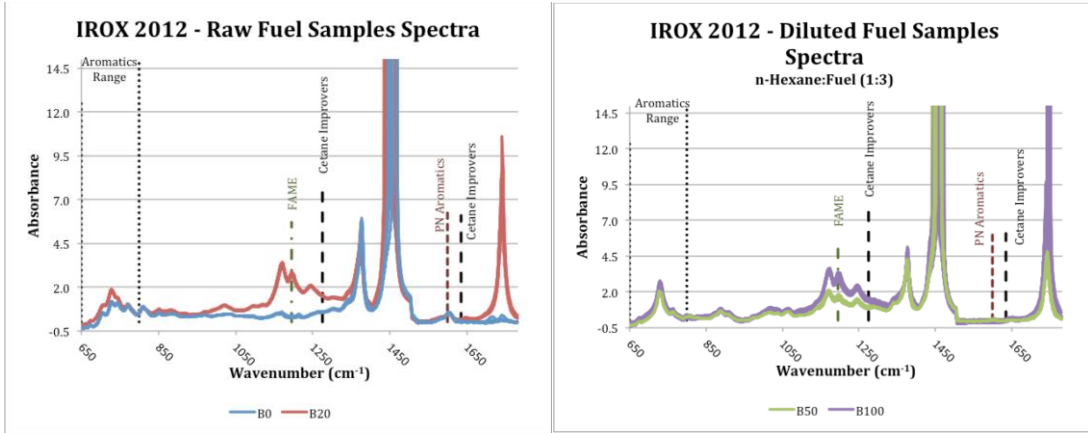


Figure 3-2. IROX Mid-FTIR Absorbance Spectra for raw B0 and B20 fuel samples (left) and B50 and B100 samples diluted to 25% with n-hexanes (right)

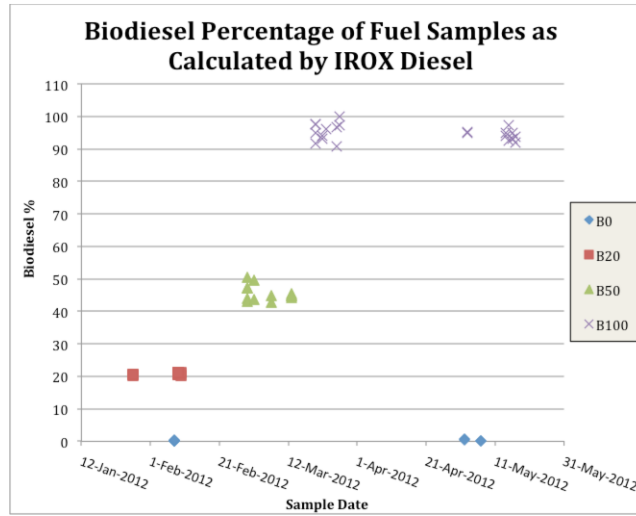


Figure 3-3. IROX results for fuel biodiesel content

Table 3-2. Mean IROX results for fuel biodiesel content

Fuel Type	Expected Value (% Bio)	Mean Actual Value (% Bio)	Mean % Diff from Expected	StDev	%CV
B0	0	0.08	0.08	0.12	1.55
B20	20	20.83	4.17	0.35	1.69
B50	12.5	11.39	8.98	0.59	5.21
B100	25	23.71	5.16	0.58	2.44

### 3.3. Engine Operation: Run-to-Run Reproducibility

#### Engine Parameters

The test-to-test performance of the CM-12 engine and dynamometer was evaluated by comparing engine load, torque, engine speed (RPM) and throttle position (Figure 3-4 and Figure 3-5) as

well as exhaust manifold temperature (**Figure 3-6**). RPM and throttle position were programmed by the operator and therefore were expected to show much less variability than the response parameters, engine torque and engine load.

For the SS40 tests, there was good reproducibility in the engine load and torque data for tests conducted with the same biodiesel fuel blend. Notably, the SS40 B20 and B0 fuel performance metrics were similar to each other and both engine torque and load were significantly lower for the B0 and B20 tests compared to B50 and B100 tests (**Figure 3-4**). Load and torque showed a pattern of increasing values with increasing biodiesel content in the fuel for blends greater than B20.

For the SS80 tests (**Figure 3-5**), both engine torque and percent load were higher for operation on B100 than B0, following the pattern observed for SS40 tests. The data for both SS40 and SS80 operation suggest that engine operating variability was highest for the petrodiesel (B0) fuel. The reason for this result is unknown because ambient conditions were not very different between replicate B0 tests on a given fuel blend.

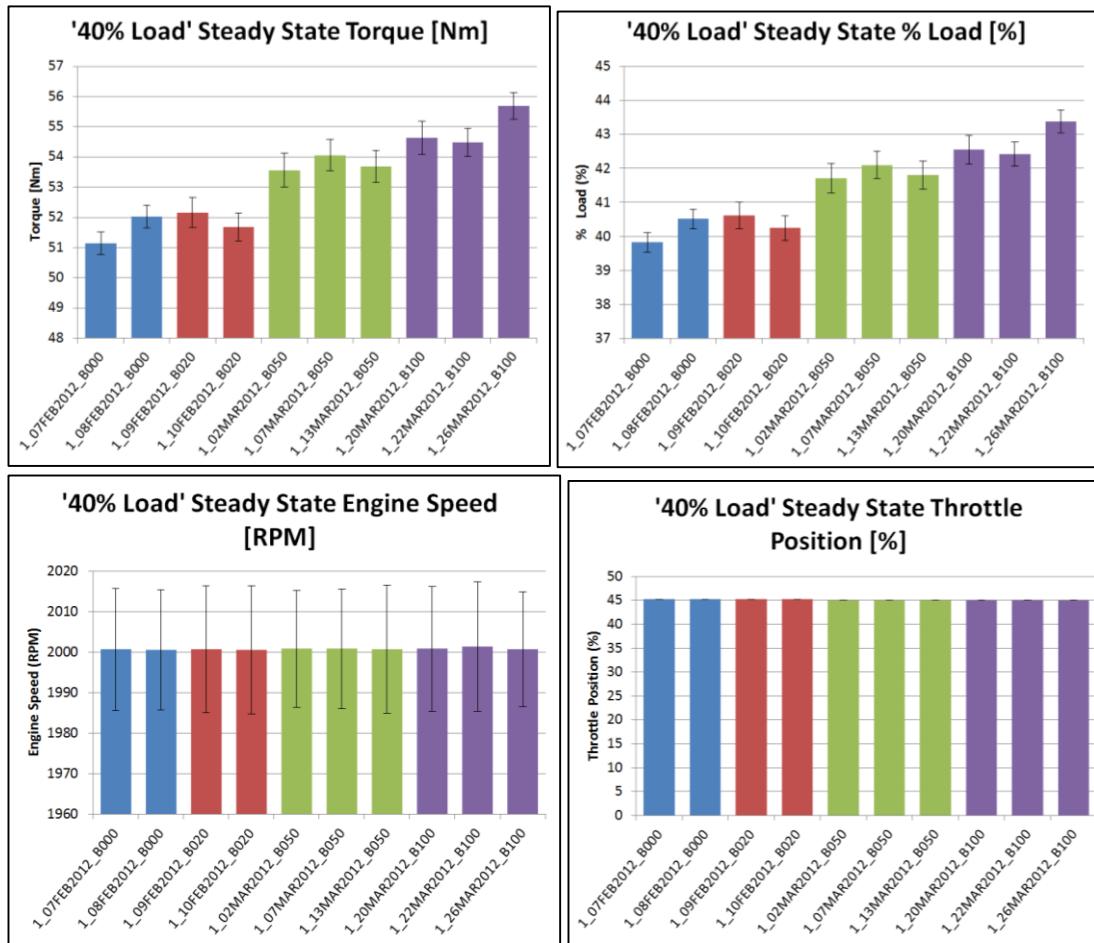


**Figure 3-4. Mean CM-12 engine operating parameters for SS40 tests: Torque, % Load, Engine Speed and Throttle Position.**

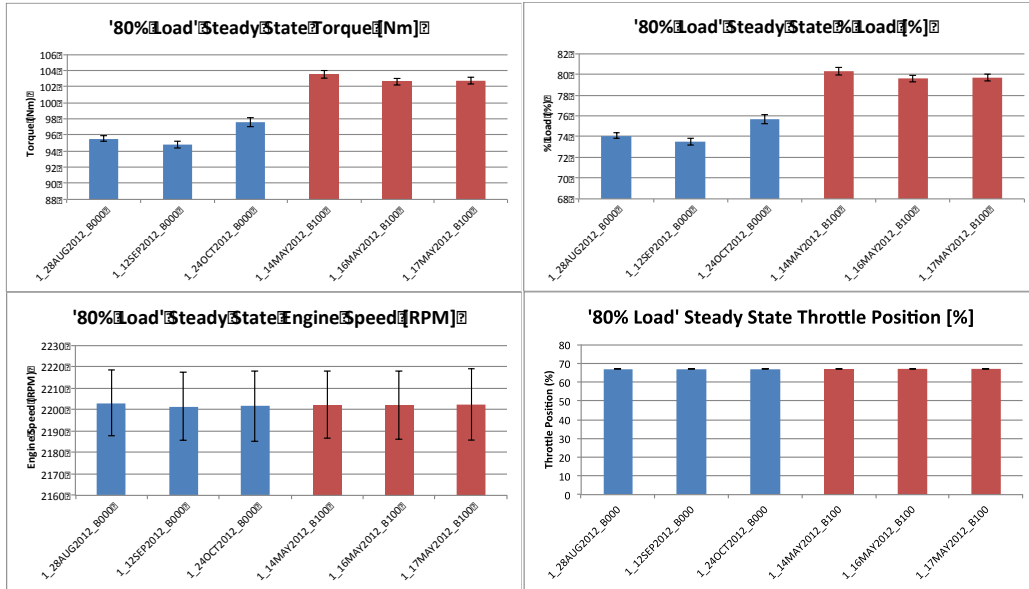


Figure 3-5. Mean CM-12 engine operating parameters for SS80 tests: Torque, % Load, Engine Speed and Throttle Position.

Measured exhaust manifold temperatures were much higher for operation at 80% load compared to 40% load, as one would expect (Figure 3-6, note y-axis ranges are different). Exhaust temperature also increased with increasing volume fraction of biodiesel in the fuel, but there was also high variability between replicate tests on a single fuel blend. For example, the B50 tests show an increasing trend. The low temperature measured on the SS40 B100 test on March 26, 2012 was likely due to a 10 degree lower ambient air temperature on that test date. (See Appendix D for table of test T and RH conditions).

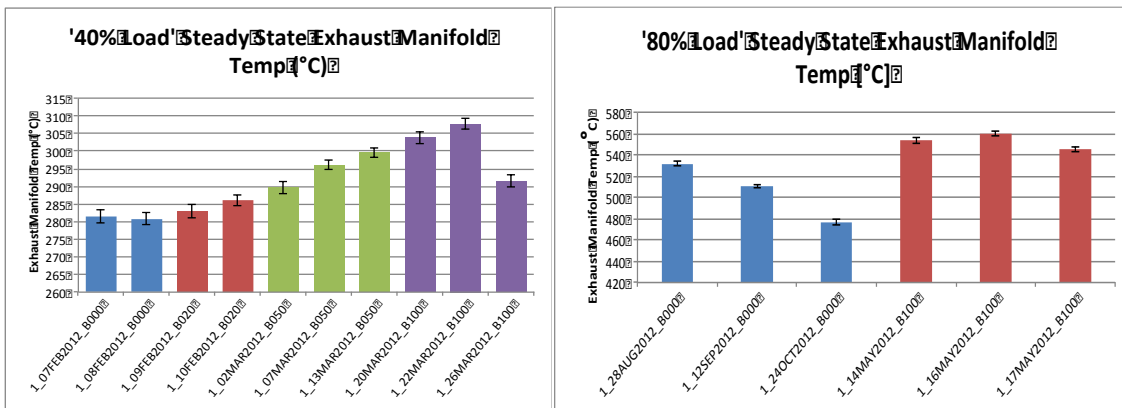
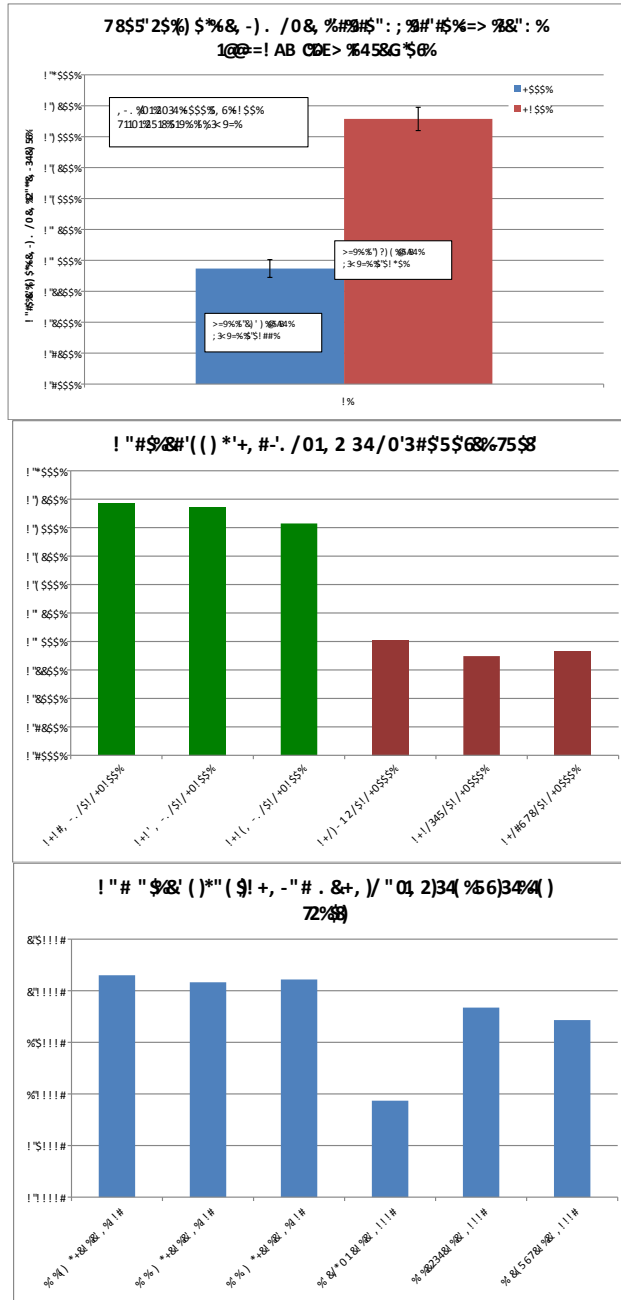


Figure 3-6. Mean CM-12 exhaust manifold temperature for SS40 (left) and SS80 (right) tests.

## Fuel Consumption

The real-time gravimetric measurements of fuel remaining in the fuel tank were available for the SS80 tests only. As the data in Figure 3-7 show, there was one test, 28AUG12, using petrodiesel fuel, that was of shorter duration because the engine ran out of fuel partway through the SS80 test. Thus, to compare the data, the average cumulative fuel consumption rates (gal/hr) were

compared by run and averaged over fuel type. Significantly higher fuel consumption rate was observed for the B100 soy biodiesel fuel compared to Trono petroleum diesel (B0). This is expected due to the approximately 10% lower *volumetric* energy content of biodiesel compared to petrodiesel (see **Table 1-1**). It should be noted that the CM-12 engine fuel injectors do not adjust for changes in fuel properties, thus the lack of adjustment may have resulted in the observed 15% (computed as percent difference) higher fuel consumption for B100 compared to B0 because of the density and viscosity properties of biodiesel fuel.



**Figure 3-7. Fuel consumption for SS80 tests determined by weight of fuel tank during test cycle. Data are averages over steady-state portion of test only.**



### 3.4 Gravimetric Total Particulate Matter (PM) Emissions

PM mass concentrations ranged from 358 for the engine blank run to over 20,000  $\mu\text{g}/\text{m}^3$  for the March 26, 2012 B100 test. The filter PM results (**Figure 3-8**) show distinct differences in the mass of particles emitted with engine operating cycle and fuel blend. First, the SS40 data show an increase in PM mass concentration with increasing percentage of soy biodiesel in the fuel. This increase with Bxx did not correlate with ambient temperature or RH (**Figure 3-8.c/d**), both factors can affect engine operation and particle emissions. The highest PM mass concentration was measured for B100 for both steady-state test cycles. Interestingly, the B100 mass concentration was lower for operation at 80% load compared to 40% load (**Figure 3-8.a/b**). A side-by-side comparison of the SS40 and SS80 runs is shown in **Appendix D**.

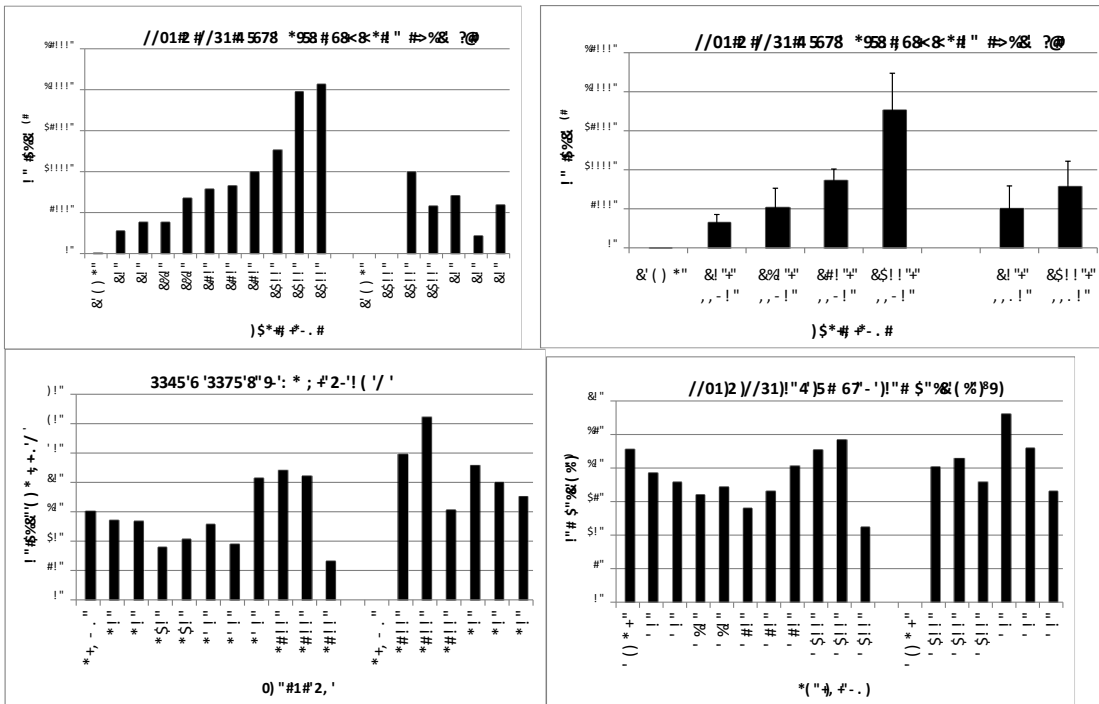


**Figure 3-8. (a and b) Gravimetric PM mass concentration ( $\mu\text{g}/\text{m}^3$ ) results and (c and d) laboratory test conditions (T and RH) for Teflo and FiberFilm filters collected directly from tailpipe without dilution for SS40 and SS80 runs with all biodiesel blends. Blends on left hand side of each plot are for SS40 runs and SS80 runs are on the right hand side.**

### 3.5 Mean Particle Number Distributions by Biodiesel Blend

Mean EEPS particle number data for each biodiesel blend during the SS40 tests are plotted as a function of particle diameter ( $D_p$ ) on a log-log basis in **Figure 3-9**. The EEPS distributions showed very good reproducibility for petrodiesel runs (red symbols in **Figure 3-9**). There were two distinct particle modes – an accumulation mode near 50 nm diameter and a nanoparticle mode at  $\sim 10$  nm. This is consistent with diesel engine PN emissions reported in the literature (see **Section 1.3**). Surprisingly, the B20 number distributions at SS40 were practically identical to those measured for B0 fuel over the entire EEPS particle diameter range (5.6 – 560 nm). This result may reflect the characteristics of the CM-12 engine during steady-state test cycles



compared to heavy-duty diesel engine and vehicle test results reported in the literature where differences have been seen between B0 and B20 emissions (see [Section 1.3](#)).

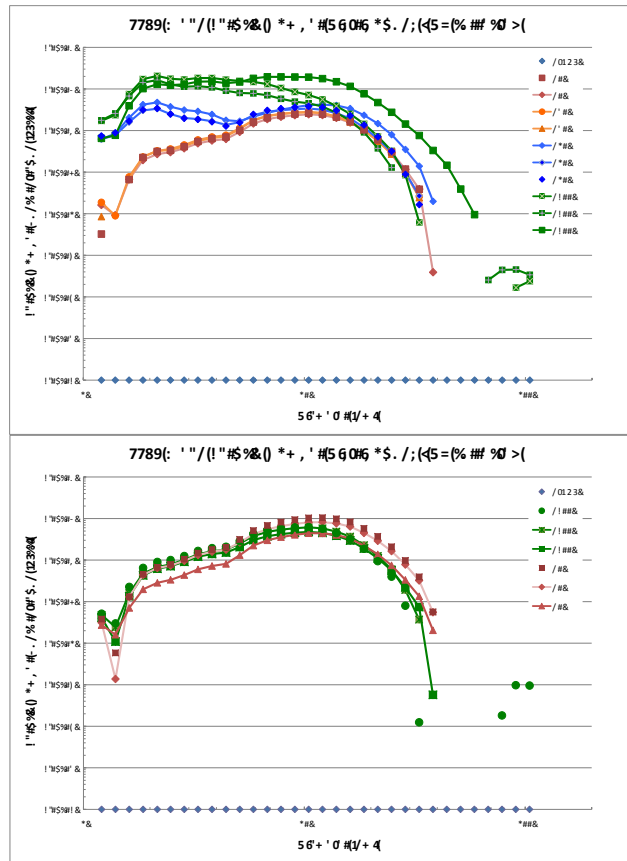


**Figure 3-9. EEPS Particle Number Distributions for SS40 and SS80 tests. Data were corrected for measured dilution ratio. Log-Log plot.**

As observed for the PM filters, the EEPS particle number distribution data (**Figure 3-aaa**) show an increase in particle emissions with increasing biodiesel content in the fuel for steady-state operation at 40% load. In contrast, at 80% load, where only the two fuel end member compositions were tested (B100 and B0), there was little difference between the B0 and B100 particle number emissions. Also at SS80, the nanoparticle mode at ~ 10nm diameter was less pronounced compared to SS40 operation on B100. This indicates that, for B100 fuel, the higher operating load (SS80) particle emissions are less likely to be comprised of the semi-volatile material that nucleates to form the smallest particles during exhaust dilution and cooling. Previous studies have shown that high engine load conditions produce more elemental carbon-rich particles compared to idle conditions where the organic carbon (OC) fraction is enhanced. It is this OC fraction generated during low-load operation that is likely to be comprised of hydrocarbons and other materials that partition easily between the gas and particle phases and lead to a pronounced nanoparticle mode.

Also notable is the high variability in B100 emissions during SS40 tests. There was a significant increase in particle number emissions (and corresponding surface area and mass) as the biodiesel content of the fuel increased, with B100 particle number concentrations up to an order of magnitude higher than B50 at some particle diameters. The shape of the B50 and B100 distributions deviated from the nearly mono-modal shape of the B0 and B20 distributions with

significantly higher emissions for particle diameters less than ~25nm. Thus, B50 and B100 fuels produced elevated nanoparticle emissions compared to B20 and B0 fuel.

The average dilution ratio for the ten 40% load steady-state tests was 55 with a standard deviation of 2.4 (CV = 4.4%). The particle number distributions measured with this system demonstrated similar trends to those found in the literature. The petrodiesel particle number distribution was unimodal (modal diameter 52.3nm) with an average peak concentration of  $2.74 \times 10^7$  particles/cc (**Figure 3-9**). As the concentration of biodiesel was increased, the PN distribution developed additional particle diameter modes. The B100 distribution showed three distinct modes centered at 10.8, 17.8, and 31.7nm particle diameters with peak concentrations averaging  $1.38 \times 10^8$ ,  $1.27 \times 10^8$ , and  $1.34 \times 10^8$  particles/cc, respectively.

The duplicate B00 and B20 data demonstrate consistent particle distributions while the B50 and B100 triplicate data show more variability. The factors that could explain this are variability in ambient conditions (temperature and relative humidity) and aerosol transfer line temperature. Both the B00 and B20 data sets were measured on consecutive days (little change in ambient conditions) while the transfer line temperature was relatively well controlled (95-115°C; sinusoidal). In contrast, both the B50 and B100 data sets were collected over several days resulting in more variable ambient conditions (as much as 15°C; 25%RH difference between the cold and dry 26MAR2012 data set and the other two B100 data sets). Temperature control of the aerosol transfer line was also more variable from day to day, ranging from ~25°C during 02MAR2012 the B50 data set to ~100°C during the 07MAR2012 data set. This variability affects particle formation, particularly through the condensation mechanism (gases condensing onto solid particles resulting in an increase in particle diameter). Figure 3-10 shows the relationship between total particle number concentration (dN, #/cc) and ambient temperature. The “outlier” at 11°C was the B100 test conducted on March 26, 2012.

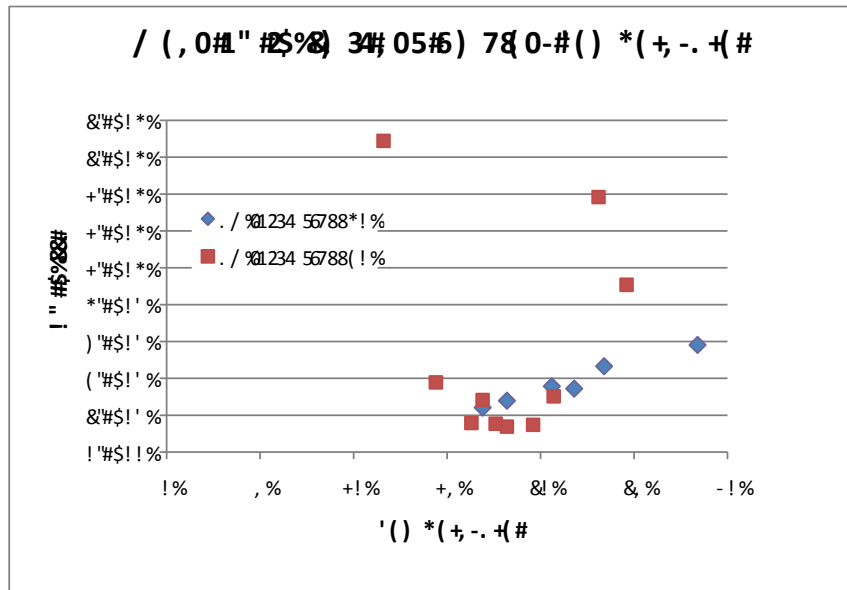


Figure 3-10. Relationship between ambient temperature and mean total particle number over SS40 and SS80 test cycle.

### 3.6 Particle Diameter Measurement

Representative “particle length” ( or “particle diameter”) concentration time-series results for EAD measurements from each fuel blend are shown in **Figures 3-11** for the entire test cycle duration. Particle diameter (PD) concentration measurements from the EAD closely tracked total particle number (TPN) concentration measurements from the EEPS over the course of each test cycle, with similar patterns of peaks in concentrations. Two trends emerge when examining the real-time particle diameter plots for tests conducted with different percentages of biodiesel. As biodiesel content increased, PD peaks associated with transient engine events, such as engine start and the transition into the warm-up phase at the beginning of the cycle, decreased in magnitude. However, while the amplitude of these peaks in B0 were almost twice that compared to B100, the PD concentration decreased more quickly after the transient event was over for lower biodiesel blends. Also, as biodiesel concentration increased in the fuel, it took much longer for the EAD signal to reach a stable level during the steady-state portion of the run. For example, PD reached a stable level after a few minutes of steady-state operation for B0 and B20 blends, after approximately 15 minutes for B50 blends, and after more than 30 minutes for B100 blends. The reason for these delays is unknown, but deserves more detailed examination of the fuel effects on engine and/or exhaust system behavior and performance.

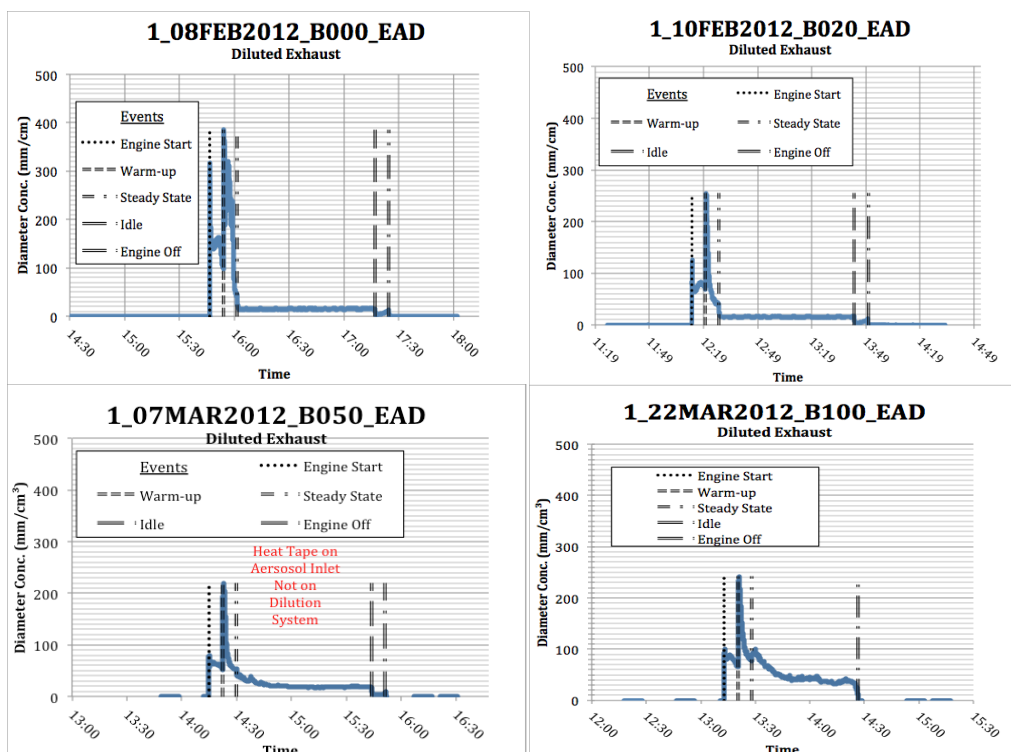


Figure 3-11. Electrical Aerosol Detector (EAD) Full Run Time Series Data for B0, B20, B50 and B100 blends.

### 3.7 Gas-Phase Emissions

In this preliminary work with the MKS FTIR instrument and biodiesel fuel blends, the manufacturer’s suggested analysis method was used for data collection. **Figure 3-12** compares the instrument check parameters for each set of biodiesel blend runs. Only for the B100 blend were any FTIR instrument parameters quite different from other tests. The B100 phase angle and

interferogram peak-to-peak ratio were much smaller than for other blends and the laser PP and laser DC voltage data were off-scale. These deviations were due to the 20MAR12 run where data were apparently not recorded properly to the stored file.

A comparison of tunnel blank data collected before and after the B0 and B20 runs in February 2011 (**Figure 3-13**) for each of the 20 gases shows that there were some tests where there were extreme differences between the ambient air gas concentrations before and after the test. A positive percent difference in **Figure 3-13** means that the pre-TB concentration exceeded that for the post-TB. These extreme differences can occur either because the TAQLab is located near a parking lot that is busy at different times of day with vehicles arriving and leaving or are related to gases with extremely low concentrations that show high variability near the instrument detection limit. The latter is likely for the high percent differences measured for ozone, an analyte not expected in the exhaust.

The mean gas-phase concentrations (ppm or % depending on gas) are listed in **Table 3-3** for the full run and for the steady-state portion of the run separately in order to evaluate how the cold-start and engine warm-up concentrations differ from that for steady operation. The 40% steady-state/total run gas concentration ratio varied from about 0.5 to 2.5 and was different between gases, but did not vary much between biodiesel blends for a given gas compound.

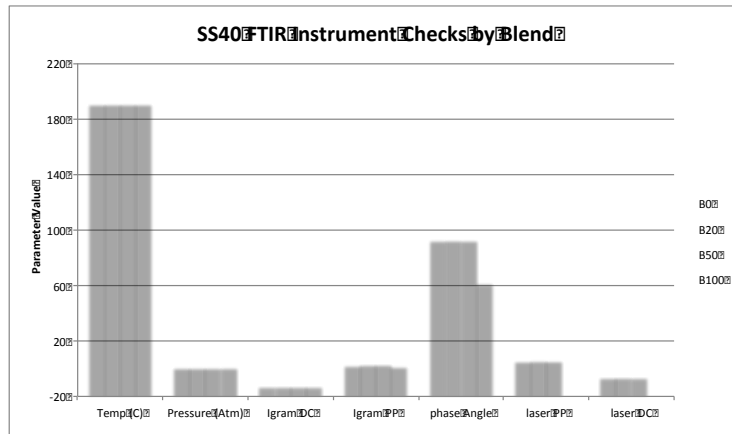


Figure 3-12. MultiGas FTIR Instrument Check Parameter Mean Values for SS40 Runs

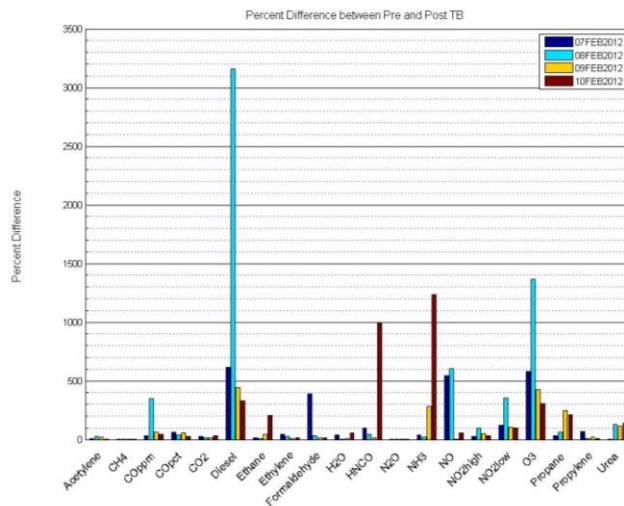


Figure 3-13. Pre- vs. Post Tunnel Blank Gas Concentration Comparison (as Percent Difference) for B0 and B20 SS40 Runs

**Table 3-3. Mean ( $\pm 1$  sd) Gas-phase Concentrations for SS40 Tests: Total Run and SS portion of run only.**

	Petrodiesel (B0)		B20 Blend		B50 Blend		Soy B100 Biodiesel	
	Total Run	SS Portion	Total Run	SS Portion	Total Run	SS Portion	Total Run	SS Portion
Acetylene (ppm)	1.1 ± 0.2	1.1 ± 0.2	1.1 ± 0.2	1.1 ± 0.2	1.1 ± 0.2	1.1 ± 0.2	1.1 ± 0.2	1.1 ± 0.2
CH <sub>4</sub> (ppm)	1.1 ± 0.2	1.1 ± 0.2	1.1 ± 0.2	1.1 ± 0.2	1.1 ± 0.2	1.1 ± 0.2	1.1 ± 0.2	1.1 ± 0.2
CO (%)	1.1 ± 0.2	1.1 ± 0.2	1.1 ± 0.2	1.1 ± 0.2	1.1 ± 0.2	1.1 ± 0.2	1.1 ± 0.2	1.1 ± 0.2
CO (ppm)	1.1 ± 0.2	1.1 ± 0.2	1.1 ± 0.2	1.1 ± 0.2	1.1 ± 0.2	1.1 ± 0.2	1.1 ± 0.2	1.1 ± 0.2
CO <sub>2</sub> (%)	1.1 ± 0.2	1.1 ± 0.2	1.1 ± 0.2	1.1 ± 0.2	1.1 ± 0.2	1.1 ± 0.2	1.1 ± 0.2	1.1 ± 0.2
Diesel (ppm)	1.1 ± 0.2	1.1 ± 0.2	1.1 ± 0.2	1.1 ± 0.2	1.1 ± 0.2	1.1 ± 0.2	1.1 ± 0.2	1.1 ± 0.2
Ethane (ppm)	1.1 ± 0.2	1.1 ± 0.2	1.1 ± 0.2	1.1 ± 0.2	1.1 ± 0.2	1.1 ± 0.2	1.1 ± 0.2	1.1 ± 0.2
Ethylene (ppm)	1.1 ± 0.2	1.1 ± 0.2	1.1 ± 0.2	1.1 ± 0.2	1.1 ± 0.2	1.1 ± 0.2	1.1 ± 0.2	1.1 ± 0.2
Formaldehyde (ppm)	1.1 ± 0.2	1.1 ± 0.2	1.1 ± 0.2	1.1 ± 0.2	1.1 ± 0.2	1.1 ± 0.2	1.1 ± 0.2	1.1 ± 0.2
H <sub>2</sub> O (%)	1.1 ± 0.2	1.1 ± 0.2	1.1 ± 0.2	1.1 ± 0.2	1.1 ± 0.2	1.1 ± 0.2	1.1 ± 0.2	1.1 ± 0.2
HNCO (ppm)	1.1 ± 0.2	1.1 ± 0.2	1.1 ± 0.2	1.1 ± 0.2	1.1 ± 0.2	1.1 ± 0.2	1.1 ± 0.2	1.1 ± 0.2
N <sub>2</sub> O (ppm)	1.1 ± 0.2	1.1 ± 0.2	1.1 ± 0.2	1.1 ± 0.2	1.1 ± 0.2	1.1 ± 0.2	1.1 ± 0.2	1.1 ± 0.2
NH <sub>3</sub> (ppm)	1.1 ± 0.2	1.1 ± 0.2	1.1 ± 0.2	1.1 ± 0.2	1.1 ± 0.2	1.1 ± 0.2	1.1 ± 0.2	1.1 ± 0.2
NO (ppm)	1.1 ± 0.2	1.1 ± 0.2	1.1 ± 0.2	1.1 ± 0.2	1.1 ± 0.2	1.1 ± 0.2	1.1 ± 0.2	1.1 ± 0.2
NO <sub>x</sub> High (ppm)	1.1 ± 0.2	1.1 ± 0.2	1.1 ± 0.2	1.1 ± 0.2	1.1 ± 0.2	1.1 ± 0.2	1.1 ± 0.2	1.1 ± 0.2
NO <sub>x</sub> Low (ppm)	1.1 ± 0.2	1.1 ± 0.2	1.1 ± 0.2	1.1 ± 0.2	1.1 ± 0.2	1.1 ± 0.2	1.1 ± 0.2	1.1 ± 0.2
O <sub>3</sub> (ppm)	1.1 ± 0.2	1.1 ± 0.2	1.1 ± 0.2	1.1 ± 0.2	1.1 ± 0.2	1.1 ± 0.2	1.1 ± 0.2	1.1 ± 0.2
Propane (ppm)	1.1 ± 0.2	1.1 ± 0.2	1.1 ± 0.2	1.1 ± 0.2	1.1 ± 0.2	1.1 ± 0.2	1.1 ± 0.2	1.1 ± 0.2
Propylene (ppm)	1.1 ± 0.2	1.1 ± 0.2	1.1 ± 0.2	1.1 ± 0.2	1.1 ± 0.2	1.1 ± 0.2	1.1 ± 0.2	1.1 ± 0.2
Urea ByProduct (ppm)	1.1 ± 0.2	1.1 ± 0.2	1.1 ± 0.2	1.1 ± 0.2	1.1 ± 0.2	1.1 ± 0.2	1.1 ± 0.2	1.1 ± 0.2

Replicate runs on the same biodiesel fuel blend showed very good reproducibility, with comparable spectra between replicate runs on a given biodiesel blend. Individual gas concentration coefficient of variation ranged from 0-65%, but most gases had CV<20% with a general increase in variability with increasing biodiesel content. Further work is needed to ensure accurate individual gas species quantitation in biodiesel exhaust, especially for carbonyl compounds like formaldehyde, a MSAT compound.

The gas-phase emissions of CO<sub>2</sub> did not vary with biodiesel blend for SS40 operation. This is surprising given that CO<sub>2</sub> emissions are tied to fuel consumption; the low 40% load operation may explain this result. The CO concentration in B0 was higher than for the biodiesel blends. Surprisingly, the NO<sub>x</sub> concentrations decreased with increasing biodiesel in the fuel blend (**Figure 3-14**). Total hydrocarbons (THC) decreased with increasing biodiesel, but ammonia increased (**Figure 3-15**).

The MKS parameter identified as “diesel” decreased in concentration from B0 to B50, but then increased to the B0 concentration when the engine operated on B100. The “diesel” analyte is based on manufacturer measurements of the volatile gas-phase compounds produced when diesel fuel was heated. Apparently, the B100 exhaust contained compounds with similar infrared absorbance bands to these “diesel” components. Further investigation of the “diesel” analyte’s characteristics is warranted to better understand the information provided by the MKS MultiGas instrument.

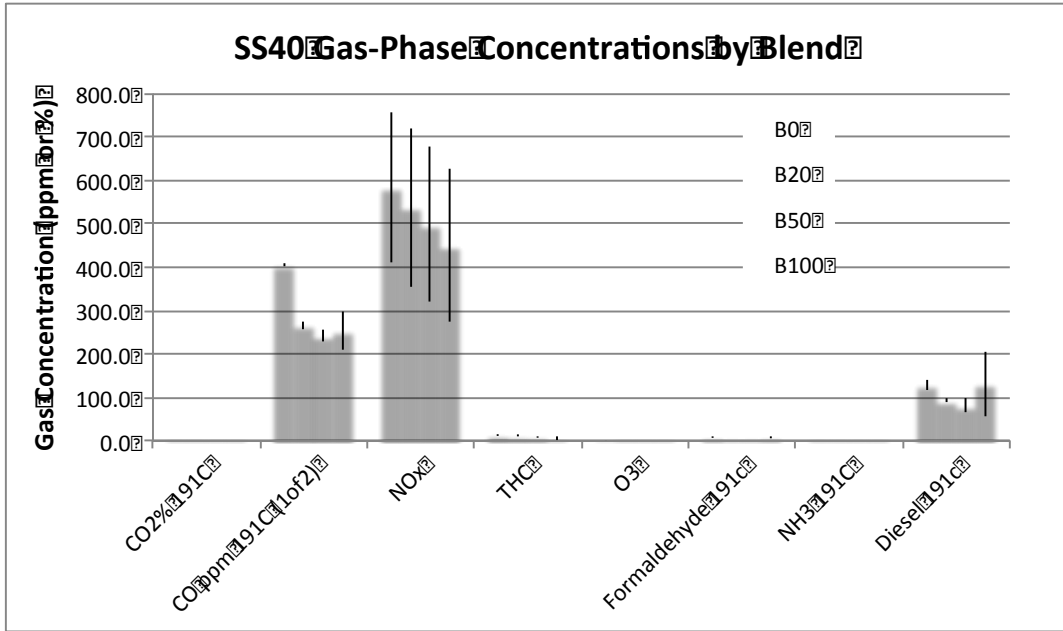


Figure 3-14. Selected Gas Concentrations for SS40 Runs (linear y-axis scale)

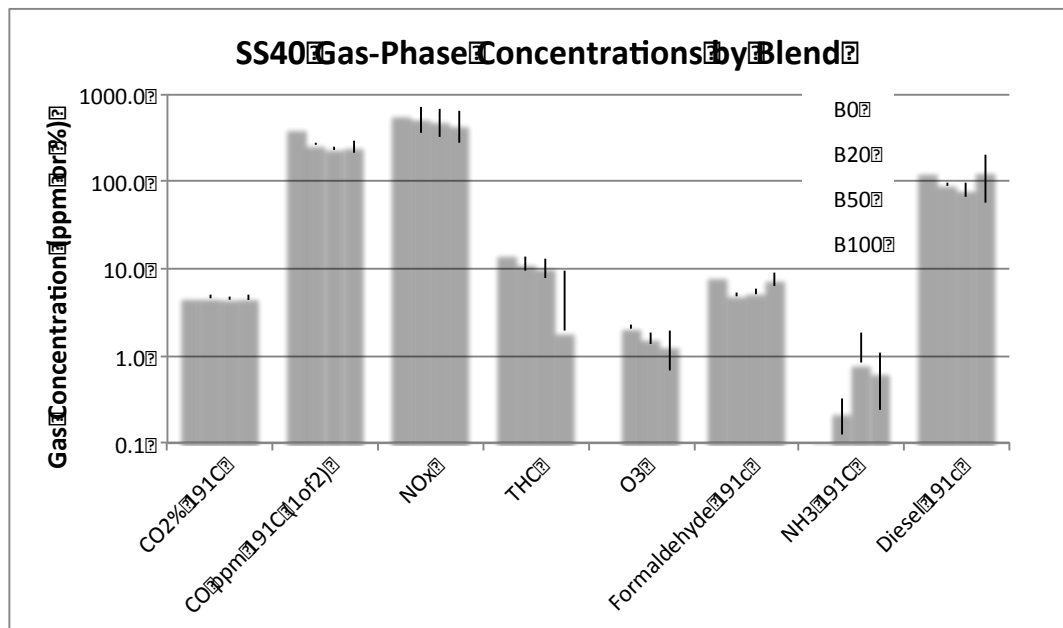


Figure 3-15. Selected Gas Concentrations for SS40 Runs (log y-axis scale). Error bars represent one standard deviation.

## 4. Conclusions

The steady-state emission test experiments enable us to make the following preliminary conclusions on (1) the capabilities of the CM-12 exhaust sampling system and (2) how biodiesel tailpipe emissions vary with blend ratio for a light-duty diesel engine.

Experimental Setup Quality and Reproducibility of Cycle and DR. The data collected thus far are promising. Dilution ratio was consistent with a 4.4% variability over a 6 month sampling period. The initial results have indicated a need for better transfer line temperature control, as the temperature in this line affects both particle evolution and flow measurement accuracy. The temperature control system was upgraded for data collection in 2013 and 2014. Now that the dilution system exhibits a consistent dilution ratio from day to day during steady-state engine operation, more realistic transient engine operation will be investigated in future emissions tests.

Fuel consumption by Bxx. Initial results determined that scantool fuel injection quantity is not an accurate measure of fuel consumption when operating on biodiesel fuels with fuel properties that deviate from those of petrodiesel. Testing of a gravimetric method for fuel consumption demonstrated the usefulness of this approach for biodiesel studies.

Fuel Bxx Composition by Mid-IR. The IROX-D instrument was determined to give reliable biodiesel blend volume % data for B0 to B100 blends as long as fuels with Bxx > 30% were carefully diluted in n-hexanes prior to analysis.

PN Distributions and Total Particle Number. The elevated 10nm particle mode observed in the B50 and B100 distributions indicates a distinct primary nanoparticle formation process occurs for these fuel blends at 40% load, but not at 80% load. In contrast, the accumulation mode (50 nm and greater) particle concentrations did not increase as much with increasing percent biodiesel or percent load.

FTIR Analyzer's Capabilities. Replicate runs on the same biodiesel fuel blend showed very good reproducibility, with comparable spectra between blends and individual gas concentrations varying up to 65% over the steady-state portion of the run for most gases. Further work is needed to ensure that quantitation of individual gases for biodiesel exhaust is reliable and calibrations should be independently verified for complex gas mixtures using GC-MS. Especially important for biodiesel exhaust will be development of FTIR methods to accurately quantify gas-phase carbonyls. Further, a FTIR data analysis method should be developed to identify a surrogate measure for Total HC that meets EPA emission test compliance.

## References Cited

1. U.S. Energy Information Administration. *Annual Energy Review 2011*. Publication DOE/EIA-0384(2011). Sep. 2012, p. 390.
2. Emission Standards: USA: Cars and Light-Duty Trucks—Tier 2. [http://www.dieselnet.com/standards/us/ld\\_t2.php](http://www.dieselnet.com/standards/us/ld_t2.php). Accessed Oct. 14, 2013.
3. Emission Standards: USA: Cars and Light-Duty Trucks—Tier 3. [http://www.dieselnet.com/standards/us/ld\\_t3.php](http://www.dieselnet.com/standards/us/ld_t3.php). Accessed Oct. 14, 2013.
4. NREL. *Biodiesel Handling and Use Guide: Fourth Edition (Revised)*. Publication DOE/GO-102008-2658, NREL/TP-540-43672, 938562. National Renewable Energy Laboratory, Golden, CO., Jan. 2009.
5. Lapuerta, M., O. Armas, and J. Rodriguezfernandez. Effect of biodiesel fuels on diesel engine emissions. *Progress in Energy and Combustion Science*, Vol. 34, No. 2, Apr. 2008, pp. 198–223.
6. Giakoumis, E. G., C. D. Rakopoulos, A. M. Dimaratos, and D. C. Rakopoulos. Exhaust emissions of diesel engines operating under transient conditions with biodiesel fuel blends. *Progress in Energy and Combustion Science*, Vol. 38, No. 5, Oct. 2012, pp. 691–715.
7. Mass-produced cleanliness: BERU Pressure Sensor Glow Plug reduces the emission of pollutants in the new VW 2.0 liter TDI | BorgWarner BERU Systems GmbH. <http://www.beru.com/bw/mass-produced-cleanliness-beru-pressure-sensor-glow-plug-reduces-the-emission-of-pollutants-in-the-n>. Accessed Jan. 31, 2014.
8. Boehman, A. L., D. Morris, J. Szybist, and E. Esen. The Impact of the Bulk Modulus of Diesel Fuels on Fuel Injection Timing. *Energy & Fuels*, Vol. 18, No. 6, Nov. 2004, pp. 1877–1882.
9. Wang, W. G., D. W. Lyons, N. N. Clark, M. Dimaratos, and P. M. Norton. Emissions from Nine Heavy Trucks Fueled by Diesel and Biodiesel Blend without Engine Modification. *Environmental Science & Technology*, Vol. 34, No. 6, Mar. 2000, pp. 933–939.
10. U.S. Environmental Protection Agency (EPA). *A Comprehensive Analysis of Biodiesel Impacts on Exhaust Emissions*. Publication EPA420-P-02-001. US EPA, Oct. 2002.
11. Durbin, T. D., J. R. Collins, J. M. Norbeck, and M. R. Smith. Effects of Biodiesel, Biodiesel Blends, and a Synthetic Diesel on Emissions from Light Heavy-Duty Diesel Vehicles. *Environmental Science & Technology*, Vol. 34, No. 3, Feb. 2000, pp. 349–355.
12. Graboski, M. S., J. D. Ross, and R. L. McCormick. *Transient Emissions from No. 2 Diesel and Biodiesel Blends in a DDC Series 60 Engine*. Publication 961166. SAE International, Warrendale, PA, May 1996.
13. Surawski, N. C., B. Miljevic, G. A. Ayoko, S. Elbagir, S. Stevanovic, K. E. Fairfull-Smith, S. E. Bottle, and Z. D. Ristovski. Physicochemical Characterization of Particulate Emissions from a Compression Ignition Engine: The Influence of Biodiesel Feedstock. *Environmental Science & Technology*, Vol. 45, No. 24, Dec. 2011, pp. 10337–10343.
14. Kittelson, D. B., M. Arnold, and W. F. Watts. Review of Diesel Particulate Matter Sampling Methods: Final Report. <http://www.me.umn.edu/centers/cdr/reports/EPAreport3.pdf>.
15. HEI Review Panel on Ultrafine Particles. *Understanding the Health Effects of Ambient Ultrafine Particles*. Health Effects Institute, Boston, MA, 2013.
16. Brook, R. D., B. Franklin, W. Cascio, Y. Hong, G. Howard, M. Lipsett, R. Luepker, M. Mittleman, J. Samet, S. C. Smith, and I. Tager. Air Pollution and Cardiovascular Disease A Statement for Healthcare Professionals From the Expert Panel on Population and Prevention Science of the American Heart Association. *Circulation*, Vol. 109, No. 21, Jun. 2004, pp. 2655–2671.
17. Gauderman, W. J., E. Avol, F. Gilliland, H. Vora, D. Thomas, K. Berhane, R. McConnell, N. Kuenzli, F. Lurmann, E. Rappaport, H. Margolis, D. Bates, and J. Peters. The Effect of Air Pollution on Lung Development from 10 to 18 Years of Age. *N Engl J Med*, Vol. 351, No. 11, Sep. 2004, pp. 1057–1067.
18. Li, N., J. R. Harkema, R. P. Lewandowski, M. Wang, L. A. Bramble, G. R. Gookin, Z. Ning, M. T. Kleinman, C. Sioutas, and A. E. Nel. Ambient ultrafine particles provide a strong adjuvant effect in the secondary immune response: implication for traffic-related asthma flares. *American Journal of Physiology - Lung Cellular and Molecular Physiology*, Vol. 299, No. 3, Sep. 2010, pp. L374–L383.
19. Wichmann, H., C. Spix, T. Tuch, G. Wölke, A. Peters, J. Heinrich, W. Kreyling, and J. Heyder. Daily mortality and fine and ultrafine particles in Erfurt, Germany part I: role of particle number and particle mass. *Res Rep Health Eff Inst*, No. 98, Nov. 2000, pp. 5–86; discussion 87–94.
20. HEI Air Toxics Review Panel. *Mobile-Source Air Toxics: A Critical Review of the Literature on Exposure and Health Effects*. Publication HEI Special Report 16. Health Effects Institute, Boston, Mass, 2007.
21. Pope, C. A., 3rd, D. G. Renlund, A. G. Kfoury, H. T. May, and B. D. Horne. Relation of heart failure hospitalization to exposure to fine particulate air pollution. *The American journal of cardiology*, Vol. 102, No. 9, Nov. 2008, pp. 1230–1234.
22. US EPA National Center for Environmental Assessment, R. T. P. N., and L. Stanek. Integrated Science Assessment for Particulate Matter (Final Report). <http://cfpub.epa.gov/ncea/cfm/recorddisplay.cfm?deid=216546>. Accessed Aug. 21, 2012.
23. Kittelson, D. B. Engines and nanoparticles. *Journal of Aerosol Science*, Vol. 29, No. 5-6, Jun. 1998, pp. 575–588.
24. Pope, C. A., 3rd, R. T. Burnett, M. J. Thun, E. E. Calle, D. Krewski, K. Ito, and G. D. Thurston. Lung cancer, cardiopulmonary mortality, and long-term exposure to fine particulate air pollution. *JAMA: the journal of the American Medical Association*, Vol. 287, No. 9, Mar. 2002, pp. 1132–1141.
25. Pope, C. A., R. T. Burnett, G. D. Thurston, M. J. Thun, E. E. Calle, D. Krewski, and J. J. Godleski. Cardiovascular Mortality and Long-Term Exposure to Particulate Air Pollution Epidemiological Evidence of General Pathophysiological Pathways of Disease. *Circulation*, Vol. 109, No. 1, Jan. 2004, pp. 71–77.
26. Emission Standards: Europe: Cars and Light Trucks. <http://www.dieselnet.com/standards/eu/ld.php>. Accessed Oct. 17, 2013.
27. Bünger, J., J. Krahl, K. Baum, O. Schröder, M. Müller, G. Westphal, P. Ruhnu, T. G. Schulz, and E. Hallier. Cytotoxic and mutagenic effects, particle size and concentration analysis of diesel engine emissions using biodiesel and petrol diesel as fuel. *Archives of toxicology*, Vol. 74, No. 8, Oct. 2000, pp. 490–498.



28. Fontaras, G., G. Karavalakis, M. Kousoulidou, T. Tzamkiozis, L. Ntziachristos, E. Bakeas, S. Stournas, and Z. Samaras. Effects of biodiesel on passenger car fuel consumption, regulated and non-regulated pollutant emissions over legislated and real-world driving cycles. *Fuel*, Vol. 88, No. 9, Sep. 2009, pp. 1608–1617.
29. Jung, H., D. B. Kittelson, and M. R. Zachariah. Characteristics of SME Biodiesel-Fueled Diesel Particle Emissions and the Kinetics of Oxidation. *Environmental Science & Technology*, Vol. 40, No. 16, Aug. 2006, pp. 4949–4955.
30. Krahl, J., A. Munack, O. Schröder, H. Stein, L. Herbst, A. Kaufmann, and J. Bünger. Fuel Design as Constructional Element with the Example of Biogenic and Fossil Diesel Fuels. *CIGR Journal*, Vol. VII, No. Manuscript EE 04 008, Mar. 2005.
31. Krahl, J., J. Bünger, O. Schröder, A. Munack, and G. Knothe. Exhaust emissions and health effects of particulate matter from agricultural tractors operating on rapeseed oil methyl ester. *Journal of the American Oil Chemists' Society*, Vol. 79, No. 7, Jul. 2002, pp. 717–724.
32. Heikkilä, J., A. Virtanen, T. Rönkkö, J. Keskinen, P. Aakko-Saksa, and T. Murtonen. Nanoparticle Emissions from a Heavy-Duty Engine Running on Alternative Diesel Fuels. *Environmental Science & Technology*, Vol. 43, No. 24, Dec. 2009, pp. 9501–9506.
33. Koo-Oshima, S., N. Hahn, and J. Van Gerpen. *Comprehensive Health and Environmental Effects of Biodiesel as an Alternative Fuel*. 1998.
34. Krahl, J., A. Munack, O. Schröder, H. Stein, and J. Bünger. *Influence of Biodiesel and Different Designed Diesel Fuels on the Exhaust Gas Emissions and Health Effects*. Publication 2003-01-3199. SAE International, Warrendale, PA, Oct. 2003.
35. Aakko, P., N.-O. Nylund, M. Westerholm, M. Marjamäki, M. Moisio, R. Hillamo, and T. Mäkelä. *EMISSIONS FROM HEAVY-DUTY ENGINE WITH AND WITHOUT AFTERTREATMENT USING SELECTED BIOFUELS*. Publication F02E195. 2002.
36. Zimmerman, N., K. J. Godri Pollitt, C.-H. Jeong, J. M. Wang, T. Jung, J. M. Cooper, J. S. Wallace, and G. J. Evans. Comparison of three nanoparticle sizing instruments: The influence of particle morphology. *Atmospheric Environment*, Vol. 86, Apr. 2014, pp. 140–147.
37. Hesterberg, T. W., C. M. Long, S. N. Sax, C. A. Lapin, R. O. McClellan, W. B. Bunn, and P. A. Valberg. Particulate matter in new technology diesel exhaust (NTDE) is quantitatively and qualitatively very different from that found in traditional diesel exhaust (TDE). *Journal of the Air & Waste Management Association (1995)*, Vol. 61, No. 9, Sep. 2011, pp. 894–913.
38. Chen, Y.-C., and C.-H. Wu. Emissions of submicron particles from a direct injection diesel engine by using biodiesel. *Journal of environmental science and health. Part A, Toxic/hazardous substances & environmental engineering*, Vol. 37, No. 5, 2002, pp. 829–843.
39. Tsolakis, A. Effects on Particle Size Distribution from the Diesel Engine Operating on RME-Biodiesel with EGR. *Energy & Fuels*, Vol. 20, No. 4, Jul. 2006, pp. 1418–1424.
40. Tinsdale, M., P. Price, and R. Chen. *The Impact of Biodiesel on Particle Number, Size and Mass Emissions from a Euro4 Diesel Vehicle*. Publication 2010-01-0796. SAE International, Warrendale, PA, Apr. 2010.
41. Hansen, K. F., and M. G. Jensen. *Chemical and Biological Characteristics of Exhaust Emissions from a DI Diesel Engine Fuelled With Rapeseed Oil Methyl Ester (RME)*. Publication 971689. SAE International, Warrendale, PA, May 1997.
42. Macor, A., F. Avella, and D. Faedo. Effects of 30% v/v biodiesel/diesel fuel blend on regulated and unregulated pollutant emissions from diesel engines. *Applied Energy*, Vol. 88, No. 12, Dec. 2011, pp. 4989–5001.
43. US EPA, O. Nitrogen Dioxide | Air & Radiation | US EPA. <http://www.epa.gov/air/nitrogenoxides/>. Accessed Feb. 25, 2014.
44. Lin, Y.-H., H. Zhang, H. O. T. Pye, Z. Zhang, W. J. Marth, S. Park, M. Arashiro, T. Cui, S. H. Budisulistiorini, K. G. Sexton, W. Vizuete, Y. Xie, D. J. Luecken, I. R. Piletic, E. O. Edney, L. J. Bartolotti, A. Gold, and J. D. Surratt. Epoxide as a precursor to secondary organic aerosol formation from isoprene photooxidation in the presence of nitrogen oxides. *Proceedings of the National Academy of Sciences of the United States of America*, Vol. 110, No. 17, Apr. 2013, pp. 6718–6723.
45. Ozone | Air & Radiation | US EPA. <http://www.epa.gov/ozone/>. Accessed Feb. 25, 2014.
46. Szybist, J. P., J. Song, M. Alam, and A. L. Boehman. Biodiesel combustion, emissions and emission control. *Fuel Processing Technology*, Vol. 88, No. 7, Jul. 2007, pp. 679–691.
47. Peterson, C. L., and D. L. Reece. *Emissions Testing with Blends of Esters of Rapeseed Oil Fuel With and Without a Catalytic Converter*. Publication 961114. SAE International, Warrendale, PA, May 1996.
48. Lapuerta, M., O. Armas, and R. Ballesteros. *Diesel Particulate Emissions from Biofuels Derived from Spanish Vegetable Oils*. Publication 2002-01-1657. SAE International, Warrendale, PA, May 2002.
49. Dorado, M. P., E. Ballesteros, J. M. Arnal, J. Gómez, and F. J. López. Exhaust emissions from a Diesel engine fueled with transesterified waste olive oil☆. *Fuel*, Vol. 82, No. 11, Jul. 2003, pp. 1311–1315.
50. Zhang, Y., and A. L. Boehman. Impact of Biodiesel on NO<sub>x</sub> Emissions in a Common Rail Direct Injection Diesel Engine. *Energy & Fuels*, Vol. 21, No. 4, Jul. 2007, pp. 2003–2012.
51. US EPA, O. Carbon Monoxide | Air & Radiation | US EPA. <http://www.epa.gov/airquality/carbonmonoxide/>. Accessed Feb. 25, 2014.
52. Health, N. C. for E. CDC - Carbon Monoxide Poisoning - Frequently Asked Questions. <http://www.cdc.gov/co/faqs.htm>. Accessed Feb. 25, 2014.
53. Buyukkaya, E. Effects of biodiesel on a DI diesel engine performance, emission and combustion characteristics. *Fuel*, Vol. 89, No. 10, Oct. 2010, pp. 3099–3105.
54. Bakeas, E., G. Karavalakis, and S. Stournas. Biodiesel emissions profile in modern diesel vehicles. Part 1: Effect of biodiesel origin on the criteria emissions. *Science of The Total Environment*, Vol. 409, No. 9, Apr. 2011, pp. 1670–1676.
55. Fontaras, G., M. Kousoulidou, G. Karavalakis, T. Tzamkiozis, P. Pistikopoulos, L. Ntziachristos, E. Bakeas, S. Stournas, and Z. Samaras. Effects of low concentration biodiesel blend application on modern passenger cars. Part I: Feedstock impact on regulated pollutants, fuel consumption and particle emissions. *Environmental Pollution*, Vol. 158, No. 5, May 2010, pp. 1451–1460.
56. U.S. EPA. *Control of Hazardous Air Pollutants From Mobile Sources*. FRN: 06-02315.
57. Karavalakis, G., V. Boutsika, S. Stournas, and E. Bakeas. Biodiesel emissions profile in modern diesel vehicles. Part 2: Effect of biodiesel origin on carbonyl, PAH, nitro-PAH and oxy-PAH emissions. *The Science of the total environment*, Vol. 409, No. 4, Jan. 2011, pp. 738–747.
58. Chien, S.-M. Effects of Biodiesel Blending on Particulate and Polycyclic Aromatic Hydrocarbon Emissions in Nano/Ultrafine/Fine/Coarse Ranges from Diesel Engine. *Aerosol and Air Quality Research*, 2009.

59. EPA (US). National Ambient Air Quality Standards (NAAQS) | Air and Radiation | US EPA. <http://www.epa.gov/air/criteria.html>. Accessed Mar. 5, 2012.
60. EPA (US). Particulate Matter | Air & Radiation | US EPA. <http://www.epa.gov/pm/>. Accessed Mar. 5, 2012.
61. EPA (US). Health | Particulate Matter | Air & Radiation | US EPA. <http://www.epa.gov/pm/health.html>. Accessed Mar. 5, 2012.
62. Abdul-Khalek, I. S., D. B. Kittelson, B. R. Graskow, Q. Wei, and F. Bear. *Diesel Exhaust Particle Size: Measurement Issues and Trends*. Publication 980525. SAE International, Warrendale, PA, Feb. 1998.
63. Seinfeld, J. H., and S. N. Pandis. *Atmospheric chemistry and physics : from air pollution to climate change*. J. Wiley, Hoboken, N.J., 2006.
64. Davis, S. C., S. W. Diegel, and R. G. Boundy. Transportation Energy Data Book. Oak Ridge National Laboratory, ORNL-6985 (Edition 29 of ORNL-5198). *Center for Transportation Analysis, Energy and Transportation Science Division*, 2010.
65. Black, K. N., F. Divita Jr, R. A. Margiotta, and R. Guensler. Correlating Particulate Matter Mobile Source Emissions to Ambient Air Quality. 2004.
66. Davis, S. C., S. W. Diegel, and R. G. Boundy. *Transportation Energy Data Book: Edition 30*. Publication ORNL/TM-2011/229, 1020812. Jul. 2011.
67. U.S. Clean Diesel Auto Sales Increase 35 Percent in 1st Quarter of 2012 - MarketWatch. <http://www.marketwatch.com/story/us-clean-diesel-auto-sales-increase-35-percent-in-1st-quarter-of-2012-2012-04-17>. Accessed May 29, 2012.

## Appendices

Information on instrument setup details, standard operating procedures for fuel blending and tables of raw experimental results are provided in the following 5 appendices.

<b>APPENDICES .....</b>	<b>53</b>
<b>Appendix A. Experimental Sampling Setup Instrumentation Detail .....</b>	<b>54</b>
<b>Appendix B. Biodiesel Fuel Blending Procedures .....</b>	<b>56</b>
<b>Appendix C. Sampling Logsheets .....</b>	<b>65</b>
<b>Appendix D. Raw Data Tables .....</b>	<b>71</b>
<b>Appendix E. Biodiesel .....</b>	<b>Error! Bookmark not defined.</b>

## Appendix A. Experimental Sampling Setup Instrumentation Detail

Table A.1. CM-12 Light-Duty Diesel Engine Dynamometer Test Equipment

Equipment List			
Description	Use	QTY	Model Number
<b>PM Collection</b>			
1	Gas Pump	Filter Sampling	3 714645-V114-D303X
2	Gas Pump	Impinger/Filter Sampling	1 0523-101Q-G588DX
3	Pall/Gelman 7mm Filter Holders	Filter Sampling	8 2220
<b>Gas Phase Pollutant Collection</b>			
4	MKS FTIR	Gas Phase Pollutant Collection	1 Multigas 2030HS
5	Cole-Parmer Sample Pump	FTIR Sample Pump	1 L-79200-00
6	Applus+ AutoLogic Inc. Gas Analyzer	Gas Phase Pollutant Collection	1 310-0120REV.B
7	URG Denuders	Gas Phase Pollutant Collection	6 URG-2000-30B4-242
<b>PN Collection</b>			
8	TSI Engine Exhaust Particle Sizer	Real Time PN Distribution Collection	1 3090
9	TSI Ultrafine Condensation Particle Counter	Real Time PN Collection	1 3025A
10	TSI Electrostatic Classifier	Particle Size Selector	1 3080
11	TSI Electrical Aerosol Detector	Real Time PN Collection	1 3070A
<b>Dilution Air System</b>			
12	Craftsman Air Compressor	Pressurize and Store Room Air	1 919.167340
13	Craftsman Air Compressor	Pressurize and Store Room Air	1 919.167220
14	Condor MDR3 Pressure Switch	Compressor Control	1 31GC3FXX
15	Schneider Electric Contactor	Compressor Control	1 199AX-9
16	Artisan Delay-on-make Relay	Compressor Control	1 438USA
17	Course Pressure Regulator	Air Pressure Control	1 N/A
18	Condenser/Expansion Tank	Air Drying	1 Custom Built
19	Ingersoll Rand Precision Air Pressure Regulator	Air Pressure Control	1 PR4031-100
20	4'x2" Diameter Desiccant/Activated Charcoal Tube	Air Drying and Purification	1 Custom Built
21	Whatman HEPA-CAP 150 Filter	Air Purification	1 6702-9500
22	Ice Bath Heat Exchanger	Temperature Control	1 Custom Built
23	OMEGA Mass Flow Meter	Flow Measurement	1 FMA 1742
24	OMEGA Pressure Transducer	Pressure Measurement	1 PX319-100GI
25	Fuji Electronics Temperature Controller	Temperature Control	2 PXR3-TEY1-4V0A1
26	Carlo Gavazzi Solid State Relay	Temperature Control	2 RM1E23AA25
27	Brisk Heat Heat Cords	Temperature Control	3 HWC1060
28	Dwyer Magnehelic	Flow Measurement	2 605-1&605-0
<b>Data Collection System</b>			
29	Agilent Power Supply	Sensor Excitation	1 E3631A
30	National Instruments Electronics Enclosure	Data Acquisition Electronics	1 CA-1000

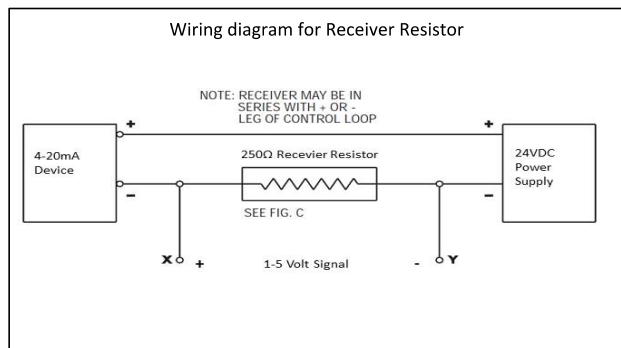
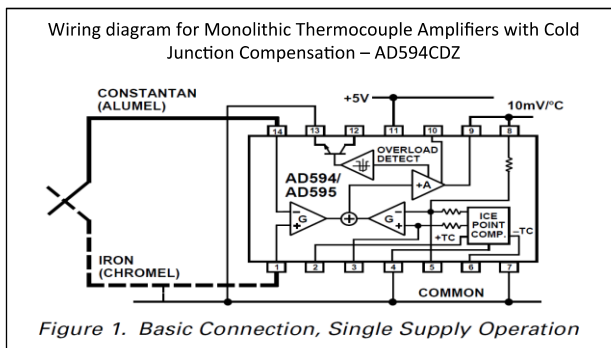
Table A.2. Scantool 8-bit Interpretation Table

8 Bit System									
bit value	1	2	4	8	16	32	64	128	
bit position	1	2	3	4	5	6	7	8	byte values
Binary	0	0	0	0	0	0	0	0	= 0
	1	0	0	0	0	0	0	0	= 1
	1	0	1	0	1	0	1	0	= 85
	1	1	1	1	1	1	1	1	= 255

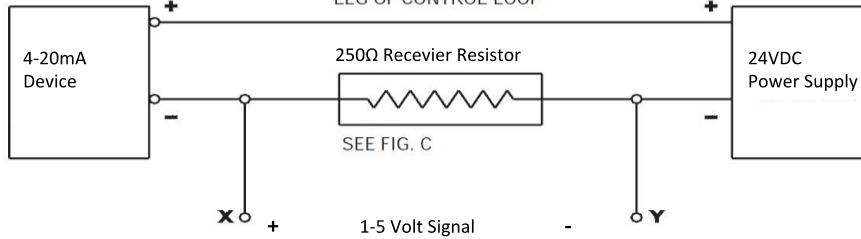
**Table A.3. Labview Channel Setup**

Physical Channel	Device	Log Order	Sensor Output	Signal Conditioning	Labview Expected Signal Range
Analog Input 0	Raw Filter/ Flow Totalizer Pressure	13	4-20mA	Receiver Resistor	1-5V
Analog Input 1	Dilution Air MAG	0	4-20mA	Receiver Resistor	0-5V
Analog Input 2	Transfer Line MAG	1	4-20mA	Receiver Resistor	0-5V
Analog Input 3	Pitot Tube MAG	2	4-20mA	Receiver Resistor	0-5V
Analog Input 4	Ambient Temp	3	4-20mA	Receiver Resistor	1-5V
Analog Input 5	Ambient RH	4	4-20mA	Receiver Resistor	1-5V
Analog Input 6	Dilution Air Pressure	5	4-20mA	Receiver Resistor	1-5V
Analog Input 7	Dilution Air Temperature	6	J-Type Thermocouple	AD594CDZ	0-1.022V
Analog Input 8	Fuel Temperature	7	J-Type Thermocouple	AD594CDZ	0-1.022V
Analog Input 9	Exhaust Temp @ Pitot Tube	8	J-Type Thermocouple	AD594CDZ	0-3.16V
Analog Input 10	Sample Manifold Temp	9	J-Type Thermocouple	AD594CDZ	0-1.022V
Analog Input 11	OMEGA Dil Air Flow Meter	10	0-5V	None	0-5V
Analog Input 12	Volkswagen MAF Sensor	11	0-5V	None	0-5V
Analog Input 13	Transfer Line Temp	12	J-Type Thermocouple	AD594CDZ	0-2.087V
Analog Input 14	-	-	-	-	-
Analog Input 15	-	-	-	-	-

Note: Labview Logs the Fuel Scale through an RS232 connection to the PC, not through the DAQ Card



NOTE: RECEIVER MAY BE IN SERIES WITH + OR - LEG OF CONTROL LOOP



## **Appendix B. Biodiesel Fuel Blending & Analysis Procedures**

### **Standard Operating Procedures for Signature Project #2**

#### **Biodiesel Emissions and Performance Testing with the Armfield CM-12 Engine Testbed.**

**This document is a compilation of a number of standard operating procedures.**

#### **Authors:**

Daryl Deprey

Tyler Feralio

Brad Haire April 22, 2011

#### **Table of contents**

- I. BXX Biodiesel Splash Blending Procedure
    - I.1. Abstract
    - I.2. Safety Precautions
    - I.3. Step by Step Procedure
    - I.4. Clean up
  - II. Fuel Purging Procedure
    - II.1. Abstract
    - II.2. Safety Precautions
    - II.3. Step by Step Procedure
  - III. IROX Diesel Fuel Analysis Procedure
- 

## **I. BXX Biodiesel Splash Blending Procedure**

### **1.1. Abstract:**

Biodiesel (B100) is typically mixed with petrodiesel for use. The mixture is denoted as BXX where XX is the percentage by volume of biodiesel to petrodiesel. For example, B85 is 85% biodiesel (B100), 15% petrodiesel by volume. B100 is 100% biodiesel. Biodiesel generally has a higher specific gravity than petrodiesel so a splash blending technique with inversion mixing will adequately blend the fuels. BXX Blends will be prepared 24 hours before usage to ensure complete mixing.

### **1.2. Safety Precautions:**

Safety goggles, gloves, and protective clothing (apron) shall be worn while mixing all fuels. The fuel blends should be prepared in a laboratory fume hood or equally well-ventilated area.

### **1.3. Step by Step Procedure:**

- I.3.1. With the desired BXX blend determined prior to mixing, appropriately label the red 6 gallon plastic fuel storage container with the following information: BXX blend; Batch Number; Date; Biodiesel Feedstock, Supplier and Date Acquired; Petrodiesel Source, and Date Acquired. Labels should be acquired for this information. The label, after it is applied and filled out, should be covered with clear packing tape to prevent the ink on the label from bleeding if it gets wet.
- I.3.2. Determine the BXX blend desired for mixing. Refer to *Table 1* below for accurate volumes of biodiesel and petrodiesel for desired blend ratio.

**Table 2: BXX Mixing Volumes to Prepare 10 Liters of Blended Biodiesel Fuel**

10 L BXX Mixing Volumes				
Designed by: Daryl Deprey & David Wheeler				
Date: 6/4/2010				
BXX	% Biodiesel	Volume Biodiesel (L)	% Petrodiesel	Volume Petrodiesel (L)
B2	2	0.2	98	9.8
B5	5	0.5	95	9.5
B15	15	1.5	85	8.5
B20	20	2	80	8
B100	100	10	0	0

- I.3.3. Using the 1L glass graduated cylinder, measure and pour the appropriate volume of petrodiesel into the designated BXX blend storage fuel tank.
- I.3.4. Using the 1L glass graduated cylinder designated for B100 biodiesel and appropriate feedstock, measure and pour the determined volume of biodiesel into the designated BXX storage fuel tank. **IMPORTANT: The biodiesel must be added to the fuel tank after the petrodiesel to ensure complete splash blending.**
- To further ensure complete blending, inversion mixing must be done. With the storage container sealed shut, slowly invert the tank every taking 3 seconds to complete the inversion 15 times to further and completely blend the fuels
- I.3.5. Place the BXX fuel mixture into the fire safety cabinet and store for 24 hours prior to experimental use to finish blending.
- I.3.6. To identify if complete blending has been achieved, remove one 30mL sample each from at the top, middle and bottom of the fuel tank with a 30mL pipet. These samples should then be placed in 30mL amber glass bottles and labeled appropriately.
- I.3.7. Analyze these samples using the IROX-Diesel FTIR instrument. The technique for testing will be done following the IROX-Diesel Analysis Procedure. Compare the sample density results; if the density values for the three samples are within 0.5% of each other then complete mixing has been achieved. Record the test name and number in both the test log and on the fuel storage container.
- I.4. Clean up:
- I.4.1. Wash all glassware down with hot soapy water.
- After the glassware is clean it will no longer smell of fuel
- I.4.2. Rinse glassware with Deionized water
- I.4.3. Rinse glassware with Acetone for quick drying

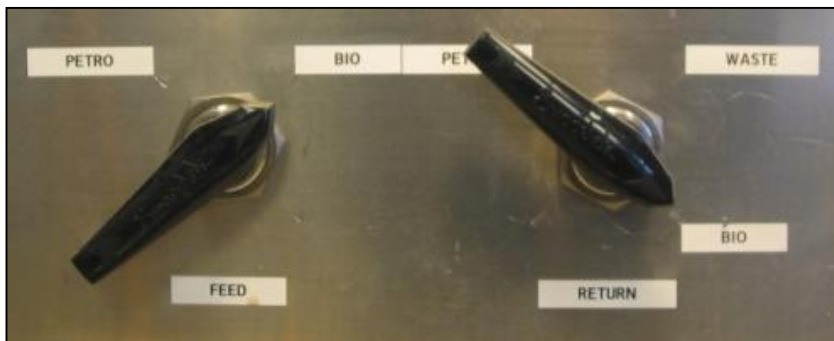
## II. Fuel Purging Procedure

This is the procedure for purging from one fuel to another for the Armfield CM-12 engine. To ensure consistent methodology and cleaning of system and to eliminate cross-contamination of fuels the fuels lines must be purged of the previous run's fuel.

**Safety.** Safety goggles, gloves, and protective clothing should be worn. Area should also be well ventilated while swapping fuels and running the Armfield engine.

### Procedure:

1. Make sure there is enough fuel in both the biodiesel and diesel fuel tanks to complete the purging process. This will be a function of the volume of fuel contained in the fuel lines, filter, and injection pump. At 0% throttle/ 0% brake the volumetric flow rate of the fuel flowing through the return fuel line has been measured to be approximately 1 Liter/min. To determine the volume of fuel and time necessary to purge the fuel system samples of fuel from the return fuel line should be taken once every minute from the time that the 'FEED' valve is changed. These samples can then be tested with the IROX-D to determine how long it takes for the fuel system to purge to the new fuel.
2. Purging from Diesel to Biodiesel:
  - a. Start engine and warm up at 0% throttle/ 0% brake for 5 minutes.



- b. Switch 'FEED' valve to 'BIO' and 'RETURN' valve to 'WASTE' as close to simultaneously as possible.
  - c. Allow engine to run for 5 minutes or until the fuel in the fuel line is known to have fully purged.
  - d. Switch 'RETURN' valve to 'BIO'
3. Purging from Biodiesel to Diesel:
    - a. Start engine and warm up at 0% throttle/ 0% brake for 5 minutes.
    - b. Switch 'FEED' valve to 'PETRO' and 'RETURN' valve to 'WASTE' as close to simultaneously as possible.
    - c. Allow engine to run for 5 minutes or until the fuel in the fuel line is known to have fully purged.
    - d. Switch 'RETURN' valve to 'PETRO'



# IROX Diesel Fuel Analysis Procedure

## Abstract:

The IROX Diesel can be used to analyze properties of petrodiesel, biodiesel, and blends of both. The IROX Diesel instrument uses Fourier transform infrared spectroscopy to determine characteristics of fuel. The IROX diesel instrument determines the mid-range infrared absorption spectrum. The mid-infrared wavenumber range analyzed is  $650\text{cm}^{-1}$  to  $3100\text{cm}^{-1}$ . This is done by an infrared source emitting the range of wavelengths through a sample. A detector then determines the absorption of the sample. Organic compounds create distinct peaks in the mid-infrared spectrum. The IROX Diesel is used to create the mid-infrared spectrum to determine the organic compounds that exist in the fuels. The purpose of this procedure is to document how the IROX Diesel instrument and IROX MiniWin program are used to analyze fuel samples.

## Safety:

Safety goggles, gloves, and protective clothing should be worn. Area should also be well ventilated while pouring fuels for IROX analysis.

## Materials:

- 30mL Amber Glass Bottles w/ Teflon Cap
- 40mL Hexanes, HPLC, 98.5%, UN1208
- IROX Diesel FTIR Instrument V3.21; Serial # 21-520-0300
- MiniWin IROX Software V2.24
- Pipettor
- 25mL Beaker
- 30mL Pipet

## 3.1 IROX Diesel Setup and Calibration

1. Switch on the instrument with the power switch above the power connector on the rear panel.
2. Wait for the instrument to run through the initiation steps which include, “warming up FTIR” and “adjusting FTIR” until the **Hexane calibration menu** appears as seen below in *Figure 1*.



Figure 1: IROX Diesel Hexane Calibration Menu

- a. **ATTENTION:** The Calibration of the FTIR spectrometer must be performed once a day before the IROX is used for sample measurements. Make sure that the machine is only completing one rinse cycle. Otherwise it will consume 5 ml extra

per rinse. Also be sure that **auto** is selected (has thick border) under **setup** menu. If it is not, move cursor to **auto** and press **TASK**. **Auto** should be highlighted when the cursor is moved to another selection. Auto uses makes the IROX-D use the auto sampler tube to acquire the sample instead of the operator using a syringe.

- b. To navigate to the calibration menu move the cursor to “**calib.**” and select **TASK**. The cursor should then be moved to “**FTIR**” and **TASK** will be selected again. This will bring you to the calibration menu as previously shown in *Figure 1*.
3. Add approximately 15mL of 98.5%, HPLC grade, Hexanes (GIVE manufacturer and catalog # currently in use) to a clean, acid washed 25mL glass beaker. This will be used for the calibration.
4. With the sample tube connected to the Luer inlet on the right side of the IROX, insert the end of the tube into the beaker of n-Hexanes, as shown in *Figure 2* below.

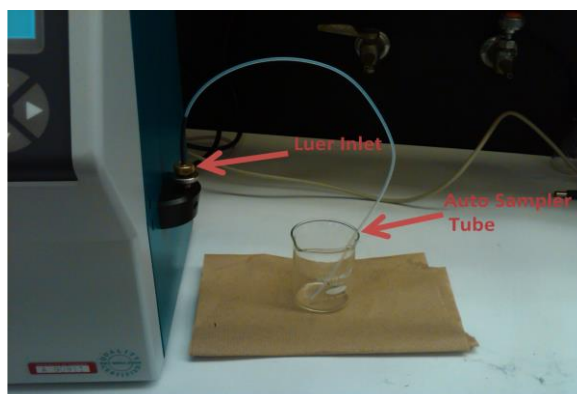


Figure 2: IROX Diesel Sampling Setup

5. Press **RUN** to start the calibration measurement and follow the instructions on the display to remove the sampling tube when prompted.
6. When the measurement is finished, the display changes to back to the Hexane calibration menu.
  - a. According to an email with the Grabner Support Team, the magnitudes of the peaks on the calibration reference spectrum are not indicative of the quality of the calibration. As long as no errors are reported by the instrument the calibration is “acceptable”. Move the cursor to **SAVE** and press **TASK**. If an error occurs the machine should be readjusted. This can be done by going selecting “**setup**” in the main menu then selecting “**adjust**” and pressing **TASK**. The calibration will then have to be repeated.
7. Shift the cursor to **END** and press **TASK**. The new reference spectrum is stored and used for further calculation of concentrations.
8. The display will show the Start-up menu as shown below in *Figure 3*.

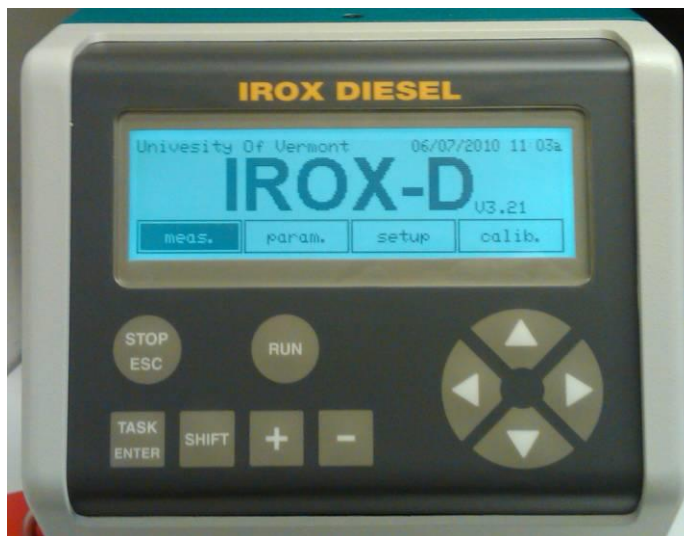


Figure 3: IROX Main Menu

### 3.2 Fuel Sampling:

Using a 30 mL pipet and pipette remove 30mL of sample fuel from the desired fuel tank. Place this sample into a 30mL amber glass bottle and close with proper Teflon cap. The sample can then be stored at room temperature or used for further testing.

### 3.3 Testing Fuel Samples Using IROX MiniWin V2.24:

1. Prepare the sample of fuel by filling a minimum of 15mL of fuel from the sample bottles into a 25 mL beaker and place the sample tube in the sample as shown in *Figure 2* above.
2. Open IROX MiniWin version 2.24 file path, C:\Program Files\Grabner Instruments\Miniwin Irox the Dell Latitude E6400 companion laptop .
3. Verify that the IROX Diesel instrument is connected to IROX MiniWin by viewing the COM status in *the bottom right corner* of the program as shown in *Figure 4*. “IROX-D V 3.21” should show up in the middle box as shown.

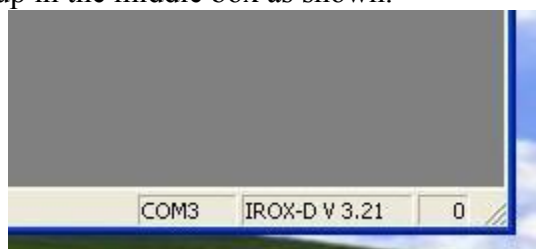


Figure 4: IROX MiniWin COM Status

4. Select the “IROX Measurement” button on the toolbar, as shown by the red arrow in *Figure 5* below.

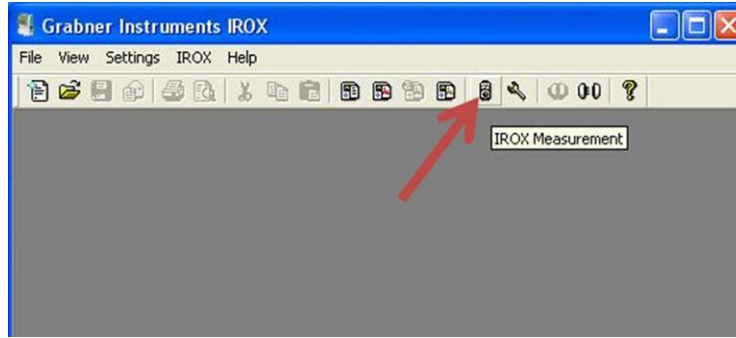


Figure 5: IROX MiniWin V2.24, Measure Button

5. The measurement window that opens is shown in *Figure 6*. In this window, properly name the test under “Sample-ID” and make sure “1” is selected under “Groups”. Select “SET” in the window to upload the test name and group number to the IROX instrument.
  - a. “Group 1” selects the default characteristics that the instrument will analyze.  
<<LIST THOSE CHARACTERISTICS HERE>>
  - b. The Sample-ID, test operator, type of fuel being testing, and date should also all be recorded IROX Logbook found near the computer.

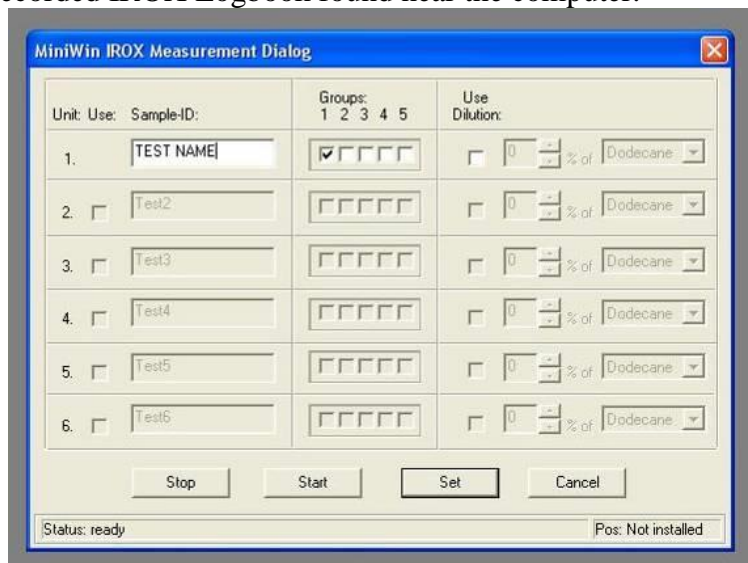


Figure 6: IROX MiniWin Measurement Window

6. Select “**Start**” in the measurement window. The instrument will begin the analysis procedure. Observe the IROX Diesel instrument display and remove the sample tube when prompted.

Always download and save the IROX spectra after the instrument has completed its task under the same name as the file name used in step 5. (Figure 7)

7. After the analysis another measurement can be performed by following these instructions.

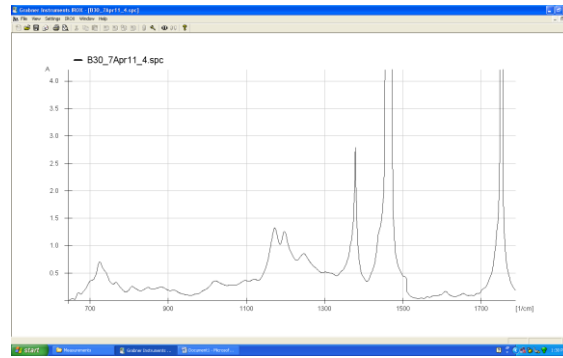


Figure 7: IROX Spectrum output

### 3.4 Viewing Results and Spectrum Using IROX MiniWin:

When the analysis is finished the WHAT KIND? (does this mean spectrum or the interpreted parameters?) results should be downloaded in IROX MiniWin. Selecting the “Download Result” button on the toolbar, as shown in *Figure 8*, downloads the result to the compiled result list. If no list is opened it will start a new list.

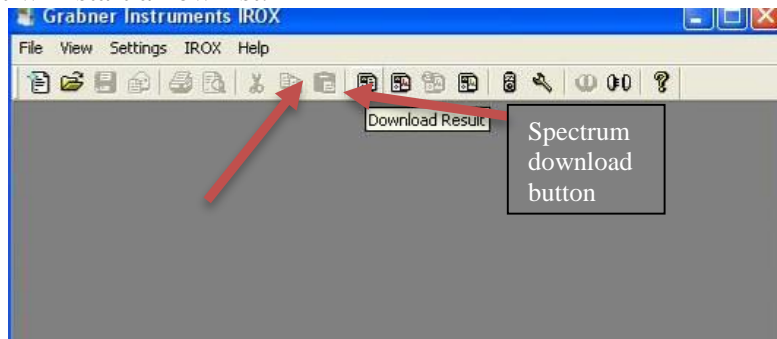


Figure 8: IROX MiniWin Download Result Button

1. To view the individual sample results, select the measurement from the list. The results will appear above the list. Scroll through the list to view desired characteristics. The results list and results are shown below in *Figure 9*. If there was a specific warning associated with the sample it would be displayed

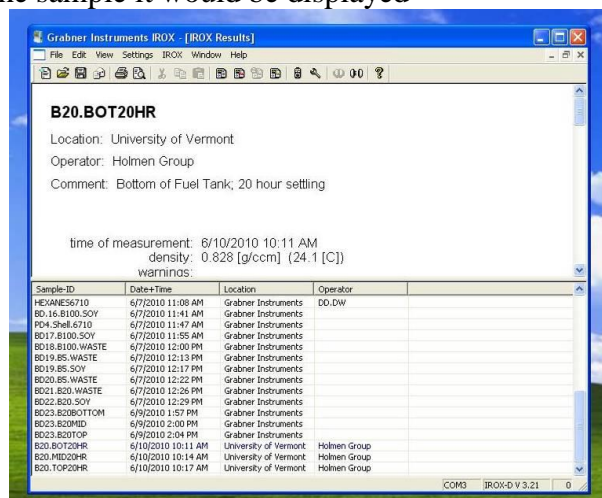


Figure 9: IROX MiniWin Results Window

- To download the FTIR spectrum produced by the instrument select “Download Spectrum” on the toolbar as shown in *Figure 9*.

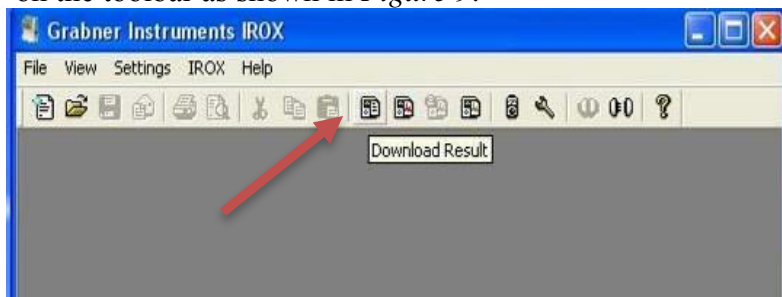


Figure 10: IROX MiniWin Download Spectrum Button

THIS FIGURE IS SAME AS FIG 8... please FIX.

- The spectrum should then be saved with the date in the folder C:\Documents and Settings\Rose\My Documents\IROX Diesel Tests\ the companion laptop.

### 3.5 Shutting Down and Cleaning the IROX Diesel Instrument

- When testing is complete for the day, fill the syringe supplied with the instrument with 5mL of n-Hexanes. With the sample tube removed, place the syringe in the Luer inlet and slowly inject the 98.5%, HPLC grade, Hexanes into the instrument.
- Using the empty syringe inject several pumps of air into the instrument. This is done to clean the instrument and eliminate contamination of the instrument after usage.
- To shut down the instrument make sure nothing is running and turn the switch located on the back of the instrument off.
- Dispose of waste fuel in a properly labeled waste container.

#### References:

- NREL: Biodiesel handling and use guide
- IROX MiniWin Manual
- IROX Quick Start Guide
- Skoog, Douglas A., and James J. Leary. *Principles of Instrumental Analysis*. Fort Worth: Saunders College Pub., 1992. Print.

Table B.1 Fuel Purchase and Delivery Log

Distributor	Fuel	Delivery Date	Quantity (Gal)	Price/Gal	Federal Tax/Gal
Burke	Soy Biodiesel	20-Sep-2010	20	3.00	
Trono	Petrodiesel	22-Oct-2010	54.5	2.68	0.244
Trono	Petrodiesel	9-Mar-2012	51.2	3.86	0.244
Burke	Soy Biodiesel	9-May-2012	20	3.00	0.1875
Trono	Petrodiesel	15-Jan-2013	104.8	3.82	0.244
UConn	Soy Biodiesel	17-Jan-2013	50		
UConn	WVO Biodiesel	17-Jan-2013	158		
Trono	Petrodiesel	19-Mar-2013	53.8	3.65	0.244

## Appendix C. Sampling Checklists and Logsheets

Figure C.1. Run Logsheet

The UNIVERSITY of VERMONT												TAQ LAB											
ARMFIELD ENGINE: EMISSIONS SAMPLING LOGSHEET												Fuel Type		Bend Date									
NOTE: Please fill all relevant sections highlighted in yellow												Test ID Code*:				Fuel Type		Bend Date					
Date:								Engine Start Time:						Notes									
Operators:								Engine End Time:															
Ambient Sampling Conditions in the Lab				Temp. (deg C)				Mini-Diluter Time ON															
				Rel. Humidity (%)				Mini-Diluter Time OFF															
Setup:																							
Husky Compressor Outlet Pressure (psi):								Impinger Solution:															
Driving cycle info:																							
Heat Tape (% / Temperature)								Time ON:				Temp:											
Heat Tape (% / Temperature)								Time ON:				Temp:											
OMEGA FM -Approximate Rate ( L/min)																							
SMPS Used				Yes/No				ELPI Used				Yes/No											
Number of Filters & their locations						Number of impingers & their locations																	
Filter ID:	Location	Pump ID	Flow Rate (L/min)	Time ON	Time OFF	Filter ID:	Location	Pump ID	Flow Rate (L/min)	Time ON	Time OFF	Total Vol. Sampled											
Magnehelic Readings					SMPS and ELPI Information																		
Time	Exhaust	Diluter	Pitot	Remarks	SMPS				ELPI														
					PC ID																		
					File Name																		
					Run Scan No.																		
					Issues				Issues														
					Mean				#DIV/0!														
					SD				#DIV/0!														
					RSD (%)				#DIV/0!														

\*Test ID Code Format: 1-09-26-10-B00  
 Run number for - Month - Day - Year- Fuel (B00=PetroDiesel)  
 the day

Figure C.2. Labels sheet for PM Filter Petri dishes

Armfield Filter	QFF Teflo	#69
	FF	
Project:		
Prewriteight:	Postweight:	Test#:
g	g	Date:
Date: By:	Date: By:	TP DS

Armfield Filter	QFF Teflo	#70
	FF	
Project:		
Prewriteight:	Postweight:	Test#:
g	g	Date:
Date: By:	Date: By:	TP DS

Armfield Filter	QFF Teflo	#71
	FF	
Project:		
Prewriteight:	Postweight:	Test#:
g	g	Date:
Date: By:	Date: By:	TP DS

Armfield Filter	QFF Teflo	#72
	FF	
Project:		
Prewriteight:	Postweight:	Test#:
g	g	Date:
Date: By:	Date: By:	TP DS







Figure C.5. Aggressive Drive Cycle Worksheet

## Aggressive Cycle Worksheet

Your Name – \_\_\_\_\_  
 People Present – \_\_\_\_\_  
 Date – \_\_\_\_\_  
 Test ID Code – \_\_\_\_\_  
 Total Time @ Start – \_\_\_\_\_ HR \_\_\_\_\_ MIN  
 Fuel Type – \_\_\_\_\_  
 Solution Type – \_\_\_\_\_  
 Mode Time – \_\_\_\_\_

- Turn Cooling Water on to approximately 15 L/min
- Time at which ignition 'radio' button selected – \_\_\_\_\_
- Scan Tool Start Time – \_\_\_\_\_
- Armfield Start Time – \_\_\_\_\_
- Labview Start Time – \_\_\_\_\_
- Start Engine (Remote, Ignition, Starter)
  - Engine Start time – \_\_\_\_\_
- Warm up Mode (0% brake, 0% throttle)
  - \*Turn radio button for Brake on\*
  - Turn control to 'automatic' and type in a set point RPM to ~100RPM lower then steady state and select 'apply'
  - Time at end of warm up – \_\_\_\_\_
- Mode 1 – RPM 3300; Throttle 40%
  - Activate 'Scheduler'
- Mode 2 - throttle down to 30% @ time \_\_\_\_\_
- Mode 3 - RPM down to 3000 @ time \_\_\_\_\_
- Mode 4 - RPM down to 2700 @ time \_\_\_\_\_
- Mode 5 - RPM down to 2400 @ time \_\_\_\_\_
- Mode 6 - RPM down to 2000 @ time \_\_\_\_\_
- Mode 7 - Throttle up to 35% @ time \_\_\_\_\_
- Mode 8 - Throttle up to 40% @ time \_\_\_\_\_
- Mode 9 - RPM up to 2700; Throttle down to 30% @ time \_\_\_\_\_
- Cool Down Mode - Lower Throttle and Brake to 0% @ time \_\_\_\_\_
- Turn engine off
  - Engine off time – \_\_\_\_\_
  - Total Time @ End – \_\_\_\_\_ HR \_\_\_\_\_ MIN
- Time @ which data logging via Armfield stopped – \_\_\_\_\_
- Time @ which data logging via Labview stopped – \_\_\_\_\_

NOTES:

**Figure C.6. Run Checklist****CM12 Run Checklist:****Pre Run:**

- If running a completely new setup, go through it with Dr. Holmen to make sure everything is in place
- If sampling equipment has been rearranged or added, perform calculation to make sure the sum of the flow required by equipment is not greater than the sample flow
- Start instrument blanks
  - See logsheets for individual pieces of equipment (FTIR, EEPS, ELPI, EAD, SMPS, 5-Gas, etc.)
- Turn compressors on making sure that the drain valves are closed and that the hoses are attached correctly
- Turn the Agilent power supply on for the Labview instruments and set to 24V
- When instrument blanks are complete and the compressors are full, open the valve to turn the dilution system on; record dilution system on time
- Turn the extraction system on
- Make sure all ports are either plugged or going to sampling equipment and that back flow will not occur.
- Start logging Labview data. Record starting time.
- Load the 'blank' impingers.
- Turn Gillian pumps on
- If using the FTIR, load new filter on the inlet and make sure its pump runs for the entirety of all tunnel blanks. If FTIR is not being used make sure the line/port is plugged.
- Start tunnel blanks
  - See logsheets for individual pieces of equipment (FTIR, EEPS, ELPI, EAD, SMPS, 5-Gas, etc.)
- Once all tunnel blanks are complete turn Gillian pumps off and clear them
- Remove and cap the 'blank' impingers and replace with 'test' impingers
- Load filters
- Check to make sure all pump connections are secure and that rotameter valves are fully open

**Starting Engine & Equipment after tunnel blanks are complete**

- Make sure scantool wire is connected
- Turn cooling water flow on
- Start Gillian and Fasco pumps, setting flow rates; record start times (~30sec before engine start)
- Select 'Remote' and 'Ignition' radio buttons in Armfield software
- Start logging scantool and Armfield data; record start times
- Start engine by clicking and holding the 'Start' radio button until the engine starts. Record start time.
  - If there is a false start, turn the 'Ignition' radio button off and back on quickly and try to start again.
- Once engine is running, select the 'Brake' radio button

- Open 'Control' and select 'Automatic'. Change the 'Set point RPM' to ~ 100RPM less than steady state and click 'Apply'.
  - Make sure the 'Brake %' changes to something other than 0 within 1 min of selecting 'Apply'
- ~7.5min after the engine was started, initiate the scheduler

**During Run**

- Monitor equipment and take manual readings during each mode. These readings should be taken after the engine has stabilized (between 1/2way through the mode and the end of the mode). Record the time of the reading.
- Make sure all information is filled out on logsheets

**Shut Down**

- Turn 'Ignition' radio button off in Armfield software to stop engine
- Stop logging through Armfield; record the stop time
- Turn Gillian and Fasco pumps off; record time off (~30sec after engine off)
- Record total volume pumped via Gillian pumps. Clear once recorded.
- Remove 'test' impingers and install 'blank' impingers
- Turn coolant water flow off
- Save Armfield & scantool data to HolmenGroup Drive
- Turn Gillian pumps back on
- Start tunnel blanks
  - See logsheets for individual pieces of equipment (FTIR, EEPS, ELPI, EAD, SMPS, 5-Gas, etc.)
- If using the FTIR, make sure FTIR pump runs to the completion of tunnel blanks for all equipment.
- Once tunnel blanks are complete, remove FTIR inlet filters, store for analysis.
- Stop Labview from logging and save to the HolmenGroup drive
- Start instrument blanks
  - See logsheets for individual pieces of equipment (FTIR, EEPS, ELPI, EAD, SMPS, 5-Gas, etc.)
- Turn off extraction system
- Turn off dilution system
- Turn off compressors
- Once instrument blanks are complete, drain compressor tanks.
- Save all instrument data to :\\HolmenGroup\\SP2\_ArmfieldEngine\\Run Logs\\(Date of run)
- Photocopy and scan all instrument and run logsheets; copies go to Dr. Holmen, scans are saved along with instrument files in a folder called LogSheets&Pics (:\\SP2\_ArmfieldEngine\\Run Logs\\(Date of run)\\LogSheets&Pic)
- Collect fuel samples from fuel tanks once a week.

# Appendix D. Raw Data Tables

**Table D.1. DILUTION RATIO AND TEST CONDITIONS TABLE.**

Date (dd-Mon-YYYY)	Test #	Fuel Blend (Biodiesel % by Vol)	Petrodiesel Feedstock (Distributor, Fuel Purchase Year)	Biodiesel Feedstock (Distributor, Oil Type, Purchase Year)	Test Cycle (Test, Purge, Aggressive, Steady State, Hot Cleanout)	Number of False Start/Cutout Events	Engine Start Time	Engine Off Time	Run Duration (min)	Engine Hours Start	Engine Hours End	Ignition Time On (min)	Log in Dil Sys?	Calculated Dilution Ratio	Notes/Issues	
<b>Changed Dilution System Orifice setup</b>																
23-Jan-2012	N/A	B0	Trono Petro 2010	None	Purge	0	17:48:50	17:59:00	10.2	105:33	105:44	11	N		Purge to B0	
24-Jan-2012	N/A	B0	Trono Petro 2010	None	Test	0	15:55:20	16:02:30	7.2	105:44	105:52	8	N		Testing Mags	
26-Jan-2012	N/A	B0	Trono Petro 2010	None	Test	0				105:52	105:55	3	N		Testing Aerosol Inlet	
30-Jan-2012	1	B0	Trono Petro 2010	None	Steady State 40%	0	14:20:57	15:45:30	84.6	105:55	107:20	85	N		"QnD" - Only collecting PM	
31-Jan-2012	1	B0	Trono Petro 2010	None	Steady State 40%	0	15:02:47	16:27:15	84.5	107:20	108:46	86	N		"QnD" - Only collecting PM	
6-Feb-2012	N/A	B0	Trono Petro 2010	None	Test	0				108:46	108:58	12	N		Testing DilSys changes	
6-Feb-2012	N/A	B0	Trono Petro 2010	None	Test	0				108:58	109:04	6	N		Testing DilSys changes	
7-Feb-2012	1	B0	Trono Petro 2010	None	Steady State 40%	0	15:13:05	16:53:30	100.4	109:04	110:46	102	N	54		-5-Gas did not detect CO2
8-Feb-2012	1	B0	Trono Petro 2010	None	Steady State 40%	0	15:47:00	17:25:00	98.0	110:46	112:32	106	N	50-51		-EEPS - "Concentration Overrange" message -scantool disconnected but was successfully reconnected
9-Feb-2012	1	B20	Trono Petro 2010	Burke Soy 2010	Steady State 40%	0	16:21:00	17:59:00	98.0	112:32	114:11	99	N	50		-Scantool disconnected
10-Feb-2012	1	B20	Trono Petro 2010	Burke Soy 2010	Steady State 40%	1	12:11:00	13:50:00	99.0	114:11	115:50	99	N	53		
1-Mar-2012	N/A	B50	Trono Petro 2010	Burke Soy 2010	Purge	0	11:55:00	12:00:00	5.0	116:17	116:24	7	N			Purged to B50
2-Mar-2012	1	B50	Trono Petro 2010	Burke Soy 2010	Steady State 40%	0	11:45:00	13:23:00	98.0	116:24	118:03	99	N	57-58		-Heat tape malfunction -EEPS - "Concentration Overrange" message -Adjusted Armfield Throttle position to match OBD-II throttle position since last run. Maintained the same OBD-II throttle position throughout runs. -Scantool disconnected -Building water left on for the night prior - cylinder head colder than usual
7-Mar-2012	1	B50	Trono Petro 2010	Burke Soy 2010	Steady State 40%	1	14:15:00	15:51:30	96.5	118:03	119:42	99	N	55-56		-Heat tape only on Aerosol Inlet -Scantool disconnected
13-Mar-2012	1	B50	Trono Petro #0 2012	Burke Soy 2010	Steady State 40%	1	14:22:30	16:00:00	97.5	119:42	121:20	98	N			-Heat tape only on Aerosol Inlet
19-Mar-2012	N/A	B100	Burke Soy 2010	Burke Soy 2010	Purge	0	17:36:00	17:41:00	5.0	121:20	121:26	6	N			Purge to B100
20-Mar-2012	1	B100	Burke Soy 2010	Burke Soy 2010	Steady State 40%	0	13:58:00	15:35:30	97.5	121:26	123:04	98	N	56-57		-EEPS turned off between pre IB & TB -Both heat tapes operational again -Adjusted both heat tape controllers to try to maintain correct temperature
22-Mar-2012	1	B100	Burke Soy 2010	Burke Soy 2010	Steady State 40%	1	13:13:00	14:26:30	73.5	123:04	124:17	73	N	56		-Engine turned off early due to low fuel -EEPS - "Concentration Overrange" message
22-Mar-2012	N/A	B100	Burke Soy 2010	Burke Soy 2010	Test	1	18:15:00			124:17	124:33	16	N			Making sure engine starts back up
26-Mar-2012	1	B100	Burke Soy 2010	Burke Soy 2010	Steady State 40%	0	15:24:30	17:02:30	98.0	124:33	126:12	99	N	55		-Adjusted heat tape setpoint to achieve correct gas temp -Much colder Ambient temp then previous B100 runs -Grounded thermocouple used to collect dilution air and transferline gas temperatures are reporting erroneously
5-Apr-2012	N/A	B0	Trono Petro #0 2012	None	Purge	0				126:18	126:27	9	N			Purge to B0
20-Apr-2012	N/A	B0	Trono Petro #0 2012	None	Test	0				145:33	145:36	3	N			Testing new fuel system
2-May-2012	1	B0	Trono Petro #0 2012	None	Steady State 80%	0	15:21:30	17:21:31	120.0	145:48	147:49	121	N	58		-Scantool disconnected momentarily but reconnected successfully (went back to idle momentarily after warm-up to reconnect)
3-May-2012	N/A	B100	Burke Soy 2010	Burke Soy 2010	Purge	0							N	58		Purge to B100
3-May-2012	1	B100	Burke Soy 2010	Burke Soy 2010	Steady State 80%	0	15:29:00	17:24:30	115.5	147:49	149:50	121	N			-Tried Armfields '2 controller project work' control. It did not work with the setting changes I made. Had to shut down and restart with control typically used. -Forgot to reinitiate Armfield data collection after restart - No Armfield data. Torque toggled between 103 and 104 Nm during SS. -Manually logged fuel tank weight
7-May-2012	1	B0	Trono Petro #0 2012	None	Steady State 80%	0	13:12:00	15:10:00	118.0	149:50	151:48	118	N			Purged to B0 during warm-up Aerosol Inlet orifice clogged
11-May-2012	N/A	B100	Burke Soy 2012	Burke Soy 2012	Purge	0	16:15:00	16:22:30	7.5	151:48	151:56	8	N			Purge to B100
14-May-2012	1	B100	Burke Soy 2012	Burke Soy 2012	Steady State 80%	0	10:03:15	12:00:00	116.8	151:56	153:53	117	N	86.33		Day 1 of 3 day exposures - 10 mice SMPs data - many scans, one sample
15-May-2012	1	B100	Burke Soy 2012	Burke Soy 2012	Steady State 80%	0	9:28:00	11:23:30	115.5	153:53	155:52	119	Y	128.59		Day 2 - Aerosol Inlet orifice clogged
16-May-2012	1	B100	Burke Soy 2012	Burke Soy 2012	Steady State 80%	0	9:18:00	11:13:30	115.5	155:52	157:48	116	N	85.8		Redo day 2 of 3 day exposures - 10 mice 5-Gas missed engine start & warm-up
17-May-2012	1	B100	Burke Soy 2012	Burke Soy 2012	Steady State 80%	0	8:34:00	10:29:30	115.5	157:48	159:44	116	N	85.11		Day 3 of 3 day exposures - 10 mice
24-May-2012	N/A	B100	Burke Soy 2012	Burke Soy 2012	Steady State	0	14:26:30	14:49:00	22.5	159:44	160:06	22	N			Determining source of odor
8-Jun-2012	1	B0	Trono Petro #0 2012	None	Steady State 40%	0	13:42:00	15:14:00	92.0	160:06	161:39	93	N	82		Dilution System Manifold Test
27-Jun-2012	1	B0	Trono Petro #0 2012	None	Steady State 40%	0	11:18:00	14:00:32	162.5	161:39	164:21	162	N	82.95		Dilution System Manifold Test
28-Aug-2012	1	B0	Trono Petro #0 2012	None	Steady State 80%	0	13:24:30	14:50:00	85.5	164:21	165:47	86	Y	85.24		Impinger Redesign Test - Tall Impinger
6-Sep-2012	1	B0	Trono Petro #0 2012	None	Steady State 80%	0	11:03:43	12:28:30	84.8	165:56	167:22	86	Y	99.07		Impinger Redesign Test - Vortex Impinger Clog in Aerosol Inlet
10-Sep-2012	N/A	B0	Trono Petro #0 2012	None	Test	0	10:57:20	10:59:40	2.3	167:22	167:32		N	83.32		Testing Scantool measuring block
10-Sep-2012	N/A	B0	Trono Petro #0 2012	None	Test	1	17:28:00	17:33:49	5.8	167:32	167:49	17	N			Testing Scantool measuring block
12-Sep-2012	1	B0	Trono Petro #0 2012	None	Steady State 80%	0	10:30:30	12:26:00	115.5	168:42	170:38	116	N			Impinger Redesign Test - Vortex Impinger
21-Sep-2012	1	B0	Trono Petro #0 2012	None	Steady State 80%	0	11:18:30	12:47:30	89.0	171:04	172:34	90	Y	88.63		Impinger Redesign Test - Diffused Impinger Clog in Aerosol Inlet
5-Oct-2012	N/A	B0	Trono Petro #0 2012	None	Test	0				172:34	172:44	10	N			Testing cold air intake
8-Oct-2012	N/A	B0	Trono Petro #0 2012	None	Test	0				172:44	172:50	6	N			Demonstrating engine operation
16-Oct-2012	N/A	B0	Trono Petro #0 2012	None	Transient	0				172:50	172:52	2	N			Testing Transient Cycle schedule
24-Oct-2012	1	B0	Trono Petro #0 2012	None	Steady State 80%	0	15:04:30	16:58:00	113.5	172:52	174:46	114	Y	91.57		Impinger Redesign Test - Swirling Impinger
8-Nov-2012	1	B0	Trono Petro #0 2012	None	Steady State 80%	1	10:13:00	12:20:00	127.0	174:46	176:53	127	Y	85.73		
12-Nov-2012	1	B0	Trono Petro #0 2012	None	Steady State 80%	0	10:09:00	12:04:00	115.0	176:54	178:49	115	N	64.87		Impinger Test - Heat Exchanger, Swirling Imp
21-Nov-2012	N/A	B0	Trono Petro #0 2012	None	Transient	0	13:16:30	13:22:30	6.0	178:54	179:01	7	N			Developing Transient Cycle
27-Nov-2012	N/A	B0	Trono Petro #0 2012	None	Transient	0	14:50:30	14:57:00	6.5	179:01	179:09	8	N			Developing Transient Cycle
11-Dec-2012	1	B0	Trono Petro #0 2012	None	Steady State 80%	0	14:15:00	16:10:00	115.0	179:23	181:18	115	N	83.81		Impinger Test - Heat Exchanger w/ catch-can
17-Dec-2012	N/A	B0	Trono Petro #0 2012	None	Transient	0	15:50:00	16:05:00	15.0	181:18			N			Developing Transient Cycle
17-Dec-2012	N/A	B0	Trono Petro #0 2012	None	Transient	0	16:15:30	16:30:00	14.5	181:34	181:49	15	N			Developing Transient Cycle

**Table D.2. Steady-State Test Run Mean Engine Parameters**

Steady-State 40%:

Parameter	1_07FEB2012_B000	1_08FEB2012_B000	1_09FEB2012_B020	1_10FEB2012_B020	1_02MAR2012_B050	1_07MAR2012_B050	1_13MAR2012_B050	1_20MAR2012_B100	1_22MAR2012_B100	1_26MAR2012_B100
Amount of Time at SS (h)	0.87	0.84	0.84	0.83	0.83	0.81	0.83	0.83	0.41	0.83
Average Corrected Torque [Nm]	51.14	52.02	52.16	51.68	53.56	54.06	53.68	54.63	54.48	55.69
StDev Corrected Torque	0.37	0.37	0.50	0.47	0.56	0.52	0.52	0.54	0.46	0.43
Average Corrected % Load (%)	39.82	40.51	40.62	40.24	41.71	42.09	41.80	42.54	42.42	43.36
StDev Corrected % Load	0.29	0.29	0.39	0.36	0.43	0.41	0.40	0.42	0.35	0.34
Average Engine Speed (RPM)	2000.66	2000.56	2000.72	2000.57	2000.82	2000.84	2000.66	2000.82	2001.36	2000.72
StDev Engine Speed	15.02	14.84	15.62	15.82	14.39	14.74	15.78	15.39	15.92	14.22
Average Throttle Position (%)	45.24	45.24	45.24	45.24	45.00	45.00	45.00	45.00	45.00	45.00
StDev Throttle Position	0.00	0.00	0.00	0.00	0.00	0.00	0.00	0.00	0.00	0.00
Average Exhaust Temperature (°C)	281.59	280.88	282.94	286.12	289.68	296.06	299.68	303.82	307.75	291.42
StDev Exhaust Temperature	1.92	1.69	1.86	1.56	1.70	1.41	1.41	1.64	1.52	1.72

Steady-State 80%:

Parameter	1_28AUG2012_B000	1_12SEP2012_B000	1_24OCT2012_B000	1_14MAY2012_B100	1_16MAY2012_B100	1_17MAY2012_B100
Amount of Time at SS (h)	0.62	1.12	1.10	1.14	1.13	1.13
Average Corrected Torque [Nm]	95.53	94.76	97.55	103.52	102.63	102.72
StDev Corrected Torque	0.37	0.40	0.58	0.47	0.43	0.43
Average Corrected % Load (%)	74.10	73.49	75.66	80.29	79.60	79.67
StDev Corrected % Load	0.29	0.31	0.45	0.36	0.34	0.34
Average Engine Speed (RPM)	2203.03	2201.44	2201.64	2202.04	2202.16	2202.33
StDev Engine Speed	15.23	15.75	16.43	15.61	16.00	16.56
Average Throttle Position (%)	67.00	67.00	67.00	67.00	67.00	67.00
StDev Throttle Position	0.00	0.00	0.00	0.00	0.00	0.00
Average Exhaust Temperature (°C)	531.74	510.42	476.92	553.97	560.16	545.62
StDev Exhaust Temperature	1.94	1.85	2.66	3.01	2.35	2.40

**Table D.3. Particulate Matter Filter Mass Concentrations**

Filter		Engine Run Setup					PM Mass Collected on Filter		Notes
Filter Type	Sample Filter#	Filter Sampling Location	Exhaust Sample Type	Fuel Blend	% Load	Test Date (mm/dd/yy)	Difference post-wt-pre-wt (Δmg)	Mass Concentration (μg/m <sup>3</sup> )	
QFF	144	DL-C	Diluted	B000	40	7-Feb-2012	0.532	595.11	
QFF	145	DL-C	Diluted	B000	40	8-Feb-2012	0.532	366.92	
FF	171	DL-C	Diluted	B000	40	8-Jun-2012	0.084	65.12	
QFF	146	DL-C	Diluted	B020	40	9-Feb-2012	0.489	305.02	
QFF	147	DL-C	Diluted	B020	40	10-Feb-2012	0.187	128.51	
QFF	150	DL-C	Diluted	B050	40	2-Mar-2012	0.451	318.84	
QFF	148	DL-C	Diluted	B050	40	7-Mar-2012	-0.371	-285.22	Filter may have been torn in corner
QFF	149	DL-C	Diluted	B050	40	13-Mar-2012	0.376	250.97	
QFF	151	DL-C	Diluted	B100	40	20-Mar-2012	0.388	262.75	
QFF	179	DL-C	Diluted	B100	40	22-Mar-2012	0.288	250.62	Run ended early
QFF	180	DL-C	Diluted	B100	40	26-Mar-2012	0.919	601.86	
QFF	202	DL-C	Diluted	B000	80	2-May-2012	0.942	561.04	
QFF	181	DL-C	Diluted	B000	80	7-May-2012	0.062	36.33	Orifice logged in Aerosol Inlet
QFF	203	DL-C	Diluted	B100	80	3-May-2012	0.559	335.45	
QFF	204	DL-C	Diluted	B100	80	14-May-2012	0.638	372.52	
QFF	205	DL-C	Diluted	B100	80	15-May-2012	0.497	292.68	Orifice logged in Aerosol Inlet
QFF	206	DL-C	Diluted	B100	80	16-May-2012	0.622	377.16	Small tear on edge post-run
QFF	210	DL-C	Diluted	B100	80	17-May-2012	0.616	372.62	
QFF	142	DL-C	Diluted	None	None	27-Jan-2012	0.084	81.66	From dry run Black specks present on filter after run
QFF	212	DL-E	Diluted	B000	40	8-Jun-2012	0.414	367.46	
QFF	211	DL-E	Diluted	B100	80	17-May-2012	0.561	308.37	Denuder in line before filter
QFF	143	DL-H	Diluted	B000	40	7-Feb-2012	0.403	255.40	
FF	167	DL-H	Diluted	B100	80	14-May-2012	0.066	63.14	
FF	168	DL-H	Diluted	B100	80	15-May-2012	0.003	2.89	Orifice logged in Aerosol Inlet
FF	169	DL-H	Diluted	B100	80	16-May-2012	0.088	84.53	Torn on edge post-run
Teflo	152	DL-H	Diluted	None	None	27-Jan-2012	-0.114	-125.54	From dry run
Teflo	155	TP	Raw	B000	40	30-Jan-2012	2.182	3978.63	Q-n-D run
Teflo	155	TP	Raw	B000	40	30-Jan-2012	2.150	3920.28	2nd weigh
Teflo	155	TP	Raw	B000	40	30-Jan-2012	2.113	3853.42	3rd weigh
Teflo	156	TP	Raw	B000	40	31-Jan-2012	5.777	5974.42	Q-n-D run #2
Teflo	156	TP	Raw	B000	40	31-Jan-2012	5.586	5776.88	2nd weigh
Teflo	158	TP	Raw	B000	40	7-Feb-2012	3.143	3077.29	
Teflo	159	TP	Raw	B000	40	8-Feb-2012	4.833	4072.63	
Teflo	161	TP	Raw	B020	40	9-Feb-2012	3.889	4103.01	
Teflo	173	TP	Raw	B020	40	10-Feb-2012	5.576	7032.51	
Teflo	176	TP	Raw	B050	40	2-Mar-2012	7.017	8105.03	
Teflo	178	TP	Raw	B050	40	7-Mar-2012	7.144	8534.42	
Teflo	189	TP	Raw	B050	40	13-Mar-2012	7.153	10244.23	
Teflo	190	TP	Raw	B100	40	20-Mar-2012	11.125	12861.47	
Teflo	192	TP	Raw	B100	40	22-Mar-2012	11.669	19972.47	Run ended early
Teflo	194	TP	Raw	B100	40	26-Mar-2012	21.261	20975.73	Spotty collection pattern Cold ambient conditions
Teflo	195	TP	Raw	B000	80	2-May-2012	5.720	6683.95	
FF	163	TP	Raw	B000	80	7-May-2012	14.150	12589.96	Orifice logged in Aerosol Inlet
FF	183	TP	Raw	B000	80	6-Sep-2012	6.017	12396.63	Pre-wt checked 5:59:7.98mg
FF	184	TP	Raw	B000	80	12-Sep-2012	7.485	10240.40	Pre-wt checked 12:57:10.1mg
FF	185	TP	Raw	B000	80	21-Sep-2012	10.963	20953.75	Pre-wt checked 19:57:7.61mg
FF	186	TP	Raw	B000	80	24-Oct-2012	5.242	6113.99	Pre-wt checked 10:24:37.0.373mg
Teflo	199	TP	Raw	B000	80	8-Nov-2012	3.848	4048.82	First Engine Run for mass collection
Teflo	199	TP	Raw	B000	80	12-Nov-2012	4.124	4328.66	Second Engine Run for mass collection
Teflo	200	TP	Raw	B000	80	11-Dec-2012	5.933	6405.04	Sampled horizontally with catch-can
Teflo	196	TP	Raw	B100	80	3-May-2012	3.567	2091.52	No post-run low-rate recorded
Teflo	197	TP	Raw	B100	80	14-May-2012	8.413	7349.79	
FF	164	TP	Raw	B100	80	15-May-2012	9.636	6614.42	Orifice logged in Aerosol Inlet
Teflo	198	TP	Raw	B100	80	16-May-2012	3.071	2424.10	
FF	166	TP	Raw	B100	80	17-May-2012	5.426	6260.45	
FF	162	TP	Raw	None	None	27-Jan-2012	0.078	358.15	From dry run Black specks present on filter after run
Teflo	160	TP-FTIR	Raw	B000	40	8-Feb-2012	3.481	2841.36	Degradation visible on back of filter
Teflo	172	TP-FTIR	Raw	B020	40	9-Feb-2012	2.070	1626.74	
Teflo	174	TP-FTIR	Raw	B020	40	10-Feb-2012	2.066	1631.67	Metallic particles on filter after run
Teflo	177	TP-FTIR	Raw	B050	40	2-Mar-2012	2.548	2151.24	
Teflo	187	TP-FTIR	Raw	B050	40	7-Mar-2012	1.774	1432.08	Filter torn after run
Teflo	188	TP-FTIR	Raw	B050	40	13-Mar-2012	1.798	1435.32	
Teflo	191	TP-FTIR	Raw	B100	40	20-Mar-2012	1.623	1310.45	Metallic particles on filter after run
Teflo	193	TP-FTIR	Raw	B100	40	22-Mar-2012	1.320	1466.06	Run ended early
QFF	182	TP-FTIR	Raw	B000	80	7-May-2012	4.985	3946.83	Orifice logged in Aerosol Inlet
QFF	207	TP-FTIR	Raw	B100	80	14-May-2012	2.423	1926.03	
QFF	208	TP-FTIR	Raw	B100	80	15-May-2012	2.073	1678.44	Orifice logged in Aerosol Inlet
QFF	209	TP-FTIR	Raw	B100	80	16-May-2012	2.626	2124.13	Some of filter left on ring post-run
FF	170	TP-FTIR	Raw	B100	80	17-May-2012	0.733	588.43	O-ring did not seal correctly
Teflo	157	TP-imp	Raw	B000	40	31-Jan-2012	0.734	4125.47	Q-n-D run #2 flow given by imp pump
Teflo	157	TP-imp	Raw	B000	40	31-Jan-2012	0.698	3923.22	2nd weigh

**Table D.4. Ambient conditions recorded from ExTech Temperature and Humidity Logger at beginning of Engine Runs**

Engine Run Date	Temp (°C)	R.H. (%)	RunType
31-Jan-2012	19.4	31.8	SS40%1
7-Feb-2012	19.6	27.8	
8-Feb-2012	18.2	27.7	
9-Feb-2012	16.3	18.9	
10-Feb-2012	17.6	21.5	
2-Mar-2012	14.4	26.5	
7-Mar-2012	16.9	19.7	
13-Mar-2012	20.7	42.2	
20-Mar-2012	23.1	44.7	
22-Mar-2012	24.6	43	
26-Mar-2012	11.6	13.9	
2-May-2012	21.1	43.3	SS80%1
3-May-2012	20.7	50	
7-May-2012	21.3	19.7	
14-May-2012	20.6	50.3	
15-May-2012	20.4	68.6	
16-May-2012	21.8	63	
17-May-2012	18.2	31.4	
8-Jun-2012	24.8	46.2	SS40%2
27-Jun-2012	21.9	49.4	
28-Aug-2012	28.4	46.6	SS80%2
6-Sep-2012	25.9	60.4	
12-Sep-2012	23.4	40.8	
21-Sep-2012	21.4	50.5	
24-Oct-2012	16.9	36.1	



**Table D.5. IROX RESULTS FOR 2012 CM-12 TEST FUELS**

IROX Run Date/Time	IROX Run Name	Date Sample Taken	Sample Type	Biodies el Info	Petro Info	Dilution Factor BXX.X%	BXX.X %Diff	Density (g/cc)	Total Aromatics %	PAH %	Cetane No.	Cetane Improv (ppm)	T_90	T_95	FAEE	FAME Temp	1195cm <sup>-1</sup> FAME Peak	Comments
4/16/12 13:08	09FEB2012BQpre	2/8/12	80	N/A	Trono 2010	0	0	0.816	24.1	2.9	44.2	607	327.9	248	0.1	0.6	26.2	0.27948
4/16/12 13:48	09FEB2012BQpreM	2/8/12	80	N/A	Trono 2010	0	0	0.817	24.5	2.4	44.6	538	328.2	348.4	0.2	1.2	26	0.26785
4/16/12 13:53	09FEB2012BQpreB	2/8/12	80	N/A	Trono 2010	0	0	0.817	25	2.6	44	464	329.4	350	0.2	1.2	26.1	0.260712
4/16/12 14:02	09FEB2012BQpreT	2/8/12	80	N/A	Trono 2010	0	0	0.817	23.9	2.7	44.6	527	328.4	348.4	0.1	0.6	26.4	0.285431
4/16/12 14:05	09FEB2012BQpreM	2/8/12	80	N/A	Trono 2010	0.1	0.1	0.817	23.9	2.2	44.3	467	325.9	345.6	0.2	1.2	26.6	0.287491
4/16/12 14:09	09FEB2012BQpreB	2/8/12	80	N/A	Trono 2010	0.3	0.3	0.815	22.7	3	44.2	468	324.7	344.3	0.3	1.8	26.8	0.302643
4/16/12 14:14	27JAN2012BQ20op	1/27/12	B20	Burke Soy	Trono 2010	20.4	2	0.828	23.3	1.9	59.3	760	380.5	396.8	15.9	95.4	27.1	2.794861
4/16/12 14:19	27JAN2012BQ20mid	1/27/12	B20	Burke Soy	Trono 2010	20.5	2.5	0.829	24.2	2	59.7	747	380.8	398.4	18.9	113.4	27.3	2.739426
4/16/12 14:23	27JAN2012BQ20bot	1/27/12	B20	Burke Soy	Trono 2010	20.5	2.5	0.828	24.5	1.4	59.1	612	376.9	394.4	25.1	150.6	27.4	2.703568
4/16/12 14:28	09FEB2012BQ20op	2/9/12	B20	Burke Soy	Trono 2010	15.9	20.5	0.829	19.6	5.6	54.3	811	417.6	439	12.9	77.4	27.6	Warning #10 - CO2 peak not found
4/16/12 14:33	09FEB2012BQ20op	2/9/12	B20	Burke Soy	Trono 2010	21.2	6	0.828	23.4	1.3	59.6	684	375.9	391.9	30.8	184.8	27.7	2.910995
4/16/12 14:42	09FEB2012BQ20mid	2/9/12	B20	Burke Soy	Trono 2010	21.2	6	0.828	23.7	1.7	60.1	633	381	398.1	18.1	108.6	27.7	2.770187
4/16/12 14:51	09FEB2012BQ20pre	2/9/12	B20	Burke Soy	Trono 2010	20.7	3.5	0.828	24.2	2.1	60.1	621	389.9	407.5	69	414	27.7	2.751938
4/16/12 14:55	09FEB2012BQ20preT	2/9/12	B20	Burke Soy	Trono 2010	20.9	4.5	0.828	23.5	1.9	60.1	704	385.9	403.2	68.9	413.4	27.7	2.793945
4/16/12 15:02	09FEB2012BQ20preB	2/9/12	B20	Burke Soy	Trono 2010	21.2	6	0.828	24.1	1.5	59.5	503	380	396.9	69	414	27.9	2.742157
4/16/12 15:41	16APR2012_HEX_1		n-Hexane	N/A	N/A	0	0.1	0.659	4	6.6	50.6	671	295.5	287.6	0.5	3	27.3	
4/16/12 15:55	16APR2012_HEX_1		n-Hexane	N/A	N/A	0	0	0.655	2.6	7.4	49.3	692	294.4	289.0	0	0	27.3	0.072357
4/16/12 16:04	09FEB2012BQ20preM	2/9/12	B20	Burke Soy	Trono 2010	20.6	3	0.827	25.2	2.6	60.3	584	382.6	401	14.8	88.8	27.3	2.600861
4/16/12 16:13	10FEB2012BQ20pre	2/10/12	B20	Burke Soy	Trono 2010	20.4	2	0.828	26.2	2.4	59.5	547	385.8	404.8	69.1	414.6	27.4	2.607346
4/16/12 16:19	10FEB2012BQ20preT	2/10/12	B20	Burke Soy	Trono 2010	21.1	5.5	0.828	23.1	1.6	59.7	785	377.7	394.1	20.8	124.8	27.4	2.880295
4/16/12 14:59	09FEB2012BQ20preM	2/9/12	B20	Burke Soy	Trono 2010	21.3	6.5	0.828	24.9	2.2	60.6	671	385.2	403.9	20	120	27.8	2.779495
4/18/12 15:08	29FEB2012BQ20op	2/29/12	B50	Burke Soy	Trono 2010	44	12	0.705	7.1	5.8	56.1	634	338.1	336.9	11.4	68.4	27.6	1.658356
4/18/12 15:14	29FEB2012BQ20pre	2/29/12	B50	Burke Soy	Trono 2010	43.9	12.2	0.845	25.7	0.4	82.2	866	447.1	459.4	68.9	413.4	27.8	5.729477
4/18/12 15:25	29FEB2012BQ20mid	2/29/12	B50	Burke Soy	Trono 2010	50.4	0.8	0.709	7.9	5.7	57.2	660	341.2	340	12.3	73.8	28.1	1.864258
4/18/12 15:30	29FEB2012BQ20preT	2/29/12	B50	Burke Soy	Trono 2010	42.4	15.2	0.846	26.1	0.1	82.3	804	444.5	457.7	69	414	28.2	5.7388
4/18/12 15:44	29FEB2012BQ20bot	2/29/12	B50	Burke Soy	Trono 2010	47.2	5.6	0.707	8.8	6	58.2	690	341.8	339.5	12.1	72.6	28.6	1.741074
4/18/12 15:48	29FEB2012BQ20pre	2/29/12	B50	Burke Soy	Trono 2010	40.9	18.2	0.846	25	0	80.6	786	430.5	440.7	68.9	413.4	28.5	5.518921
4/18/12 15:54	29FEB2012BQ20preB	2/29/12	B50	Burke Soy	Trono 2010	47.2	5.6	0.707	8.3	5.7	56.2	559	339.1	337.7	11.8	70.8	28.8	1.709061
4/18/12 17:01	02MAR2012BQ20pre	3/2/12	B50	Burke Soy	Trono 2010	43.2	13.6	0.702	8.9	5.5	57.1	654	340.6	339.7	11	66	27.8	1.529785
4/18/12 17:10	02MAR2012BQ20preM	3/2/12	B50	Burke Soy	Trono 2010	43.6	12.8	0.705	7.7	5.7	56.4	590	337	335.5	11.6	69.6	27.8	1.562515
4/18/12 17:17	07MAR2012BQ20pre	3/7/12	B50	Burke Soy	Trono 2010	49.6	0.8	0.709	9	5.7	58.6	1000	329.2	327.9	11.2	67.2	27.8	1.720627
4/18/12 17:34	07MAR2012BQ20preT	3/7/12	B50	Burke Soy	Trono 2010	42.8	14.4	0.705	7.9	5.7	56.5	579	337	335.2	11.6	69.6	27.9	1.544388
4/18/12 17:41	13MAR2012BQ20pre	3/13/12	B50	Burke Soy	Trono 2012	44.8	10.4	0.705	8.7	5.7	57.4	645	329.2	327	11.5	69	27.9	1.57785
4/18/12 17:49	13MAR2012BQ20preM	3/13/12	B50	Burke Soy	Trono 2012	45.6	8.8	0.705	9.3	5.5	59	652	329	326.6	11.5	69	28	1.57634
4/18/12 18:01	13MAR2012BQ20preB	3/13/12	B50	Burke Soy	Trono 2012	44.4	11.2	0.702	7.5	5.9	57.5	789	342.2	341.5	10.9	65.4	28.1	1.584351
4/18/12 18:08	13MAR2012BQ20preT	3/13/12	B50	Burke Soy	Trono 2012	44.8	10.4	0.705	8.2	5.6	57.2	601	333.5	333.5	11.4	68.4	28.1	1.553162
4/18/12 18:20	13MAR2012BQ20preM	3/13/12	B50	Burke Soy	Trono 2012	44.8	10.4	0.705	7	6.1	56.6	670	333.2	332.1	10.6	63.6	28.1	1.625946
4/18/12 18:24	18APR2012_HEX_1		n-Hexane	N/A	N/A	0	0	0.655	3.1	6.8	49.9	547	294.7	288.1	0	0	28.2	-0.052704
4/19/12 18:59	20MAR2012BQ20op	3/20/12	B100	Burke Soy	Trono 2012	97.6	2.4	0.713	11.2	5.3	68.9	788	371.7	368.5	69	414	27.2	2.995392
4/19/12 19:12	20MAR2012BQ20mid	3/20/12	B100	Burke Soy	Trono 2012	97.6	2.4	0.713	8.7	4.8	66.3	569	356.8	353.6	17.5	105	27.6	3.047745
4/19/12 19:15	20MAR2012BQ20pre	3/20/12	B100	Burke Soy	Trono 2012	94.8	5.2	0.713	11.2	5.3	68.2	708	363.4	361.1	18.9	113.4	27.8	2.793961
4/19/12 19:20	22MAR2012BQ20pre	3/22/12	B100	Burke Soy	Trono 2012	94	6	0.713	10.6	5.2	67.2	582	367.6	365.3	68.9	413.4	28.2	2.858948
4/19/12 19:26	22MAR2012BQ20preM	3/22/12	B100	Burke Soy	Trono 2012	93.2	6.8	0.713	10.5	5.2	68.4	673	369.7	367.3	68.9	413.4	28.5	2.761414
4/19/12 19:32	20MAR2012BQ20preB	3/20/12	B100	Burke Soy	Trono 2012	91.6	8.4	0.712	9.2	5.4	65.9	557	378.7	376.3	68.8	412.8	28.7	2.735596
4/19/12 19:39	23MAR2012BQ20preT	3/23/12	B100	Burke Soy	Trono 2012	96	4	0.712	10.2	4.4	66.8	643	354.1	351	18.1	108.6	28.7	2.881393
4/19/12 19:45	27MAR2012BQ20pre	3/27/12	B100	Burke Soy	Trono 2012	97.2	2.8	0.712	10.3	5.3	68.6	739	365.8	363.4	23.1	138.6	28.7	2.833313
4/19/12 19:50	27MAR2012BQ20preM	3/27/12	B100	Burke Soy	Trono 2012	100	0	0.712	8.8	4.7	67.5	791	352.4	349.9	13.5	81	28.8	3.084427
4/19/12 19:54	28MAR2012BQ20preB	3/26/12	B100	Burke Soy	Trono 2012	96.8	3.2	0.712	9.8	4.8	67	681	357.3	354.8	16.8	100.8	28.9	2.934875
4/19/12 20:03	28MAR2012BQ20preT	3/26/12	B100	Burke Soy	Trono 2012	90.8	9.2	0.712	9.8	5.4	66.2	520	372.3	369.5	68.9	413.4	29	2.759552
4/19/12 20:07	19APR2012_HEX_1		n-Hexane	N/A	N/A	0	0	0.654	2.7	7.1	48.1	544	285.3	281.1	0	0	29	-1.8074
9/27/12 10:27	27SEP2012_HEX_1		n-Hexane	N/A	N/A	0	0	0.655	4.3	6.7	51.1	555	296	289.2	0	0	27.6	-0.015381
9/27/12 17:27	03MAY2012BQ20pre	2-May	80	N/A	Trono 2012	2.4	0.6	0.816	20.3	3.5	45.9	469	321.7	336.9	0.8	4.8	26.5	0.372589
9/27/12 17:33	03MAY2012BQ20preM	2-May	80	N/A	Trono 2012	1.2	0.3	0.817	22.4	2.7	44.1	301	322.1	338.8	0.4	2.4	26.7	0.291791
9/27/12 17:40	27SEP2012_HEX_2		n-Hexane	N/A	N/A	0	0	0.673	5.1	6.7	50	664	294.9	291.8	0	0	27.1	-0.0109
9/27/12 17:45	03MAY2012BQ20preB	3-May	B100	Burke Soy	Trono 2012	94.8	5.2	0.713	8.3	4.1	69.6	868	359.1	356.2	15.1	90.6	27.2	3.342163
9/27/12 17:50	03MAY2012BQ20preT	3-May	B100	Burke Soy	Trono 2012	95.2	4.8	0.713	10.2	5	69.6	660	368.2	365.2	23.3	139.8		

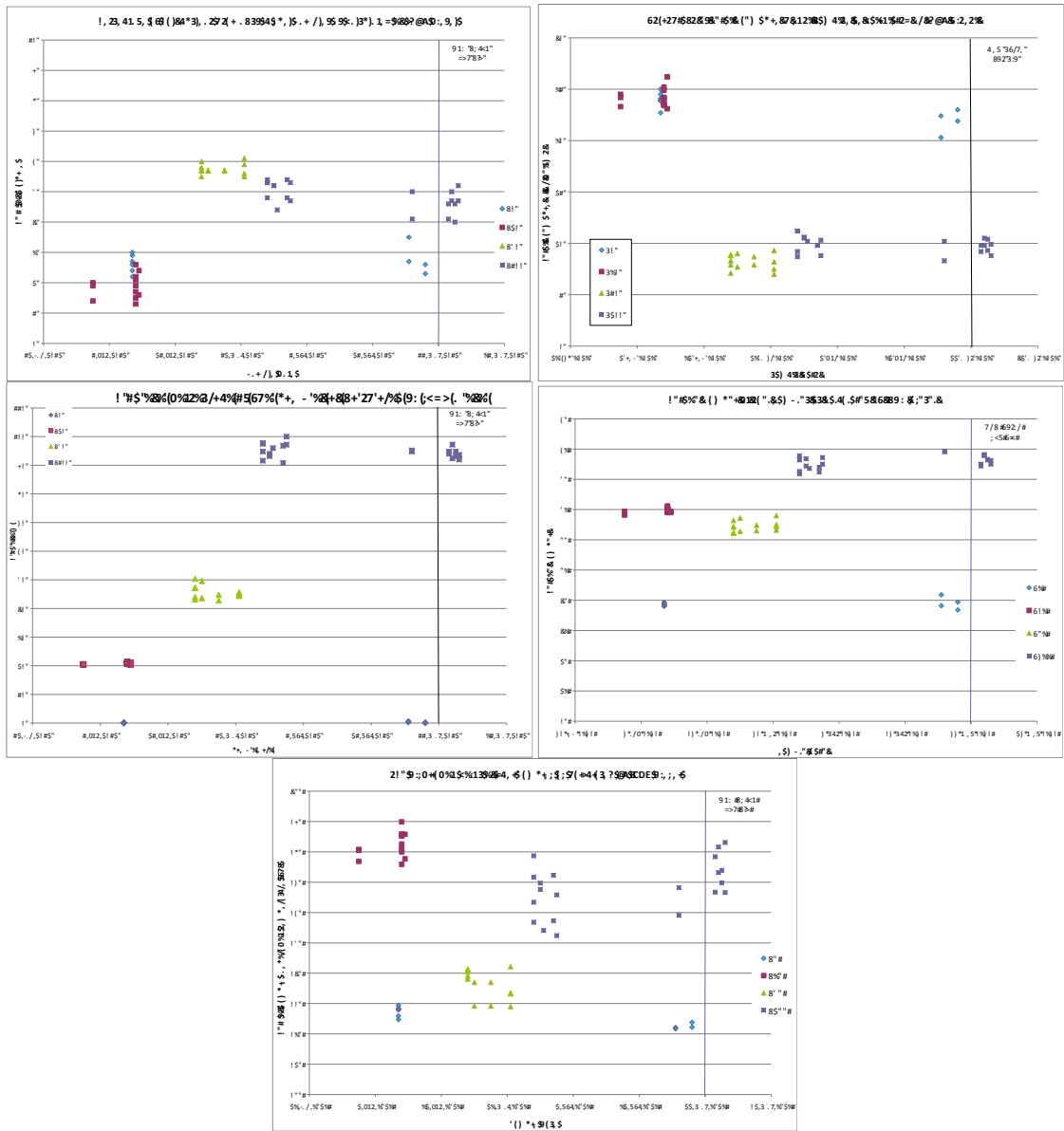


Figure D.1. IROX-Diesel Fuel Properties for fuel samples collected from the fuel tanks, before and after CM-12 tests.

**Table D.6. Steady-State 40% Load Engine Tests from Winter-Spring 2012**

SS40 (Steady-State, 40% Engine Load) TESTS from WINTER-SPRING 2012													
Filter ID #	Test #	Test Date MM/DD/YYYY	FUEL	Filter Type	Sampling location	PM Mass Collected (mg)	Flow rate (L/min)	Minutes sampled	Total Flow (L)	PM Concentration (µg/m <sup>3</sup> )	Measured by:	Notes	CHEMICAL ANALYSIS DATE
142	1	1/27/12	None	QFF	DL-C	0.084	16.2	63.50	1029	82	JD	Run Blank - First 2012 Sample	Feb-13
152	1	1/27/12	None	Teflo	DL-H	-0.114	14.3	63.50	908	-126	JD	Run Blank - First 2012 Sample	
162	1	1/27/12	None	FF	TP	0.078	3.415	63.50	217	358	JD	Run Blank - First 2012 Sample	
143	1	2/7/12	B000	QFF	DL-H	0.403	20.47	77.08	1578	255	JD		Jun-13
144	1	2/7/12	B000	QFF	DL-C	0.532	11.59	77.08	893	595	JD		Jun-13
158	1	2/7/12	B000	Teflo	TP	3.143	13.25	77.08	1021	3077	JD		
145	1	2/8/12	B000	QFF	DL-C	0.532	19.44	74.58	1450	367	JD		
159	1	2/8/12	B000	Teflo	TP	4.833	15.91	74.58	1187	4073	JD		
160	1	2/8/12	B000	Teflo	TP-FTIR	3.481	12.5	98.00	1225	2841	JD	Degradation visible on back of filter	
146	1	2/9/12	B020	QFF	DL-C	0.489	21.65	74.05	1603	305	JD		Jun-13
161	1	2/9/12	B020	Teflo	TP	3.889	12.8	74.05	948	4103	JD		
172	1	2/9/12	B020	Teflo	TP-FTIR	2.070	13	97.88	1272	1627	JD		
147	1	2/10/12	B020	QFF	DL-C	0.187	19.875	73.22	1455	129	JD		Jun-13
173	1	2/10/12	B020	Teflo	TP	5.576	10.83	73.22	793	7033	JD		
174	1	2/10/12	B020	Teflo	TP-FTIR	2.066	13	97.38	1266	1632	JD	Metallic particles on filter after run	
150	1	3/2/12	B050	QFF	DL-C	0.451	19.115	74.00	1415	319	JD		Jun-13
176	1	3/2/12	B050	Teflo	TP	7.017	11.7	74.00	866	8105	JD		
177	1	3/2/12	B050	Teflo	TP-FTIR	2.548	12.1	97.90	1185	2151	JD		
148	1	3/7/12	B050	QFF	DL-C	-0.371	17.9	72.67	1301	-285	JD	Torn along edge post-run	
178	1	3/7/12	B050	Teflo	TP	7.144	11.52	72.67	837	8534	JD		
187	1	3/7/12	B050	Teflo	TP-FTIR	1.774	12.85	96.38	1239	1432	JD	Filter torn after run	
149	1	3/13/12	B050	QFF	DL-C	0.376	20.2	74.17	1498	251	JD		Jun-13
188	1	3/13/12	B050	Teflo	TP-FTIR	1.798	12.85	97.47	1252	1435	JD		
189	1	3/13/12	B050	Teflo	TP	7.153	9.415	74.17	698	10244	JD		
151	1	3/20/12	B100	QFF	DL-C	0.388	19.905	74.25	1478	263	JD		Jun-13
190	1	3/20/12	B100	Teflo	TP	11.125	11.65	74.25	865	12861	JD		
191	1	3/20/12	B100	Teflo	TP-FTIR	1.623	12.7	97.50	1238	1310	JD	Metallic particles on filter after run	
179	1	3/22/12	B100	QFF	DL-C	0.288	19.4	59.17	1148	251	JD	Run ended early	
192	1	3/22/12	B100	Teflo	TP	11.669	9.875	59.17	584	19972	JD	Run ended early	
193	1	3/22/12	B100	Teflo	TP-FTIR	1.320	12.25	73.50	900	1466	JD	Run ended early	
180	1	3/26/12	B100	QFF	DL-C	0.919	20.45	74.67	1527	602	JD		Jun-13
194	1	3/26/12	B100	Teflo	TP	21.261	13.575	74.67	1014	20976	JD	Splotchy collection pattern	

**Table D.7. Steady-State 80% Load Engine Tests from Winter-Spring 2012**

SS80 (Steady-State, 40% Engine Load) TESTS from WINTER-SPRING 2012											
Filter ID #	Test #	Test Date MM/DD/YY	FUEL	Filter Type	Sampling location	PM Mass Collected (mg)	Flow rate (L/min)	Minutes sampled	Total Flow (L)	PM Concentration ( $\mu\text{g}/\text{m}^3$ )	Notes
167	1	5/14/12	B100	FF	DL-H	0.066	11.35	91.63	1040	63	
197	1	5/14/12	B100	Teflo	TP	8.413	9.825	116.50	1145	7350	
204	1	5/14/12	B100	QFF	DL-C	0.638	18.7	91.63	1714	373	
207	1	5/14/12	B100	QFF	TP-FTIR	2.423	10.8	116.50	1258	1926	
164	1	5/15/12	B100	FF	TP	9.636	15.95	91.33	1457	6614	Orifice clogged in Aerosol Inlet
168	1	5/15/12	B100	FF	DL-H	0.003	11.38	91.33	1039	3	Orifice clogged in Aerosol Inlet
205	1	5/15/12	B100	QFF	DL-C	0.497	18.58	91.33	1697	293	Orifice clogged in Aerosol Inlet
208	1	5/15/12	B100	QFF	TP-FTIR	2.073	10.695	115.50	1235	1678	Some of filter left on o-ring post-run
169	1	5/16/12	B100	FF	DL-H	0.088	11.37	91.22	1037	85	Torn along edge post-run
198	1	5/16/12	B100	Teflo	TP	3.071	13.89	91.22	1267	2424	
206	1	5/16/12	B100	QFF	DL-C	0.622	18.07	91.22	1648	377	Small tear on edge post-run
209	1	5/16/12	B100	QFF	TP-FTIR	2.626	10.705	115.50	1236	2124	
166	1	5/17/12	B100	FF	TP	5.426	9.515	91.08	867	6260	
170	1	5/17/12	B100	FF	TP-FTIR	0.733	10.79	115.50	1246	588	O-ring did not seal correctly
210	1	5/17/12	B100	QFF	DL-C	0.616	18.15	91.08	1402	439	
211	1	5/17/12	B100	QFF	DL-E	0.561	19.985	91.08	2153	261	Denuder in line before filter
171	1	6/8/12	B000	FF	DL-C	0.084	20.945	61.58	1290	65	
212	1	6/8/12	B000	QFF	DL-E	0.414	18.28	61.58	1404	295	
183	1	9/6/12	B000	FF	TP	6.017	8.056	60.25	485	12397	Pre-wt check 9/5: 69.798mg
184	1	9/12/12	B000	FF	TP	7.485	8.084	90.42	731	10240	Pre-wt check 9/12: 67.101mg
185	1	9/21/12	B000	FF	TP	10.963	8.72	60.00	523	20954	Pre-wt check 9/19: 67.761mg
186	1	10/24/12	B000	FF	TP	5.242	9.585	89.45	857	6114	Splotchy collection pattern

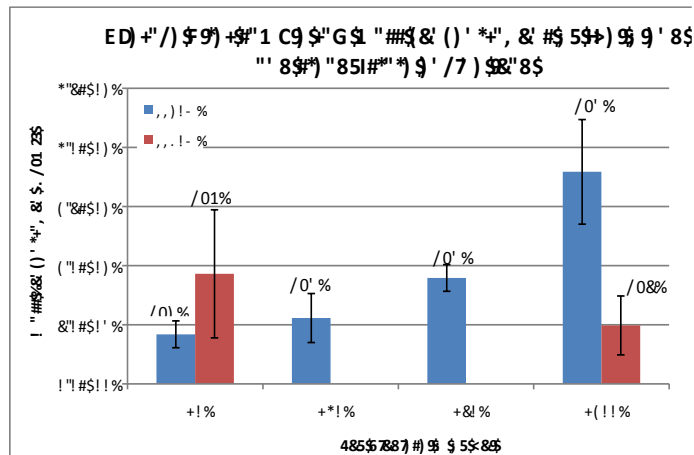


**Figure D.2. SS40 and SS80 Average Tailpipe PM Mass Concentrations. n = number of replicate samples. Error bars are one standard deviation.**



### Effect of Dilution Ratio Correction on EEPS PN Distributions

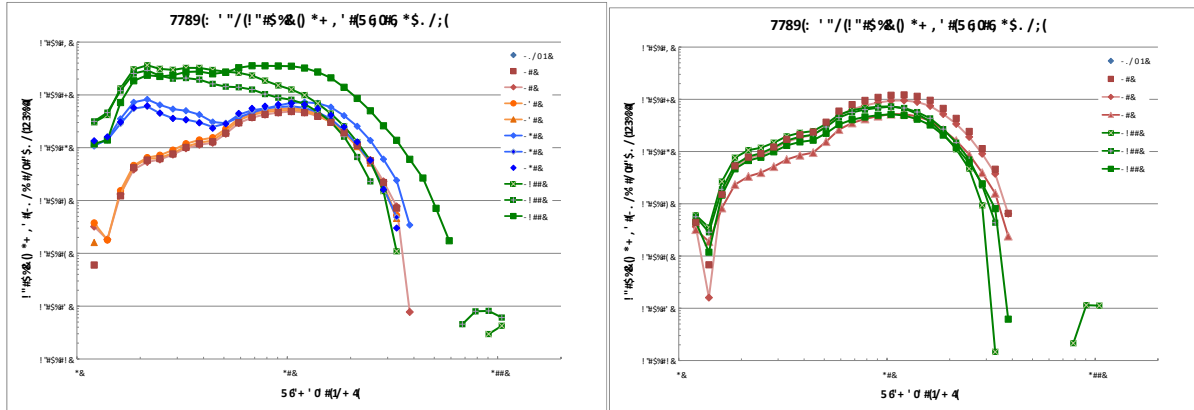


Figure D.3. Uncorrected EEPS mean number distributions by run.

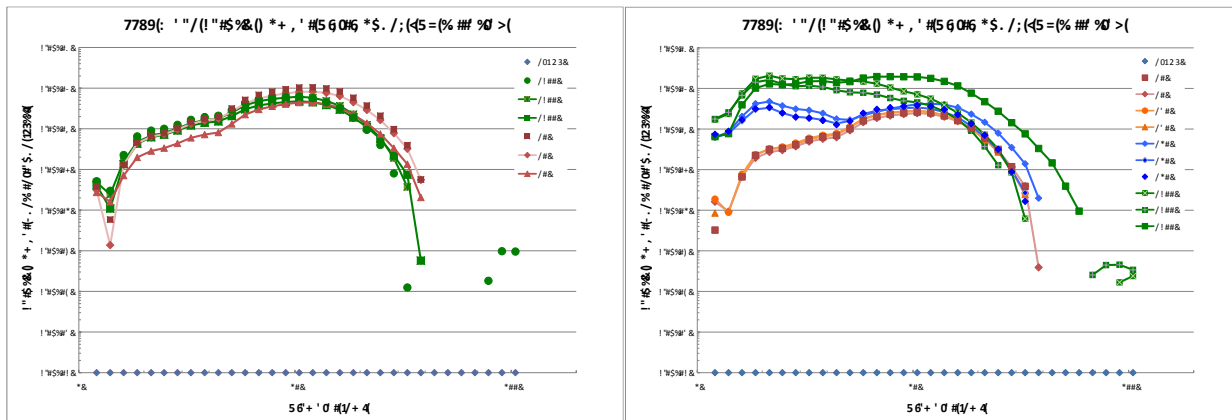
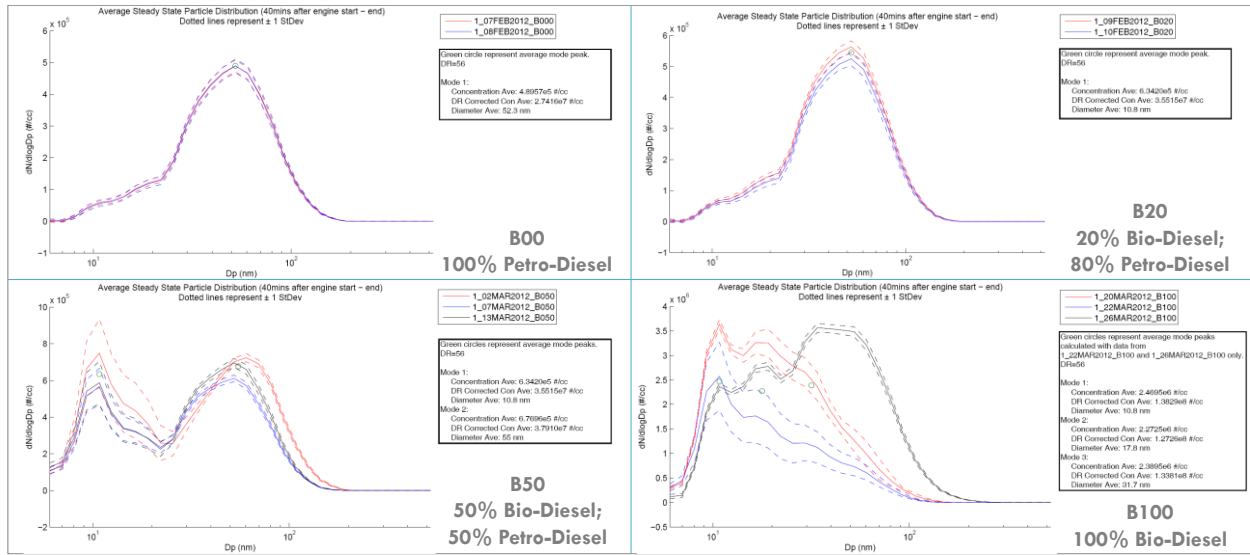


Figure D.4. EEPS Particle Number Distributions for SS40 and SS80 tests. Data were corrected for measured dilution ratio.



**Figure D.5. Average Particle Number Distributions for replicate steady-state emissions tests at each biodiesel blend ratio. EEPS data are not corrected for tunnel blank and dilution ratio here.**

**Table D.9. Particle Number Distribution Diameter Modes and Corresponding DR-Corrected Concentrations by Blend**

— 1\_09FEB2012\_B020  
 — 1\_10FEB2012\_B020

Green circle represent average mode peak.  
 DR=56

Mode 1:  
 Concentration Ave: 6.3420e5 #/cc  
 DR Corrected Con Ave: 3.5515e7 #/cc  
 Diameter Ave: 10.8 nm

— 1\_07FEB2012\_B000  
 — 1\_08FEB2012\_B000

Green circle represent average mode peak.  
 DR=56

Mode 1:  
 Concentration Ave: 4.8957e5 #/cc  
 DR Corrected Con Ave: 2.7416e7 #/cc  
 Diameter Ave: 52.3 nm

— 1\_20MAR2012\_B100  
 — 1\_22MAR2012\_B100  
 — 1\_26MAR2012\_B100

— 1\_02MAR2012\_B050  
 — 1\_07MAR2012\_B050  
 — 1\_13MAR2012\_B050

Green circles represent average mode peaks.  
 DR=56

Mode 1:  
 Concentration Ave: 6.3420e5 #/cc  
 DR Corrected Con Ave: 3.5515e7 #/cc  
 Diameter Ave: 10.8 nm

Mode 2:  
 Concentration Ave: 6.7696e5 #/cc  
 DR Corrected Con Ave: 3.7910e7 #/cc  
 Diameter Ave: 55 nm

Green circles represent average mode peaks  
 calculated with data from  
 1\_22MAR2012\_B100 and 1\_26MAR2012\_B100 only.  
 DR=56

Mode 1:  
 Concentration Ave: 2.4695e6 #/cc  
 DR Corrected Con Ave: 1.3829e8 #/cc  
 Diameter Ave: 10.8 nm

Mode 2:  
 Concentration Ave: 2.2725e6 #/cc  
 DR Corrected Con Ave: 1.2726e8 #/cc  
 Diameter Ave: 17.8 nm

Mode 3:  
 Concentration Ave: 2.3895e6 #/cc  
 DR Corrected Con Ave: 1.3381e8 #/cc  
 Diameter Ave: 31.7 nm



**Table D.10. FTIR Gas-Phase Concentrations for SS40 Biodiesel Runs**

Acetylene (ppm)		Ethylene (ppm)		NO <sub>2</sub> High (ppm)	
B000Total	2.853±0.01005	B000Total	5.27±0.6410	B000Total	88.65±0.032
B000SS	1.818±0.1367	B000SS	7.463±0.2318	B000SS	94.34±0.542
B020Total	1.877±0.4419	B020Total	7.695±0.5533	B020Total	66.26±0.227
B020SS	1.705±0.3599	B020SS	5.555±0.1080	B020SS	73.30±0.554
B050Total	2.014±0.4254	B050Total	7.886±0.3154	B050Total	76.12±0.201
B050SS	1.463±0.7633	B050SS	6.100±0.2773	B050SS	61.38±0.369
B100Total	3.160±0.3143	B100Total	11.81±0.946	B100Total	53.75±0.032
B100SS	2.653±0.4686	B100SS	9.014±0.525	B100SS	35.20±0.205
CH <sub>4</sub> (ppm)		Formaldehyde (ppm)		NO <sub>2</sub> Low (ppm)	
B000Total	5.452±0.1533	B000Total	19.88±1.125	B000Total	90.12±0.5920
B000SS	3.284±0.1189	B000SS	8.206±0.6255	B000SS	96.22±0.2728
B020Total	3.593±0.4477	B020Total	18.95±0.3283	B020Total	67.35±0.265
B020SS	2.958±0.3760	B020SS	5.099±0.2739	B020SS	74.20±0.838
B050Total	4.326±0.4612	B050Total	8.841±0.5144	B050Total	62.29±0.709
B050SS	3.233±0.1261	B050SS	5.434±0.3478	B050SS	65.62±0.181
B100Total	4.740±0.5839	B100Total	11.69±0.469	B100Total	63.42±0.588
B100SS	3.740±0.3939	B100SS	7.682±0.349	B100SS	62.45±0.099
CO (ppm)		H <sub>2</sub> O (%)		O <sub>3</sub> Low (ppm)	
B000Total	567.1±24.29	B000Total	8.805±0.03191	B000Total	3.545±0.7148
B000SS	405.5±3.294	B000SS	4.478±0.03300	B000SS	-0.8245±0.082
B020Total	313.2±3.25	B020Total	3.566±0.1882	B020Total	10.924±0.1634
B020SS	266.9±3.344	B020SS	2.469±0.1434	B020SS	2.149±0.1362
B050Total	290.2±5.22	B050Total	3.906±0.2876	B050Total	11.70±0.045
B050SS	241.8±2.37	B050SS	4.667±0.1716	B050SS	1.618±0.2495
B100Total	323.1±6.60	B100Total	4.500±0.3105	B100Total	5.645±0.856
B100SS	253.3±3.32	B100SS	4.931±0.4265	B100SS	1.328±0.6632
CO <sub>2</sub> (%)		HNCO (ppm)		Propane (ppm)	
B000Total	0.05029±0.0008585	B000Total	0.0865±0.211	B000Total	4.884±0.6515
B000SS	0.03696±0.0004504	B000SS	-0.08540±0.633	B000SS	0.7533±0.1457
B020Total	0.02750±0.001994	B020Total	2.515±0.242	B020Total	2.119±0.8333
B020SS	0.02404±0.0009327	B020SS	0.2527±0.002	B020SS	1.361±0.207
B050Total	0.02548±0.001331	B050Total	2.190±0.7653	B050Total	6.804±0.464
B050SS	0.02164±0.001139	B050SS	0.3902±0.7932	B050SS	-0.7980±0.996
B100Total	0.02827±0.004511	B100Total	1.383±0.6284	B100Total	-3.281±0.864
B100SS	0.02248±0.003623	B100SS	-0.4008±0.8098	B100SS	-13.29±0.083
CO <sub>2</sub> (%)		N <sub>2</sub> O (ppm)		Propylene (ppm)	
B000Total	3.999±0.02376	B000Total	0.7429±0.09737	B000Total	3.805±0.3100
B000SS	4.756±0.08028	B000SS	0.7569±0.09524	B000SS	1.081±0.5882
B020Total	3.698±0.2399	B020Total	0.6884±0.008956	B020Total	1.265±0.2351
B020SS	3.763±0.1843	B020SS	0.7449±0.0009089	B020SS	0.6646±0.1591
B050Total	3.755±0.2842	B050Total	0.5990±0.09176	B050Total	0.5764±0.1051
B050SS	4.651±0.2491	B050SS	0.6340±0.08320	B050SS	0.9510±0.1220
B100Total	4.115±0.1916	B100Total	0.6534±0.03582	B100Total	1.040±0.5305
B100SS	4.712±0.3518	B100SS	0.6612±0.04275	B100SS	1.127±0.3134
Diesel (ppm)		NH <sub>3</sub> (ppm)		Urea by-product (ppm)	
B000Total	202.9±9.74	B000Total	0.1321±0.05015	B000Total	0.02533±0.004947
B000SS	128.5±1.55	B000SS	0.4702±0.05394	B000SS	-0.02211±0.0007208
B020Total	193.98±6.825	B020Total	0.1853±0.06539	B020Total	-0.01111±0.005215
B020SS	193.72±5.162	B020SS	0.2284±0.1025	B020SS	0.004286±0.009627
B050Total	116.5±6.95	B050Total	0.4358±0.7504	B050Total	-0.02032±0.002876
B050SS	81.87±5.97	B050SS	0.8205±0.017	B050SS	-0.01427±0.005106
B100Total	105.8±3.95	B100Total	0.4229±0.3009	B100Total	-0.02222±0.005904
B100SS	131.2±74.52	B100SS	0.6564±0.4158	B100SS	-0.01272±0.007969
Ethane (ppm)		NO (ppm)			
B000Total	1.737±0.1338	B000Total	301.3±0.758		
B000SS	0.3618±0.01526	B000SS	392.5±2.62		
B020Total	0.2177±0.2345	B020Total	283.9±5.76		
B020SS	0.629±0.1591	B020SS	390.3±1.93		
B050Total	0.9860±0.3098	B050Total	279.7±29.40		
B050SS	-0.8162±0.3806	B050SS	371.8±1.02		
B100Total	-0.5688±0.3806	B100Total	283.7±3.25		
B100SS	-1.346±0.2478	B100SS	352.4±34.40		

B000: Feb 7, Feb 8  
 B020: Feb 9, Feb 10  
 B050: Mar 2, Mar 7, Mar 13  
 B100: Mar 20, Mar 22, Mar 26

Total: Entire Run  
 SS: 2000-5000 Sec after Engine Start

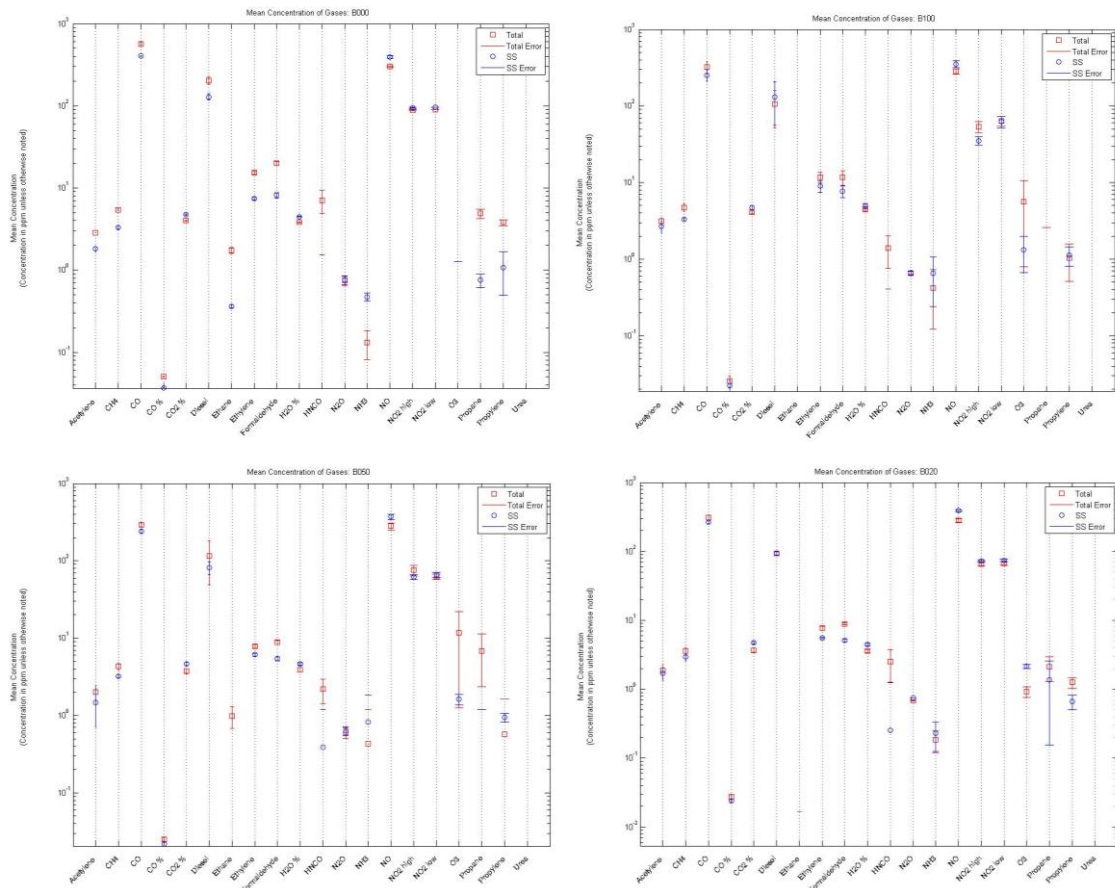


**Figure D.6. Mean Exhaust Gas Species Concentrations for (a) B0, (b) B20, (c) B50 and (d) B100 fuel blends. Error bars are one standard deviation.**